

CENTRAL RESEARCH LIBRARY
DOCUMENT COLLECTION

MARTIN MARIETTA ENERGY SYSTEMS LIBRARIES



3 4456 0361518 5

ORNL-2973
UC-81 - Reactors - Power

148

MOLTEN-SALT REACTOR PROGRAM
QUARTERLY PROGRESS REPORT
FOR PERIODS ENDING
JANUARY 31 AND APRIL 30, 1960

CENTRAL RESEARCH LIBRARY
DOCUMENT COLLECTION

LIBRARY LOAN COPY

DO NOT TRANSFER TO ANOTHER PERSON

If you wish someone else to see this
document, send in name with document
and the library will arrange a loan.



OAK RIDGE NATIONAL LABORATORY

operated by

UNION CARBIDE CORPORATION

for the

U.S. ATOMIC ENERGY COMMISSION

Printed in USA. Price \$2.25. Available from the
Office of Technical Services
Department of Commerce
Washington 25, D. C.

LEGAL NOTICE

This report was prepared as an account of Government sponsored work. Neither the United States, nor the Commission, nor any person acting on behalf of the Commission:

A. Makes any warranty or representation, expressed or implied, with respect to the accuracy, completeness, or usefulness of the information contained in this report, or that the use of any information, apparatus, method, or process disclosed in this report may not infringe privately owned rights; or

B. Assumes any liabilities with respect to the use of, or for damages resulting from the use of any information, apparatus, method, or process disclosed in this report.

As used in the above, "person acting on behalf of the Commission" includes any employee or contractor of the Commission, or employee of such contractor, to the extent that such employee or contractor of the Commission, or employee of such contractor prepares, disseminates, or provides access to, any information pursuant to his employment or contract with the Commission, or his employment with such contractor.

ORNL-2973
UC-81 -- Reactors -- Power
TID-4500 (15th ed.)

Contract No. W-7405-eng-26

MOLTEN-SALT REACTOR PROGRAM
QUARTERLY PROGRESS REPORT

For Periods Ending January 31 and April 30, 1960

H. G. MacPherson, Project Coordinator

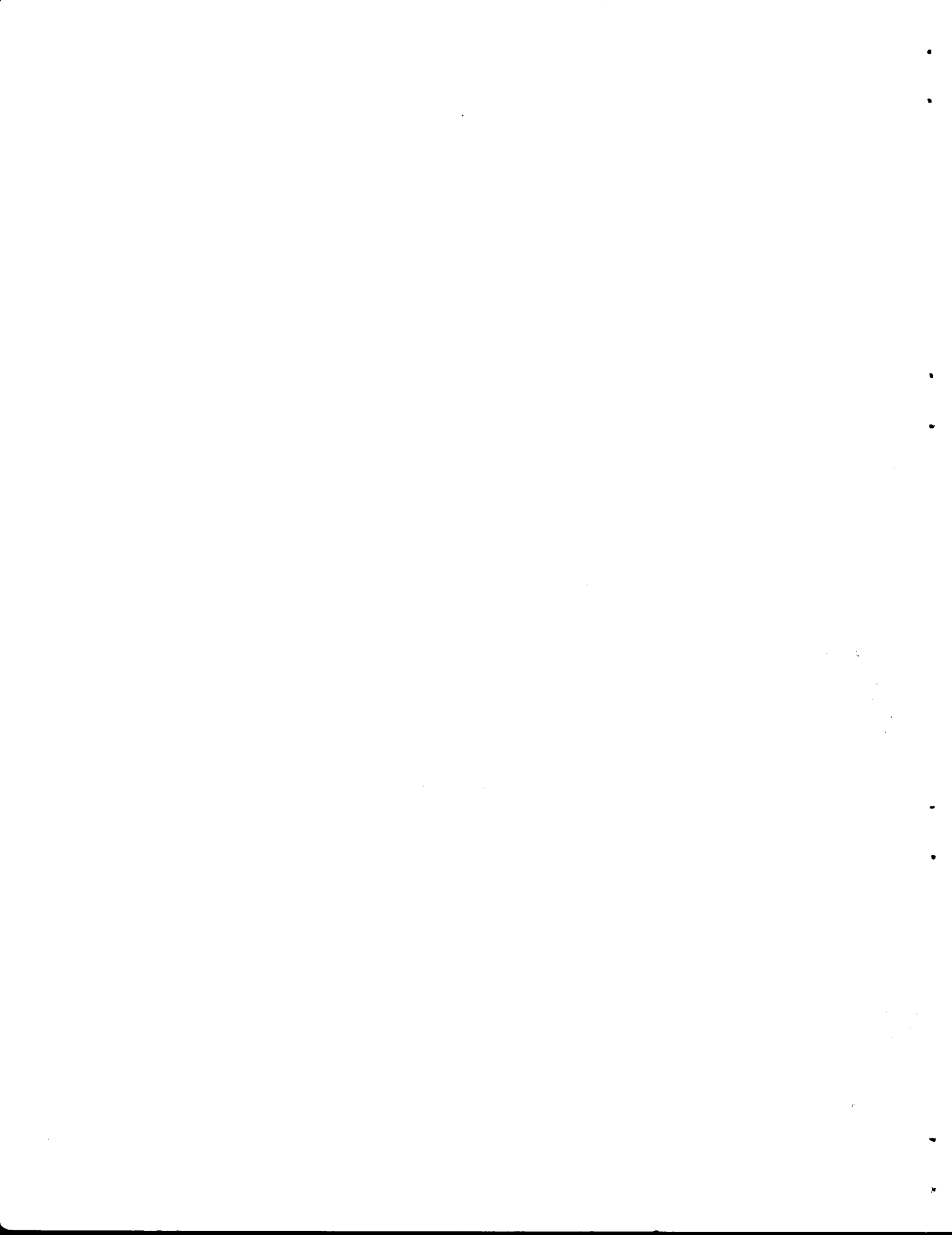
DATE ISSUED

AUG 26 1960

OAK RIDGE NATIONAL LABORATORY
Oak Ridge, Tennessee
operated by
UNION CARBIDE CORPORATION
for the
U.S. ATOMIC ENERGY COMMISSION



3 4456 0361518 5



MOLTEN-SALT REACTOR PROGRAM QUARTERLY PROGRESS REPORT

SUMMARY

Part 1. Engineering and Component Development

1.1 Component Development and Testing

Tests of molten-salt-lubricated hydrodynamic bearings continued in bearing test rigs and in the sump-type centrifugal pump. Operation of the type PKP pump, circulating NaK, with a modified Fulton Sylphon bellows seal, was suspended after 18,834 hr of continuous operation for examination of the lower seal. The seal was found to be worn and was replaced. The MF-type pump has circulated molten salt continuously for more than 25,000 hr without maintenance.

The small frozen-lead-sealed centrifugal pump has circulated molten salt continuously at 1200°F for 16,500 hr.

Molten salt was circulated at 1200°F in the Remote-Maintenance Development Facility. Following the hot operation the salt was dumped, and all maintenance operations were carried out remotely. A color motion picture with sound, demonstrating the remote removal and replacement of all major components, was completed.

Twenty-five forced-circulation corrosion loops have been placed in operation in the MSR corrosion program. Of this number, five INOR-8 loops and five Inconel loops have now been terminated for metallurgical examination; the ten loops had operated an average of 10,250 hr each.

A frozen-salt-sealed graphite-to-metal joint was tested. No leakage past the frozen joint was experienced although molten salt leaked through the porous graphite tube at 18 psi pressure.

An in-pile graphite-salt capsule was removed from the MIR after 720 hr. It is awaiting hot-cell examination. A second test continues to operate in the MIR and has accumulated more than 1000 hr of exposure at MIR power.

1.2 Engineering Research

The enthalpy of the BULT-14 mixture ($\text{LiF}-\text{BeF}_2-\text{UF}_4-\text{ThF}_4$, 67-18.5-0.5-14 mole %) was determined over the temperature range from 100 to 800°C. For

the liquid phase, the heat capacity varied from $0.367 \text{ Btu}\cdot\text{lb}^{-1}\cdot(\text{°F})^{-1}$ at 1000°F to $0.302 \text{ Btu}\cdot\text{lb}^{-1}\cdot(\text{°F})^{-1}$ at 1500°F ; the heat of fusion was 80.1 Btu/lb . Liquid heat capacities for the BeF_2 -containing salt mixtures studied to date have been summarized. The thermal conductivity for an INOR-8 rod specimen was experimentally established up to a temperature of 900°F . The results are in reasonable agreement with the thermal conductivities of several related metal alloys. The surface tension of an $\text{NaF}\text{-BeF}_2$ (64-36 mole %) mixture was measured over the range from 600 to 800°C . Comparison with data obtained previously on several $\text{LiF}\text{-BeF}_2\text{-ThF}_4\text{-UF}_4$ mixtures shows the current results to be somewhat higher. Improvements in the experimental procedure and in the instrumentation have led to increased precision in the maximum-bubble-pressure technique for surface-tension determination. Liquid densities for the $\text{NaF}\text{-BeF}_2$ mixture obtained in the course of the surface-tension experiment agree with empirical density estimates to within 7%.

Additional data have been obtained for heat transfer to BULT-14 flowing within heated Inconel and INOR-8 tubes. Approximately 4500 hr of operation have been accumulated under primarily isothermal (1150°F) conditions. No systematic variation of the heat-transfer coefficient has been observed during this time. Reanalysis of the data using recent values for the heat capacity led to an improvement in the comparison between the BULT-14 results and the general heat-transfer correlations, while adversely affecting the experimental heat balances. The previously reported discrepancy between the heat transfer in the Inconel and INOR-8 tubes has been resolved. Mean values of the heat-transfer modulus for both sets of data now agree closely; the Inconel-tube data, however, exhibit a greater experimental scatter.

Part 2. Materials Studies

2.1 Metallurgy

Examinations of nine INOR-8 thermal-convection loops, which operated with fused fluoride mixtures for one year, were completed. Five of the loops showed no attack, and the other four exhibited very light attack in the form of shallow subsurface voids. Seven Inconel thermal-convection

loops were also examined, all of which showed attack in the form of intergranular voids to depths ranging from 4 to 15 mils.

Examinations of four Inconel forced-convection loops, which operated for different periods with fluoride salt of the $\text{LiF}-\text{BeF}_2-\text{UF}_4$ system, revealed heavy subsurface-void formation in regions where loop wall temperatures exceeded 1200°F . Maximum attack ranged to 7 mils after 3000 hr of operation and to 15 mils after one year of operation.

Metallographic examinations were completed on three INOR-8 forced-convection loops which operated with fluoride mixtures for periods of one year or longer; with the exception of one loop, negligible attack was found. In that one loop, hot-leg attack, in the form of surface roughening and surface pitting, was found to a maximum depth of 1-1/2 mils. Examination of the cold-leg regions of this loop revealed the presence of metal crystals, the composition of which was determined to be predominantly nickel. The fuel mixture circulated in the loop showed appreciable oxide contamination, apparently as a result of H_2O entering the system during operation.

Chemical and metallographic examinations were carried out to investigate the thin corrosion film which has appeared in a majority of the long-term INOR-8 corrosion loops. Qualitative chemical analyses indicated the film to be composed primarily of nickel, with smaller amounts of iron, chromium, and molybdenum. Hardness data obtained indicated that the film was approximately twice as hard as the base metal.

The 48% Ti-48% Zr-4% Be alloy was used to braze an assembly of graphite tubes to an INOR-8 header in order to demonstrate the feasibility of fabricating such an assembly.

Alloys in the Au-Ni-Ta and Au-Ni-Mo ternary systems, which are resistant to corrosion by molten fluorides and which may be useful in certain applications, are under study for brazing graphite-to-graphite and graphite-to-molybdenum joints. Several alloys that melt at about 1300°C and exhibit excellent flowability have been developed. However, preliminary thermal-cycling and leak tests, coupled with metallographic examinations, indicate that these alloys are brittle and tend to crack. Thus alloys with somewhat less flowability but more ductility are being considered for future study.

Difficulty has been experienced in brazing low-porosity graphite, in contrast to experience with highly porous grades. More suitable joint designs and/or new, stronger bonding alloys are being investigated to overcome this difficulty.

Thirty-one different grades of graphite have been tested for their resistance to permeation by molten fluorides in 100-hr screening tests at 1300°F and pressures of 150 psig. Twenty-four of the grades were manufactured as low permeability; and of these, four grades, B-1, S-4-LB, GT-123-82, and CS-112-S, had less than 0.5% of their bulk volume permeated by molten fluorides in the screening test. It appears that for some grades, significant decreases in molten-fluoride-salt permeation can be accomplished by proper pressure reductions. Moderately-low-permeability grades (R-4 and S-4) were permeated to the same extent by molten fluoride salts under 150 psig at 1300°F (704°C) in 1-hr exposures as they were in 100-hr exposures.

Grade AGOT graphite was impregnated with molten bismuth and subsequently subjected to a standard fuel-permeation test. Results showed that the bismuth pretreatment suppressed the fuel pickup, but the bismuth was not completely retained in the graphite pores during the fuel-permeation test.

Two tests have been conducted to remove from graphite the oxygen contamination that causes a portion of the uranium of LiF-BeF₂-UF₄ (62-37-1 mole %, fuel 130) to precipitate as UO₂ when this fuel is exposed to the graphite at 1300°F (704°C) in a vacuum. A 50-hr exposure of grade AGOT graphite to hydrogen preheated to 1300°F (704°) failed to detectably decrease the oxygen contamination. However, the thermal decomposition of crystals of ammonium bifluoride inside a grade AGOT graphite crucible apparently was successful in removing the oxygen contamination. Fuel 130 has been exposed for 1000 hr to this graphite at 1300°F (704°C) without any uranium precipitation that could be detected by radiography.

INOR-8 was carburized to a depth of 14 mils while in direct contact for 3400 hr with grade TSF graphite at 1000 psi in fuel 30 (NaF-ZrF₄-UF₄, 50-46-4 mole %) at 1300°F (704°C).

Three nickel-base brazing alloys (Coast Metals No. 52 and 53, and General Electric No. 81), the 82% Au-18% Ni alloy, and the pure copper brazing material showed good corrosion resistance to fuel 130 (LiF-BeF₂-UF₄, 62-37-1 mole %) at 1300°F (704°C) during a 10,000-hr thermal-convection loop test of INOR-8 joints. It was noted that the commercial nickel-base alloys were corroded when used with Inconel as the base metal. Results of initial corrosion studies on experimental Au-Ni-Ta alloys have indicated that they have good resistance to both the NaF-ZrF₄- and the LiF-BeF₂-base fuels. These alloys are being developed to investigate possible graphite-to-graphite and graphite-to-metal joining methods.

2.2 Chemistry and Radiation Effects

According to preliminary checks on phase behavior, the substitution or addition of ZrF₄ in LiF-BeF₂ fuels containing UF₄ and ThF₄ appears to be a feasible route to potential improvements in corrosion behavior and perhaps oxide tolerance while at the same time retaining favorable inventories and physical properties. Such quinary fuels can be regarded as ARE NaF-ZrF₄ fuels modified as follows: Substitute 67 mole % Li⁷F for all the NaF and substitute BeF₂ for half of the ZrF₄ to reduce both the melting point and the ZrF₄ volatility, giving LiF-ZrF₄-BeF₂ in a mole ratio of 6-1-1; either UF₄ or ThF₄ may then be interchanged with ZrF₄ as desired, with only minor alterations of the over-all chemical and physical properties (except density, which increases by 50% for complete interchange with the heavy elements).

Differences, as well as similarities, in the behavior of UF₄ and ThF₄, particularly when in combination with an alkali fluoride such as NaF, have been explored, and some unusual solid solutions have been found.

Selective precipitation of oxides continues to appear promising as a means of processing breeder fuels to remove protactinium and uranium from fluoride melts.

Unintended precipitation of oxides continues to be a very troublesome problem; qualitative information in this connection has been obtained by examining quenched samples from high-temperature equilibrations containing small amounts of added oxide. The margin of tolerance for oxide

without precipitation appears to be quite low, and in addition, most sources of oxide contamination during operation and maintenance also cause corrosion in direct proportion to the amount of oxide added.

In order to evaluate the applicability of information about diffusion rates of Cr^0 and their role in controlling the rate of corrosion of INOR-8 by fluoride fuels, two anisothermal convection loop tests have been studied under conditions such that the diffusion behavior could be followed. The agreement between calculated and experimental behavior was very satisfactory.

Much of a long-standing discrepancy in the behavior of NiF_2 has been resolved through a redetermination of the free energy of formation of NiF_2 by means of experiments in which HF corrodes Ni^0 under conditions such that the equilibrium constant for the reaction can be measured accurately. Periodic sampling and analysis of the corrosion products found in long-term forced-circulation corrosion test loops has been continued; some of the results are uninterpretable in terms of the expected steady-state behavior, but most of such unpredicted deviations are sufficiently pronounced to be regarded as reflecting experimental difficulties rather than inherent behavior of the intended system.

In exploring the conditions under which intercalation of graphite by salts can occur, no effect was found with NaCl-FeCl_3 (70-30 mole %) at 750°C or with NaCl-FeCl_3 (46-54 mole %) at 200°C for 7-1/2 hr, although pure FeCl_3 crumbles graphite at 300°C in 2 hr or less. Both high temperatures and dilution of the intercalatant are presumed to diminish the tendency toward reaction.

Out-of-pile studies with fuels containing tracer rare earths in contact with graphite have been initiated to provide a background for an investigation of permeated samples which have been irradiated.

The use of purified fuels in engineering and corrosion tests has been greater than had been anticipated, so that a stockpile of fuels of current interest no longer exists.

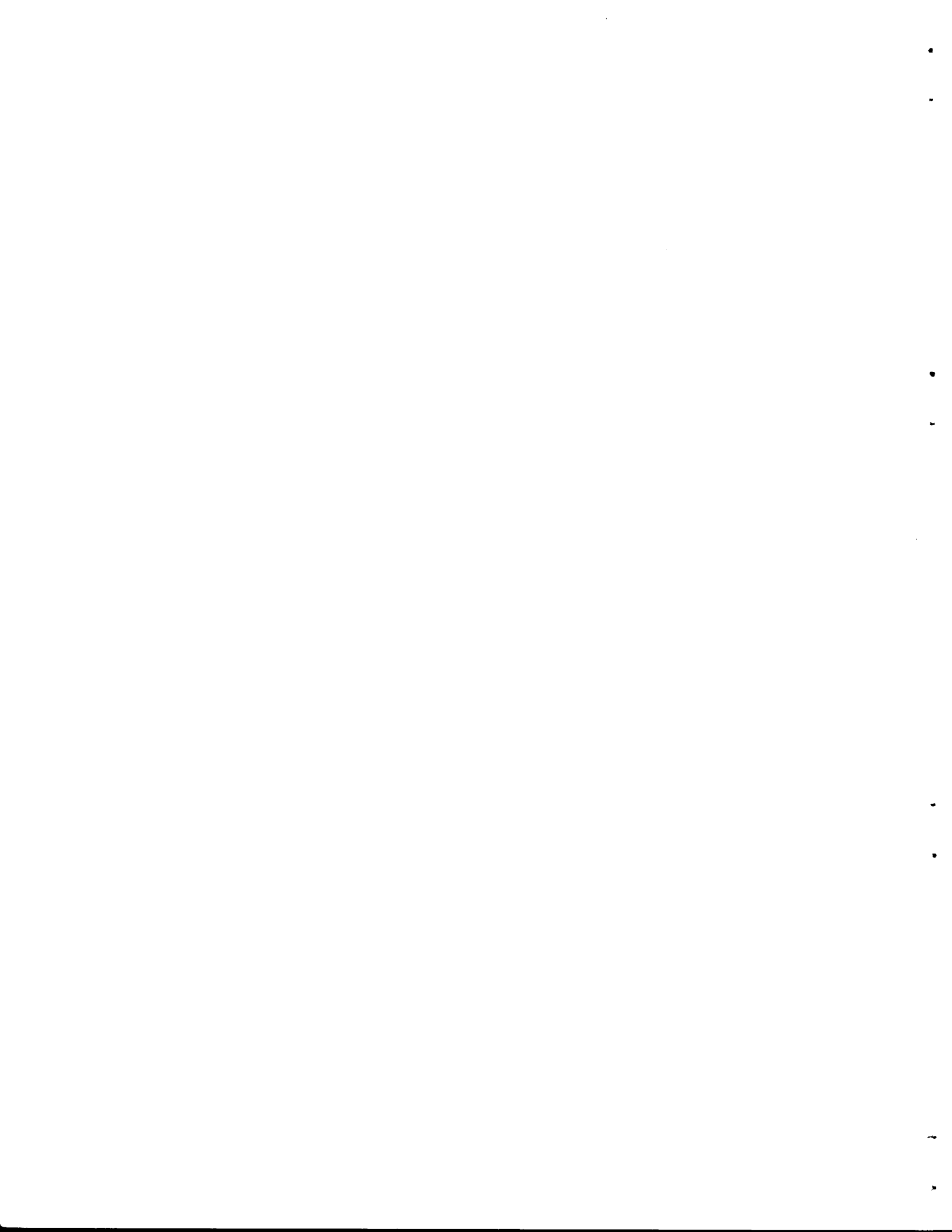
2.3 Fuel Reprocessing

Solutions of NO_2 in liquid anhydrous hydrogen fluoride appear attractive as an alternative to $\text{HF-H}_2\text{O}$ solutions for processing MSR fuel salt

containing little or no thorium. Under proper conditions the NO_2 -HF solutions dissolve UF_4 along with the LiF and BeF_2 , and decontamination from rare earths is satisfactory.

Hot saturated aqueous ammonium fluoride solutions have a reasonable solubility for thorium fluoride, but the solubility of LiF- BeF_2 - ThF_4 - UF_4 salts is much lower. No adequate processing method has yet been found for fuel salts containing ThF_4 .

In a single experiment no protactinium was removed from MSR blanket salt by fluorination at 650°C .



CONTENTS

SUMMARY..... iii

PART 1. ENGINEERING AND COMPONENT DEVELOPMENT

1.1 COMPONENT DEVELOPMENT AND TESTING..... 3

 Molten-Salt-Lubricated Bearings for Fuel Pumps..... 3

 Hydrodynamic Journal Bearings..... 3

 Test of Pump Equipped with One Molten-Salt-Lubricated
 Journal Bearing..... 3

 Self-Welding of INOR-8..... 5

 Mechanical Seals for Pumps..... 7

 Loop for Study of MF-Pump Performance..... 7

 Frozen-Lead Pump Seal..... 8

 Remote-Maintenance Development Facility..... 8

 Design, Construction, and Operation of Materials Testing
 Loops..... 12

 Forced-Circulation Corrosion Loops..... 12

 Mechanical Joints..... 19

 Design and Testing of a Frozen-Salt Metal-to-Graphite
 Joint..... 19

 In-Pile Loops..... 21

1.2 ENGINEERING RESEARCH..... 23

 Physical-Property Measurements..... 23

 Enthalpy and Heat Capacity..... 23

 Thermal Conductivity..... 23

 Surface Tension..... 26

 Heat-Transfer Studies..... 27

PART 2. MATERIALS STUDIES

2.1 METALLURGY..... 33

 Dynamic Corrosion Studies..... 33

 Thermal-Convection Loops..... 33

 Inconel Forced-Convection Loops..... 36

 INOR-8 Forced-Convection Loops..... 38

 Graphite Brazing Studies..... 45

 General Corrosion Studies..... 53

 Permeation of Graphite by Molten Salts..... 53

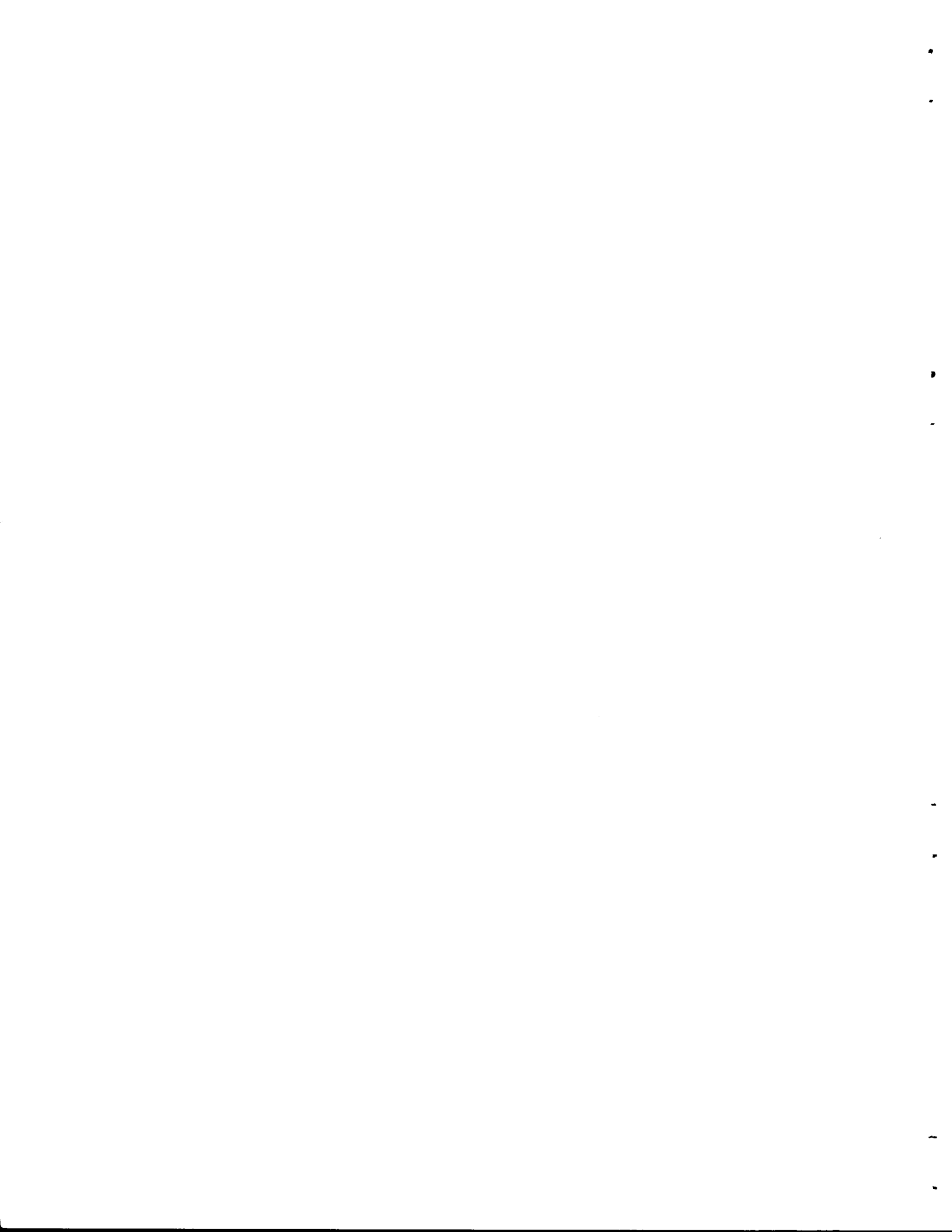
 Removal of Oxygen Contamination from Graphite..... 59

 Compatibility of INOR-8 and Graphite..... 60

 Corrosion Resistance of Brazing Alloys to
 Fluoride Fuel..... 62

2.2	CHEMISTRY AND RADIATION EFFECTS.....	65
	Phase Equilibrium Studies.....	65
	The System LiF-BeF ₂ -ZrF ₄	65
	The System NaF-ZrF ₄ -ThF ₄	65
	The System NaF-ThF ₄ -UF ₄	66
	Phase Diagrams for Fluoride Systems.....	68
	Fission-Product Behavior and Reprocessing Chemistry.....	68
	Extraction of Uranium and Protactinium from LiF-BeF ₂ -ThF ₄ Mixtures.....	68
	Chemistry of Corrosion Processes.....	74
	Effect of Oxide on LiF-BeF ₂ -ThF ₄ and LiF-BeF ₂ -ThF ₄ - UF ₄ Mixtures.....	74
	Radiotracer Studies of the Role of Cr ⁰ Diffusion as a Controlling Factor in Corrosion by Molten Fluorides....	75
	The Free Energy of Formation of NiF ₂	79
	Analysis of Corrosion Test Loops.....	80
	Corrosion Equilibria with Unalloyed Cr ⁰	81
	Melting Points of Chromous Fluoride and Chromic Fluoride.....	82
	Graphite Compatibility.....	82
	Intercalation of Graphite.....	82
	Permeation of Graphites by Molten Fluoride Fuels.....	83
	Radiation Effects.....	84
	Behavior of a Rare-Earth Fission Product in a Graphite-Molten-Salt System.....	84
	Preparation of Purified Materials.....	86
	Purification, Handling, and Service Operations.....	86
2.3	FUEL REPROCESSING.....	87
	NO ₂ -HF Solutions.....	87
	Aqueous NH ₄ F.....	87
	Protactinium Removal.....	88

PART 1
ENGINEERING AND COMPONENT DEVELOPMENT



1.1 COMPONENT DEVELOPMENT AND TESTING

Molten-Salt-Lubricated Bearings for Fuel Pumps

Hydrodynamic Journal Bearings

Investigations were continued with journal bearings operating submerged in molten salt 130 (LiF-BeF₂-UF₄, 62-37-1 mole %). Test 22, reported previously,¹ was completed. Test 18 was repeated, and two additional endurance tests were begun. A summary of the test conditions is presented in Table 1.1.1 (see also Fig. 1.1.1).

Test 22 was terminated on schedule after 494 hr. During the latter part of the test, 170 start-stop cycles were performed.

Test 23 was a repeat of test 18, with new parts, with approximately the same results. Impending seizure was evident at loads above 25 lb_f; so the test was terminated.

Test 24 was performed to investigate the endurance of the bearing at steady-state operating conditions. After 80 hr of operation the drive motor experienced a sudden power surge, and the test was suspended for examination. Examination revealed that the flow restriction at the discharge end of the grooves was not sufficient to prevent the bearing from becoming "starved."

Test 25 was a repeat of test 24, with new bearing parts. In this case the bearing grooves had a radius of 1/8 in. compared with the 1/4 in. in test 24. The test was terminated after 497 hr of operation because of seizure of the bearing. Examination revealed that the flow restriction at the discharge end of the grooves was not concentric with the bearing bore and therefore the bearing rubbed against the journal, causing the seizure. Steps are being taken to ensure concentricity with future bearings.

Test of Pump Equipped with One Molten-Salt-Lubricated Journal Bearing

Three additional tests were completed on the pump with a molten-salt-lubricated journal bearing, and another test is in progress. A summary of these tests is presented in Table 1.1.2.

¹MSR Quar. Prog. Rep. Oct. 31, 1959, ORNL-2890, p 3-5.

Table 1.1.1. Summary of Test Conditions for Testing Hydrodynamic Journal Bearings

Test No.	Material		Groove Configurations*	Speed (rpm)	Operating Temperature (°F)	Radial Load (lbf)	Operating Time (hr)	Start-Stop Cycles
	Bearing	Journal						
22	Inconel	Inconel	Axial; radius, 1/4 in.	1200	1200	200	494	170
23	INOR-8	INOR-8, carburized	Axial; radius, 1/4 in.	1200	1500	25	3	1
24	INOR-8	INOR-8, carburized	Helical; radius, 1/4 in.	1200	1200	200	80	1
25	INOR-8	INOR-8, carburized	Helical; radius, 1/8 in.	1200	1200	200	497	1

*All bearings contained three grooves. See Fig. 1.1.1 for groove details.

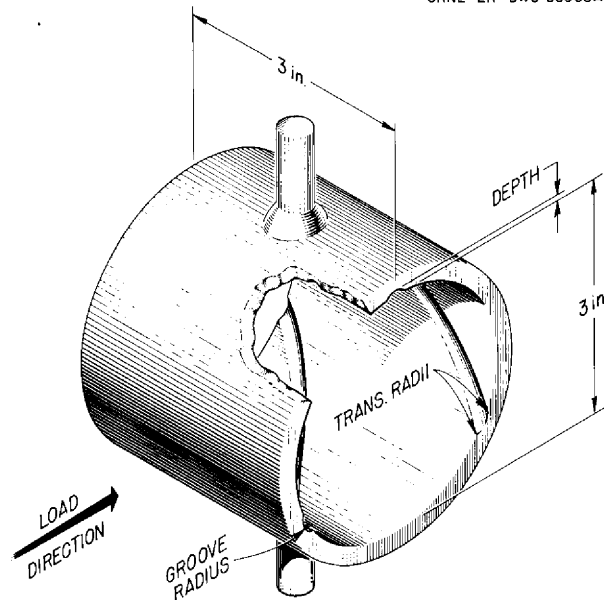


Fig. 1.1.1. Groove Details of Hydrodynamic Journal Bearing.

The journal bearing in test 3 experienced a seizure after 11 hr of operation, and subsequent examination revealed that foreign material entered the bearing clearance space, resulting in the seizure.

In tests 4, 5, and 6, the three-helical-groove bearing configuration mounted with gimbals was utilized. After 1000 hr of operation in test 4, the bearing and journal were fully suitable for further operation. At disassembly, the journal was damaged in removal from the shaft and therefore could not be re-used. The bearing and journal used in test 5 were fully suitable for further use and are under test in test 6. This test has operated for more than 850 hr, to date, and pump rotation has been stopped and started 41 times.

Self-Welding of INOR-8

One INOR-8 self-welding experiment was performed at 1500°F, on loose-fitting pins pressing against the sides of the holes, a condition encountered with gimbal-mounted bearings. The test was performed in a bath of salt 107 for 373 hr, under a load of 200 lb_F. Examination of the test pieces revealed no evidence of self-welding.

Table 1.1.2. Tests of Pumps in Molten Salt 130

	Test 1	Test 2	Test 3	Test 4	Test 5	Test 6
Bearing grooving	3, axial	3, helical	3, axial	3, helical	3, helical	3, helical
Bearing mount	Rigid	Gimbals	Rigid	Gimbals	Gimbals	Gimbals
Room-temperature radial clearance, in.	0.005	0.005	0.005	0.005	0.005	0.005
Temperature of molten salt, °F	1200	1200	1200	1200	1200	1100-1350
Shaft speed, rpm	1200	1150	1200	1400	1200	800-1400
Salt flow, gpm	50	50	50	100	50	50-260
Estimated radial load of bearing, lb _f	100	100	100	120	100	75-150
Operating time, hr	1/3	0	11	1000	105	850*
Number of start-stops	1	1	1	2	100	41*
Reason for termination	Seizure	Seizure	Seizure	Schedule	Schedule	

*Test still in progress.

Mechanical Seals for Pumps

The operation of the modified Fulton Sylphon bellows-mounted seal,² undergoing test in a PKP type of centrifugal pump circulating NaK, was suspended due to an increase of leakage of oil from the lower seal of the shaft. The total operating time was 18,834 hr at 1200 to 1225°F. The average oil leakage from the upper and lower seals, respectively, was 0.6 and 0.8 cc/day. Unaccounted-for oil leakage averaged 35 cc/day; presumably, it leaked into the process system. Examination of the pump rotary assembly revealed that (1) the lower seal faces had worn considerably; (2) the upper seal was in good condition; and (3) the impeller was in good condition, but with an etched appearance in the flow passages. The normal drainage passages to the catch basin for oil leakage past the lower seal had become filled with a viscous, greaselike substance. This plugging may well have diverted the unaccounted-for oil leakage downward through the pump-shaft annulus and into the system. The plug material was a mixture of carbon and the oxides of sodium and potassium. The pump rotary assembly, with modifications to the shaft lower seal, is being prepared for further test circulation of NaK.

Loop for Study of MF-Pump Performance

An MF type of centrifugal pump has continued in operation² and has logged more than 25,000 hr of continuous operation. Since the previous report period, the pump has continued operating in a region of cavitation at 2700 rpm, 645 gpm, and 2.5-psig pump-tank cover-gas pressure. Molten salt 30 at 1200°F is being pumped. The average seal-oil leakage collected from the upper and lower seals was 26 and 16 cc/day, respectively. An unaccounted-for loss of oil averaging 56 cc/day has been observed. Presumably, it leaks into the process system. The pump was stopped nine times: two times for 10 min each to replace brushes in the drive motor; two times for 10 min each to replace brushes in the motor-generator set; three times for 5 min each to replace the air filters in the motor-generator set; and two times for 3 min each during a scheduled power outage.

²MSR Quar. Prog. Rep. Oct. 31, 1959, ORNL-2890, p 9.

Frozen-Lead Pump Seal

The small frozen-lead-sealed pump,³ consisting of a centrifugal pump mounted vertically over a fractional-horsepower motor drive, has operated continuously during this period to accumulate 16,500 hr of continuous operation. No seal leakage occurred, and no maintenance was required during this period. The pump circulates molten salt at 1200°F.

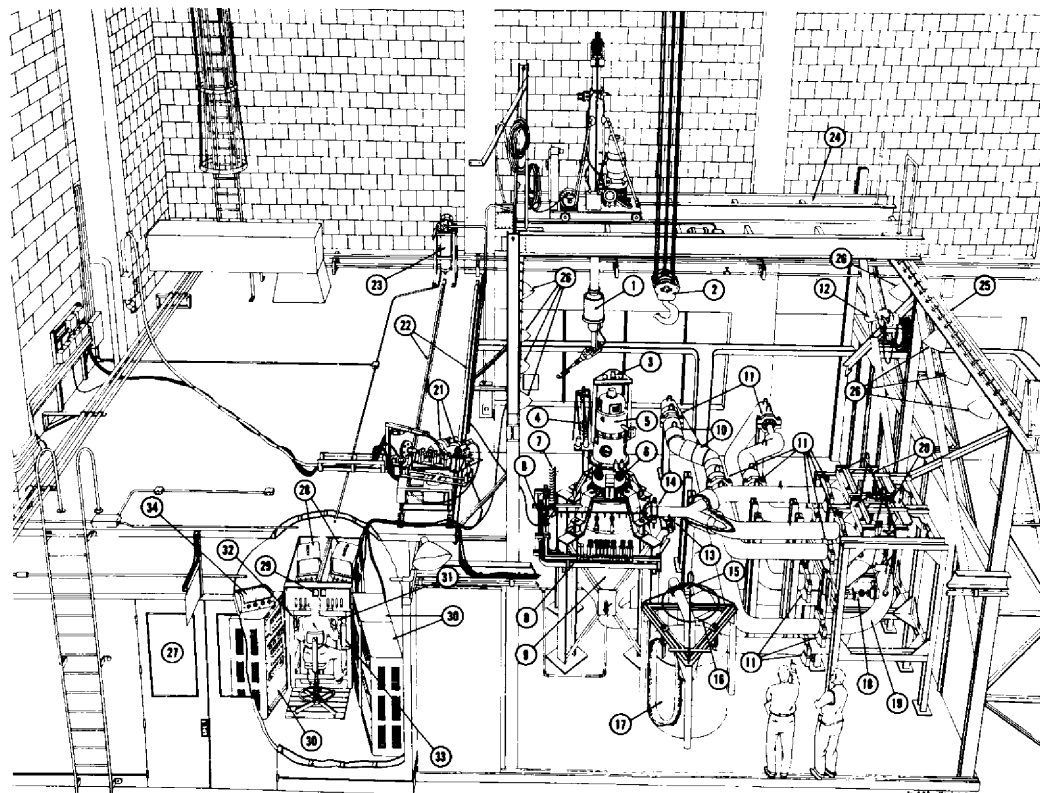
Remote-Maintenance Development Facility

A remote-maintenance facility incorporating a high-temperature (1200°F) mockup of a 20-Mw (thermal) molten-salt-fueled reactor has been constructed (see Fig. 1.1.2). The purpose is to investigate the problems involved in remotely maintaining a reactor system which cannot be approached for direct maintenance because of radioactive fission products and induced activity in the reactor components. Tools, techniques, and procedures have been developed for removing and replacing all major components, including heat exchangers, the primary fuel pump, the reactor core vessel, pipe preheaters, and piping sections. All maintenance operations are performed by a single operator from a remotely located control center, using closed-circuit television as the only means of viewing (Fig. 1.1.3).

Prior to circulating molten salt in the system, techniques and procedures were checked out by repeated performance of the required maintenance operations. Numerous modifications were incorporated in the loop, as the need arose, either to improve visibility through the cameras or to facilitate maintenance operations. A specially designed remotely operated pneumatic bolt runner and torque tool was developed to loosen and tighten the bolts on the 3 1/2- and 6-in. freeze flange clamps (see Fig. 1.1.4).

After all tools were developed, and when all operations could be performed by the operator, 120 gal of a molten-salt mixture consisting of sodium fluoride, zirconium fluoride, and uranium fluoride was circulated through the loop at 1200°F. The run was terminated and the molten

³MSR Quar. Prog. Rep. Oct. 31, 1958, ORNL-2626, p 23.



REMOTE MAINTENANCE DEVELOPMENT FACILITY
LEGEND

- 1 GENERAL MILLS MANIPULATOR
- 2 OVERHEAD TRAVELING CRANE - 5 TON
- 3 MOTOR LIFTING SLING
- 4 TOOL RACK
- 5 D.C. MOTOR - 30 H.P.
- 6 CENTRIFUGAL SUMP PUMP
- 7 RACK FOR HEATER AND THERMOCOUPLE DISCONNECTS
- 8 ELECTRIC HEATER AND THERMOCOUPLE DISCONNECTS
- 9 REACTOR VESSEL MOCK-UP
- 10 HEATER - INSULATION UNITS
- 11 FREEZE FLANGE JOINTS FOR 3 1/4 in. PIPE (Total of 16)
- 12 TELEVISION CAMERA WITH AUTO-ZOOM LENS
- 13 PIPE SUPPORT
- 14 FREEZE FLANGE JOINTS FOR 6 in. PIPE (Total of 2)
- 15 FREEZE FLANGE JOINTS FOR 1/4 in. PIPE (Total of 2)
- 16 SUMP TANK LIFTING SLING
- 17 SUMP TANK
- 18 AUXILIARY SCREW JACK FOR HEAT EXCHANGER
- 19 HEAT EXCHANGER MOCK-UP
- 20 LIFTING SLINGS AND DOLLIES FOR HEAT EXCHANGERS
- 21 STEREO TELEVISION CAMERAS
- 22 TRACK FOR TELEVISION CAMERAS
- 23 FILTER FOR FREEZE FLANGE AIR COOLING SUPPLY
- 24 BRIDGE FOR MANIPULATOR DOLLY
- 25 TRACK FOR MANIPULATOR BRIDGE
- 26 CELL LIGHTS
- 27 CONTROL ROOM
- 28 STEREO TELEVISION RECEIVERS
- 29 PRISMS OF STEREO VIEWER
- 30 TELEVISION CAMERA AND CAMERA DOLLY CONTROLS
- 31 MANIPULATOR CONSOLE
- 32 CONTROL VALVE FOR PNEUMATIC TOOLS
- 33 OVERHEAD CRANE CONTROLS
- 34 SOUND AMPLIFIER FOR CELL MICROPHONES

Fig. 1.1.2. Remote-Maintenance Development Facility.



Fig. 1.1.3. Closed-Circuit-Television Stereo Viewer.

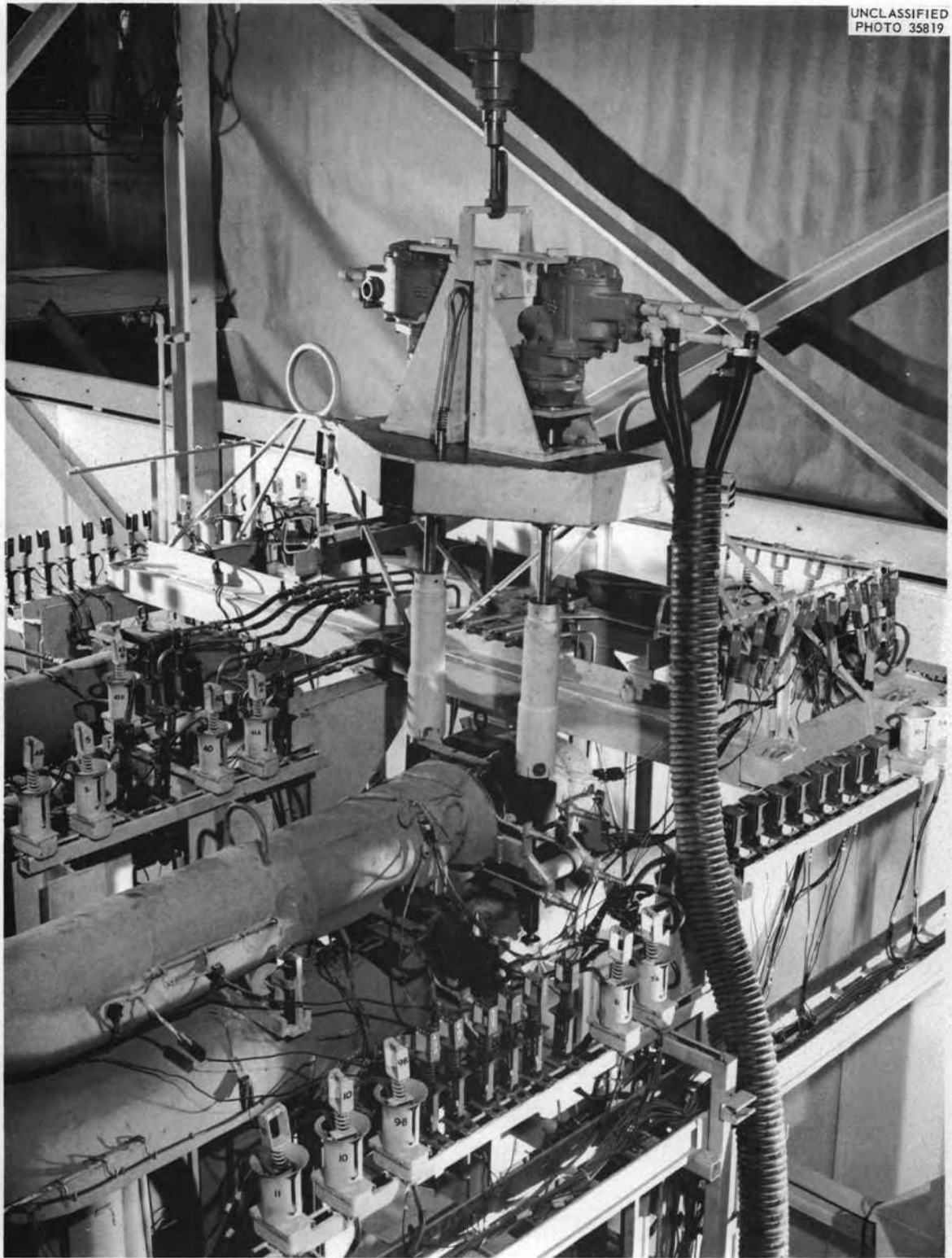


Fig. 1.1.4. Pneumatic Bolt Runner and Torque Tool.

salt returned to the sump tank, as scheduled, after 3 hr of salt circulation.

Following hot operations, maintenance operations were repeated in order to determine the effect of salt contamination on maintenance operations to be performed on the circulating pump for the molten salt, the pump motor, the reactor vessel, the heat exchanger, and the pipe preheater. These components were successfully removed, and work is continuing on their replacement. (See Figs. 1.1.5 through 1.1.8.)

To remove and replace a component, it must be possible to remotely break and remake pipe connections to leak-tight specifications. The freeze flange developed at the Laboratory is used at 20 locations in this system. Such a joint takes advantage of the ability of the molten salt to form a frozen seal between flange faces (see Fig. 1.1.9).

Shooting of the color motion picture, "Remote Maintenance of Molten-Salt Reactors," was completed.

Design, Construction, and Operation of Materials Testing Loops

Forced-Circulation Corrosion Loops

The operation of long-term forced-circulation corrosion-testing loops was continued. Including this and previous report periods, a total of 25 of these loops,⁴ in various configurations and with various fluoride salts, have operated in the MSR corrosion program. Of this number, five each of INOR-8 and of Inconel have been terminated for examination, after an average of 10,250 hr of operation. Three have been terminated for examination after less than a year of operation.

Loops presently operating and those terminated during this period are shown in Table 1.1.3. Eight of the operating loops have exceeded a year, while three more recently operated loops have less than a year of operation at ΔT conditions.

Three INOR-8 loops, 9354-1, MSRP-13, and 9354-4, were terminated during this period. INOR-8 loop 9354-1 was terminated after 14,378 hr when a salt leak occurred in the second heater section. Loop MSRP-13 was

⁴MSR Quar. Prog. Reps. from Jan. 31, 1958, ORNL-2475, through Oct. 31, 1959, ORNL-2890.

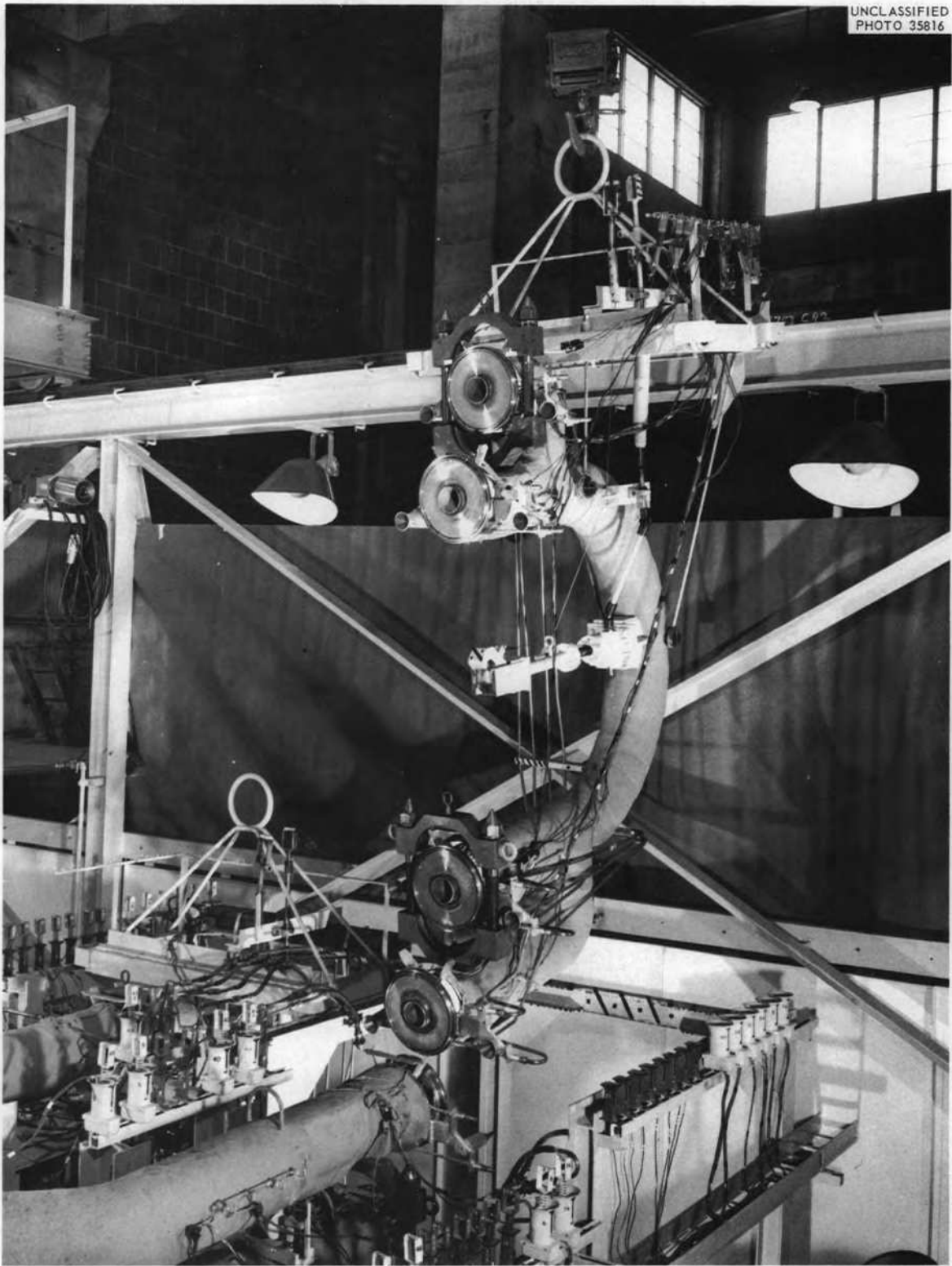


Fig. 1.1.5. Heat Exchanger After Salt Run.

UNCLASSIFIED
PHOTO 35374

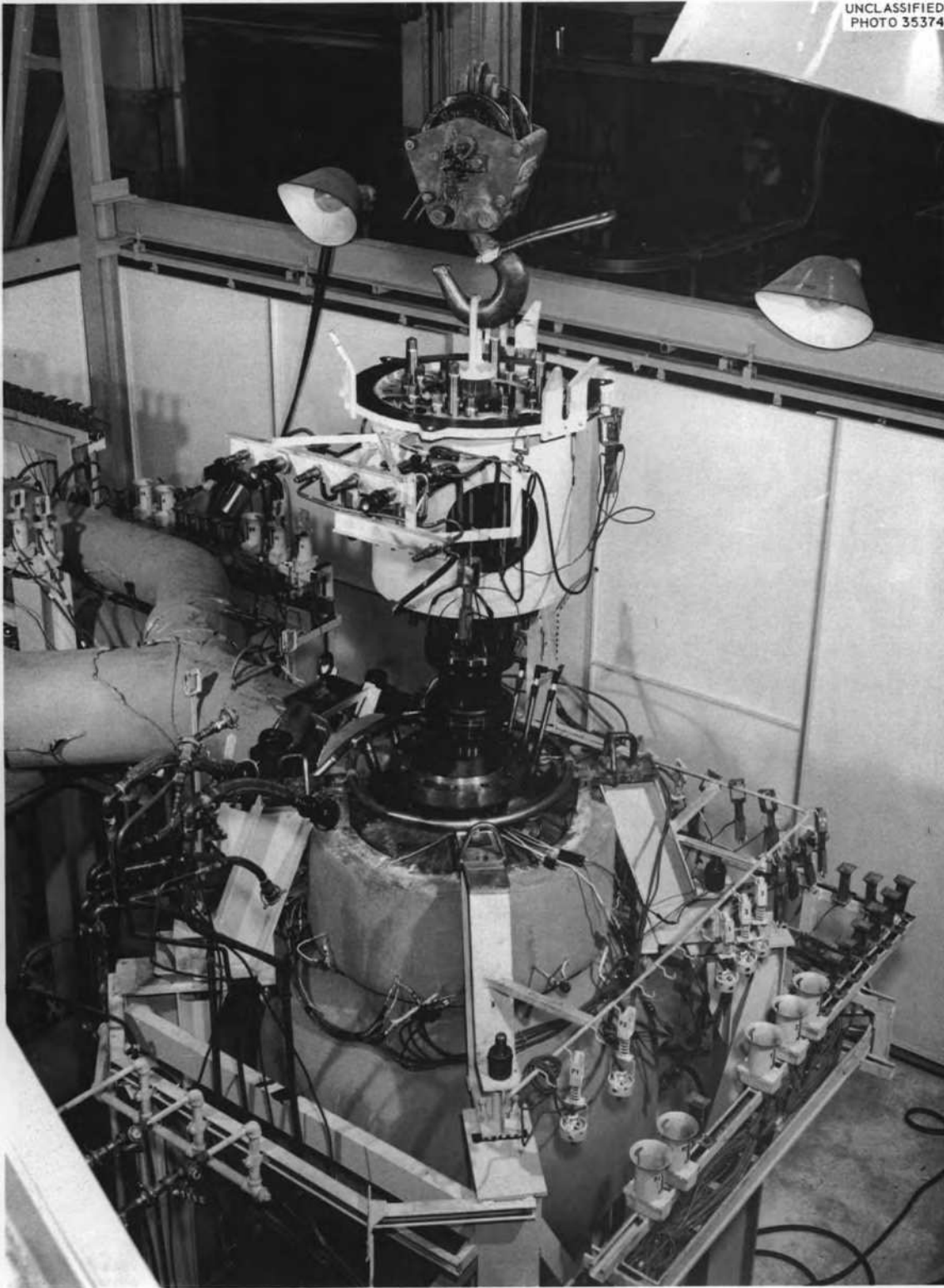


Fig. 1.1.6. Pump After Salt Run.

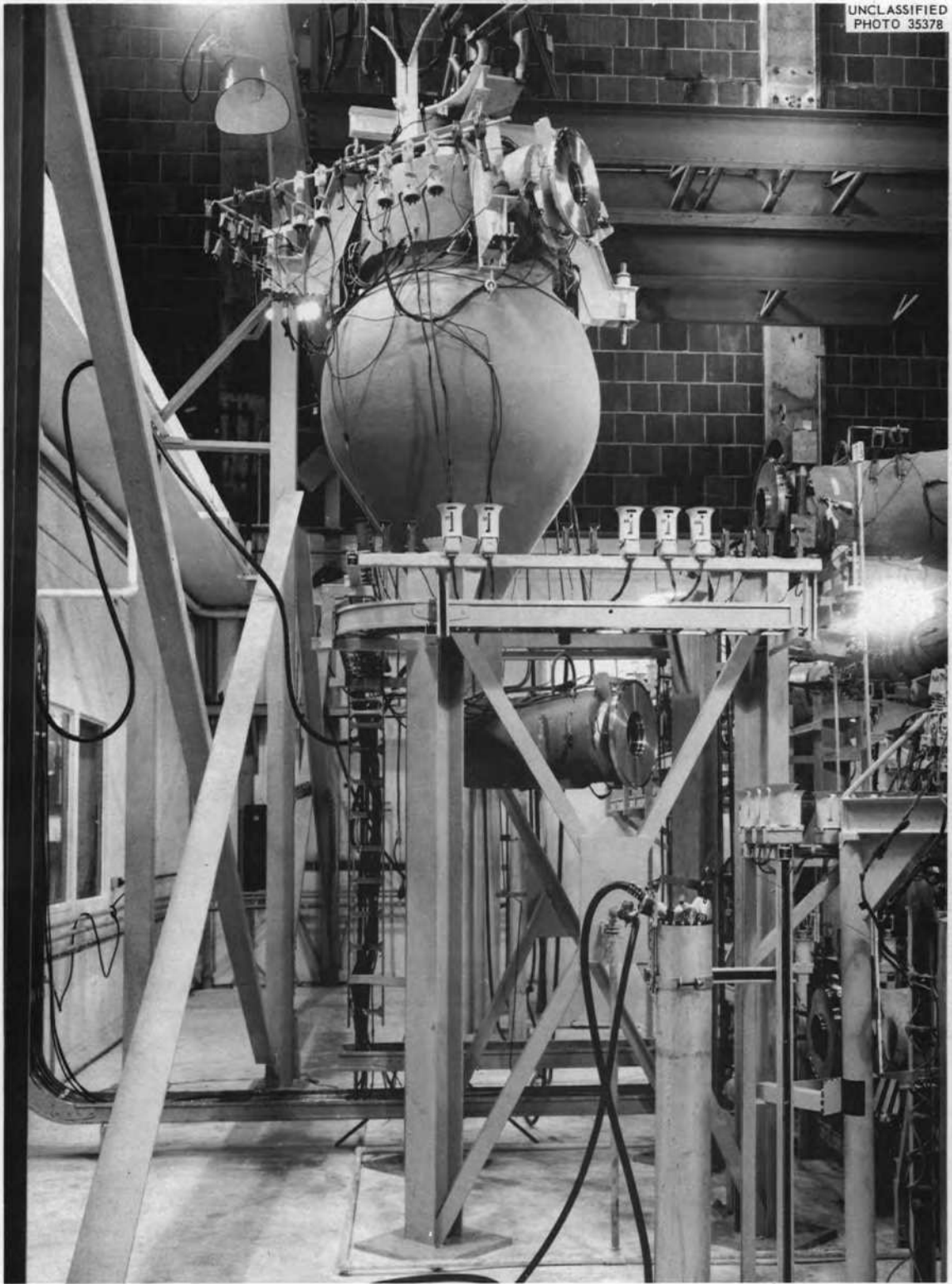


Fig. 1.1.7. Reactor Vessel Suspended.

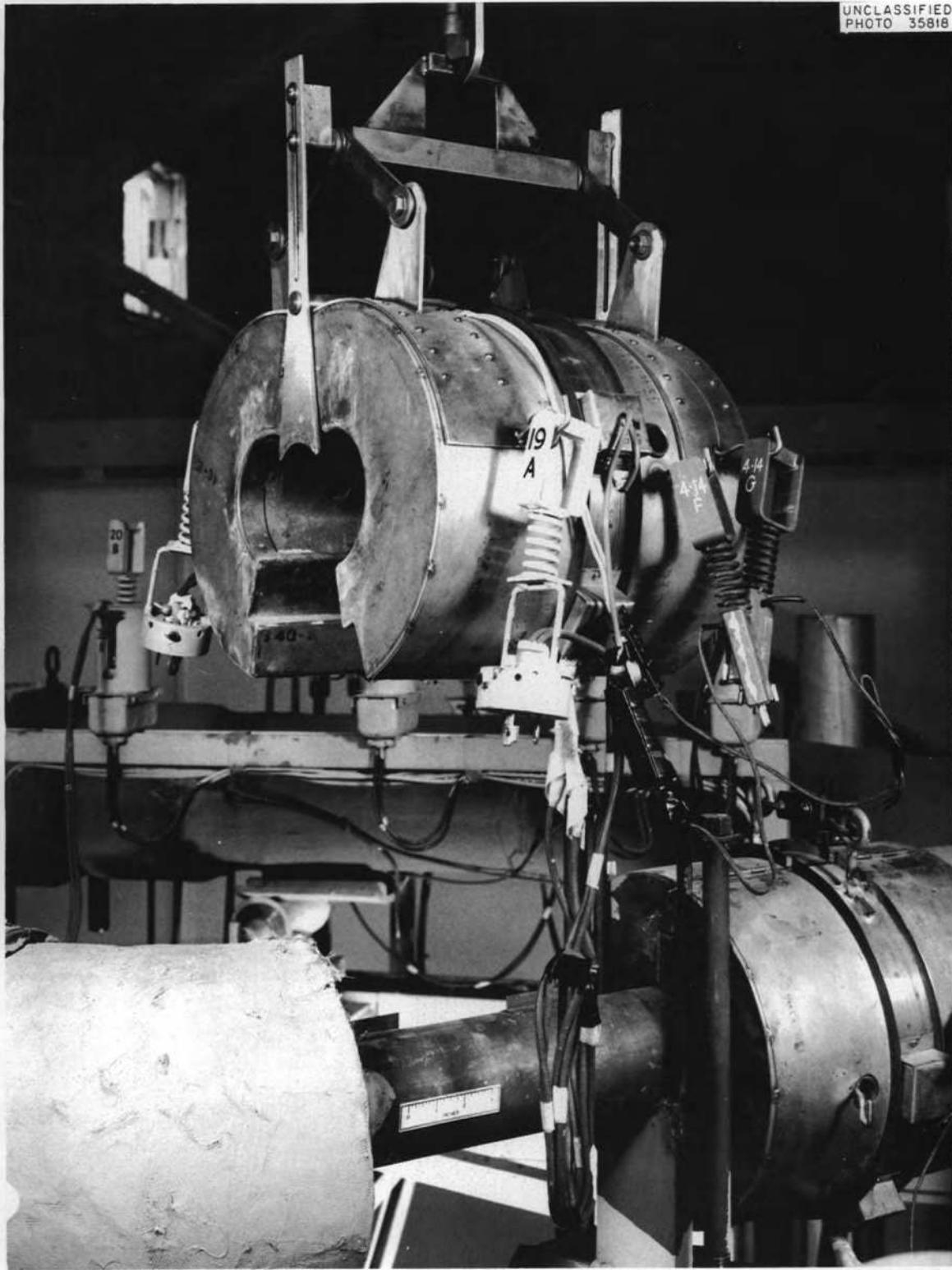


Fig. 1.1.8. Pipe Preheater After Salt Run.

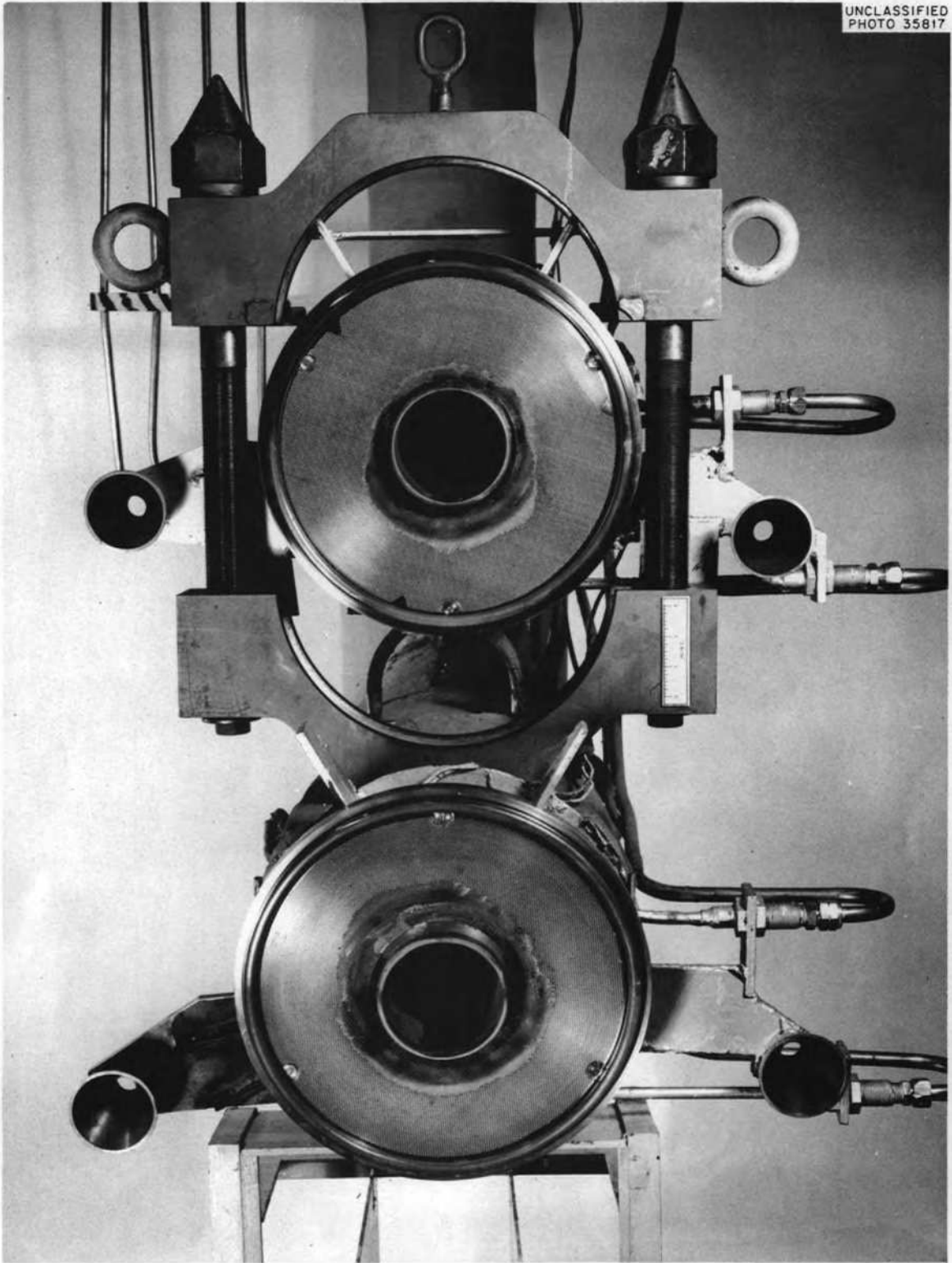


Fig. 1.1.9. Freeze Flanges on Heat Exchanger After Salt Run, Showing Salt Seal.

Table 1.1.3. Molten-Salt Forced-Circulation Corrosion-Loop Operations Summary as of April 30, 1960

Loop Designation	Loop Material	Composition Number of Fluid*	Hours of Operation at Test Conditions	High Wall Temperature (°F)	Comments
9354-3	INOR-8	84	16,586	1200	Resumed operation after pump change
9354-4	INOR-8	130	15,140	1300	Terminated 5/3/60 for removal of final sleeve insert (see ref 5)
MSRP-7	INOR-8	133	14,713	1300	Normal operation
MSRP-6	INOR-8	134	14,636	1300	Normal operation
9354-1	INOR-8	126	14,378	1300	Terminated 11/27/59
MSRP-10	INOR-8	135	13,879	1300	Normal operation
MSRP-11	INOR-8	123	13,607	1300	Normal operation
MSRP-12	INOR-8	134	13,075	1300	Normal operation
9377-5	Inconel	134	12,353	1300	Normal operation
9377-6	Inconel	133	9,835	1300	Normal operation
MSRP-13	INOR-8	136	8,110	1300	Terminated 3/14/60
MSRP-15	INOR-8	BULT-14	4,493	1400	Contains double-walled inserts (see ref 6)
MSRP-14	INOR-8	BULT-14	4,255	1300	Contains double-walled inserts
MSRP-16	INOR-8	BULT-14	2,081	1500	Began operation 11/4/59; contains double-walled inserts

*Composition numbers, components, and mole percentages of components are shown below.

Salt No.	Composition	Mole Per Cent	Salt No.	Composition	Mole Per Cent
84	NaF-LiF-BeF ₂	27-35-38	134	LiF-BeF ₂ -ThF ₄ -UF ₄	62-36.5-1-0.5
123	NaF-BeF ₂ -UF ₄	53-46-1	135	NaF-BeF ₂ -ThF ₄ -UF ₄	53-45.5-1-0.5
126	LiF-BeF ₂ -UF ₄	53-46-1	136	LiF-BeF ₂ -UF ₄	70-10-20
130	LiF-BeF ₂ -UF ₄	62-37-1	BULT-14	LiF-BeF ₂ -ThF ₄ -UF ₄	67-18.5-14-0.5
133	LiF-BeF ₂ -ThF ₄	71-16-13			

terminated after 8110 hr when a pump failure indirectly caused rupture of the cooler coil. Loop 9354-4,⁵ which began operation with three double-walled inserts, was terminated on schedule after 15,140 hr of operation. An insert was removed after each 5000 hr of operation for weight-loss determination. The results of the examination of these loops, when completed, will be reported by the Metallurgy section.

One new INOR-8 loop, MSRP-16, was placed in operation on Nov. 4, 1959, with salt mixture BULT-14. This loop is equipped with a sampling device for molten salt and incorporates three double-walled inserts in the second heater section.⁶ The sections will be removed at different operating intervals for weight-loss determination. This loop operates at a high wall temperature of 1500°F and at a 200°F ΔT .

Mechanical Joints

A complete report on the development of mechanical joints will be issued soon under the title "Mechanical-Joint Testing Program for the Molten-Salt Reactor Project."

Design and Testing of a Frozen-Salt Metal-to-Graphite Joint

During the past quarter, a frozen-salt graphite-to-metal joint was tested in a circulating-salt system. The purpose of this test was to indicate the feasibility of a frozen-salt seal between the core and blanket salts of a graphite-moderated molten-salt reactor.

The test was conducted with a molten-salt pump and loop coupled to the test piece shown in Fig. 1.1.10. The crucible was machined from a molded block of type S-4 graphite. The frozen-salt seal was formed in the annulus between the outside diameter of the graphite crucible and the inside diameter of an Inconel cylinder which was water-cooled. The configuration simulates the inlet or outlet header of a molten-salt containment vessel.

⁵MSR Quar. Prog. Rep. Jan. 31, 1958, ORNL-2474, p 32.

⁶MSR Quar. Prog. Rep. Oct. 31, 1959, ORNL-2890, p 16.

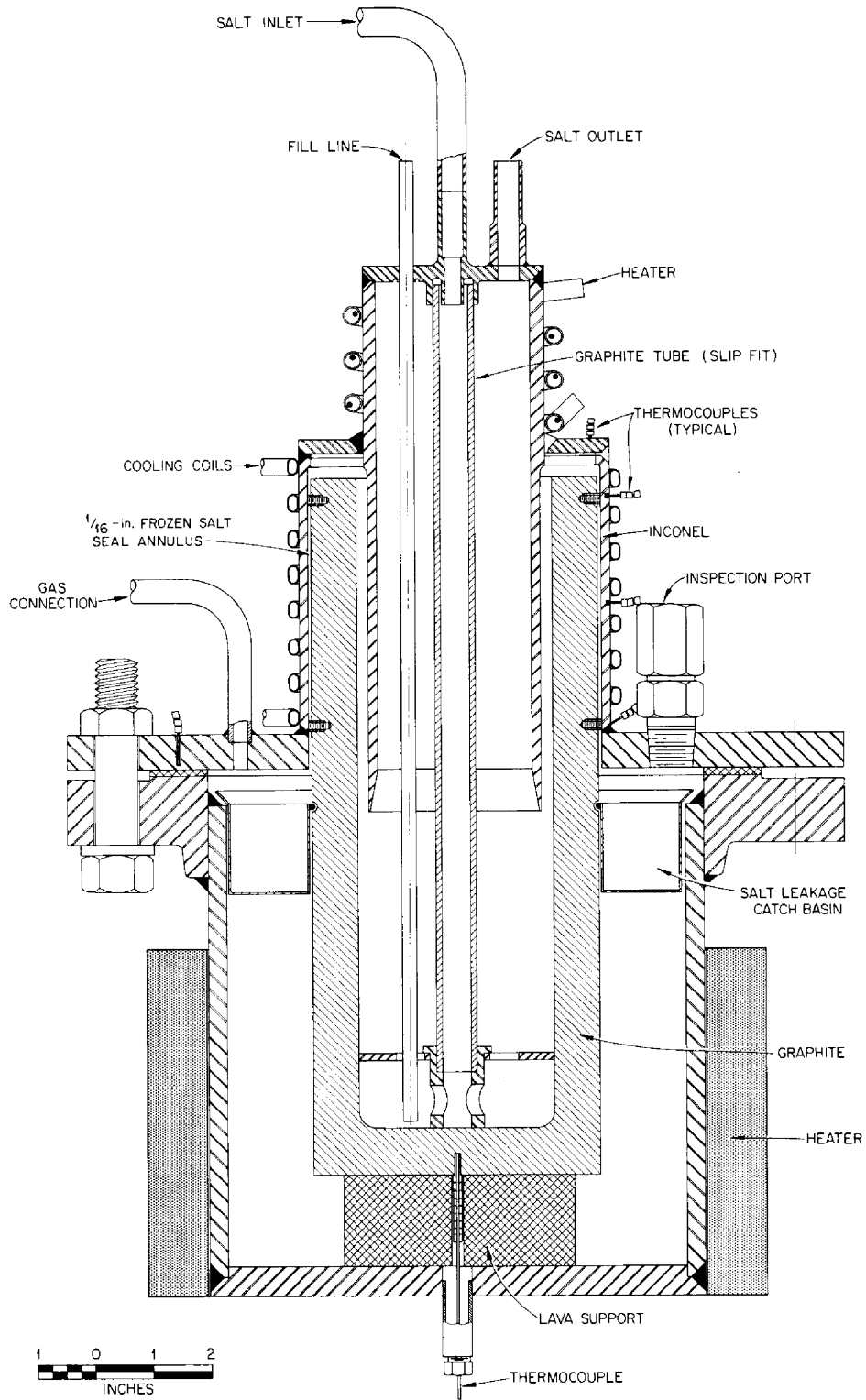


Fig. 1.1.10. Frozen-Salt Metal-to-Graphite Joint.

The salt flow entered the top of the test piece through the small, center graphite tube and up the crucible past the seal area to the outlet. The Inconel skirt extending past the seal area serves as a thermal barrier.

The test joint was operated under two conditions of differential pressure across the seal. The seal differential pressure, which was controlled by pump head and helium backup pressure on the outside of the crucible, was held at 0.5 and 18 psi for the two tests. There was no salt leakage past the seal into the catch basin in either test. However, the salt did extrude through the crucible walls during the second test. A complete report of test conditions is in process.⁷

The test piece was dismantled after the second test, as shown in Fig. 1.1.11. The upper flange, containing the graphite crucible and Inconel joint, was removed from the pot and cut as shown at 1. The frozen-salt seal annulus formed can be seen at 2. The salt frozen in the thermal-barrier annulus formed by the Inconel skirt can be seen at 3. The upper rim and lower portion of the graphite crucible are shown at 4 and 5, respectively.

In-Pile Loops

The first graphite-fuel capsule irradiation test, designated ORNL-MTR-47-1, has been completed. This test was for the purpose of studying fuel and fission-product penetration into graphite under conditions simulating those of a graphite-core molten-salt reactor. The capsules have been shipped back to ORNL and now are awaiting disassembly. The only difficulty experienced in this test, which lasted 720 hr, was the loss of the sodium-tank heaters. Operation continued without interruption.

The second test, designated ORNL-MTR-47-2, was inserted in the MTR during the March 28 shutdown and is scheduled to be removed June 20. This test has operated satisfactorily for 1000 hr, to date.

⁷J. L. Crowley and W. B. McDonald, A Metal to Graphite Joint for a Molten Salt System (to be published).

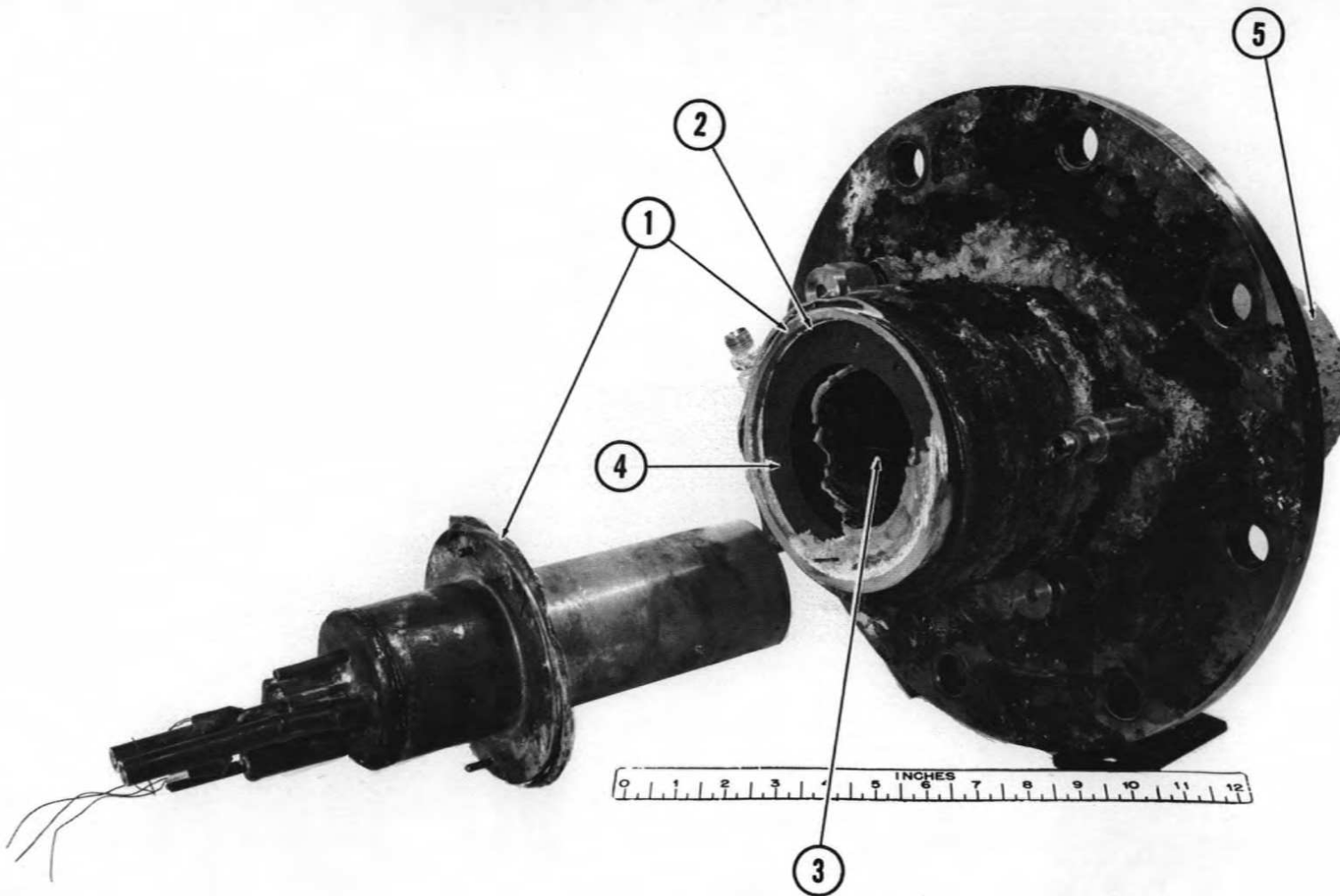


Fig. 1.1.11. Graphite-to-Metal Joint Dismantled, Showing Frozen-Salt Annuli.

1.2 ENGINEERING RESEARCH

Physical-Property Measurements

Enthalpy and Heat Capacity

Analysis of the previously reported data¹ on the enthalpy of the BULT-14 mixture (LiF-BeF₂-UF₄-ThF₄, 67-18.5-0.5-14 mole %) has been completed. The results can be expressed as follows:

1. For the solid (100-400°C),

$$H_t - H_{30} \text{ (cal/g)} = -5.0 + 0.185t + (7.8 \times 10^{-5})t^2 \quad ,$$

where t is the temperature (°C).

2. For the liquid (500-800°C),

$$H_t - H_{30} \text{ (cal/g)} = -61.5 + 0.493t - (11.71 \times 10^{-5})t^2 \quad .$$

3. The heat of fusion at 450°C is 44.5 cal/g.

The heat capacities in the liquid state of the BeF₂-containing salt mixtures studied to date are summarized in Table 1.2.1.

Thermal Conductivity

A longitudinal-heat-flow comparison-type apparatus has been used to measure the thermal conductivity of an INOR-8 specimen at temperatures up to 1000°F. The essential features of the experimental device are illustrated in Fig. 1.2.1. The test specimen (a 6-in.-long, 1-in.-dia rod) is contained between cylindrical heat meters of Armco iron of like diameter. Thermocouples (located at the axial center line in radial wells) are spaced 1 in. apart along the length of the apparatus. Radial guard heating is provided at discrete intervals by a set of heated plates. An electrical heat source at the top of the upper heat meter and a water sink below the lower meter complete the apparatus. The entire assembly is contained within an inert-atmosphere box to ensure against surface oxidation at the higher operating temperatures.

A typical longitudinal temperature profile is shown in Fig. 1.2.2; the temperature was observed to vary linearly with distance in both the

¹MSR Quar. Prog. Rep. Oct. 31, 1959, ORNL-2890, p 21.

Table 1.2.1. Liquid-Phase Heat Capacities of BeF₂-Containing Salts

Salt Mixture	Composition (mole %)					Empirical Constants*	
	LiF	NaF	BeF ₂	UF ₄	ThF ₄	a	b
							× 10 ⁻⁵
1		76	12	12		0.325	
3		25	60	15		0.315	
123		53	46	1		0.312	21.74
126	53		46	1		0.539	-3.80
130	62		37	1		0.488	5.04
133	71		16		13	0.473	-23.80
134	62		36.5	0.5	1	0.545	-8.06
136	70		10	20		0.289	-6.42
BeLT-15	67		18		15	0.418	-14.00
BULT-14	67		18.5	0.5	14	0.493	-23.42

*Constants appear in the equation $c_p [\text{cal} \cdot \text{g}^{-1} \cdot (\text{°C})^{-1}] = a + bt$, for the temperature t expressed in °C.

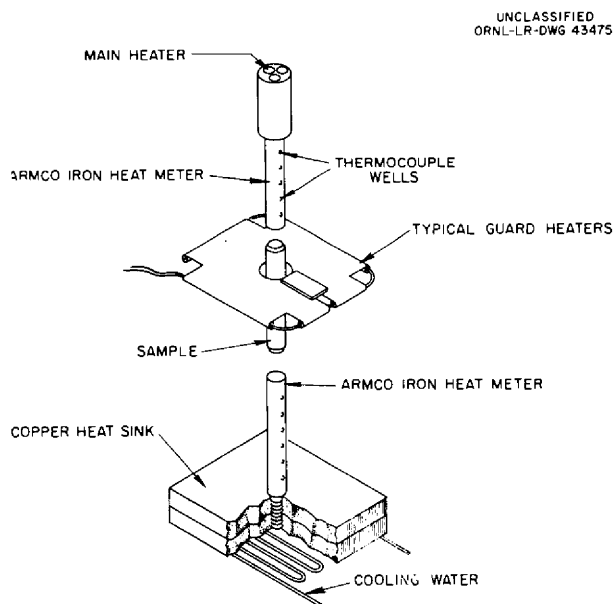


Fig. 1.2.1. Thermal Conductivity Apparatus.

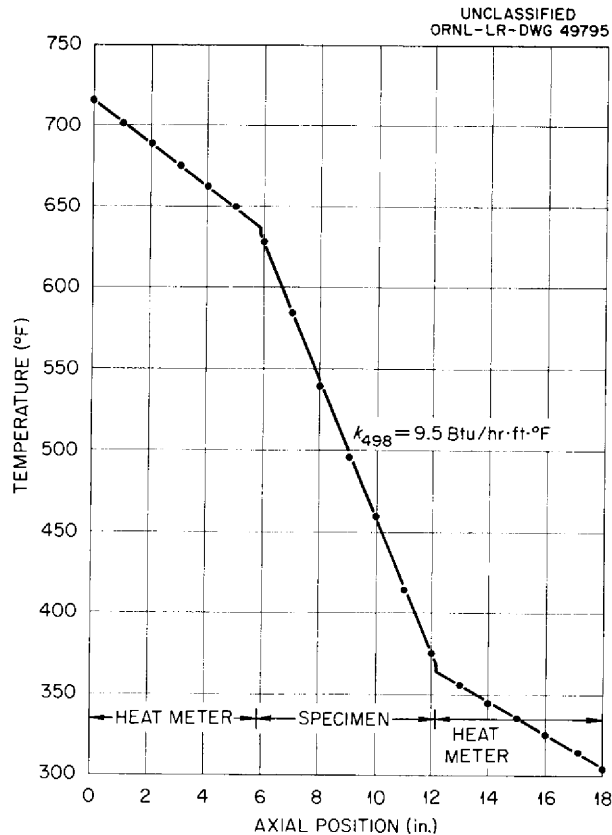


Fig. 1.2.2. Typical Longitudinal Temperature Profile Obtained in Study of Thermal Conductivity of an INOR-8 Specimen.

heat-meter and specimen regions. Although thin disks of a low-melting solder were located between the INOR-8 bar and the Armco rods to provide a low-thermal-resistance bond at operating temperatures, the small discontinuities ($\sim 5^\circ\text{F}$) at each end of the specimen show that this was not completely effective. It is probable that the tin solder did not wet the INOR-8 surface. This results in an increased radial heat flow, and a subsequent loss in experimental precision. Thus, for the case illustrated in Fig. 1.2.2, a 10% difference exists between the heat flows in the upper and lower heat meters. Since the thermal conductivity of the specimen is based on the heat flux indicated by the heat meters, a $\pm 5\%$ variation is introduced into the value for the thermal conductivity of the INOR-8 rod. This is shown in Fig. 1.2.3, which summarizes the results of the measurements with INOR-8 in the temperature range of 300 to 900°F. The correlating line, which has been included to indicate the trend of the data

with temperature, can be represented to within $\pm 5\%$ by the equation

$$k[\text{Btu}\cdot\text{hr}^{-1}\cdot\text{ft}^{-1}\cdot(^{\circ}\text{F})^{-1}] = 7.2 + 0.0045t$$

for t in $^{\circ}\text{F}$. These results are compared further in Fig. 1.2.4 with data obtained at the Battelle Memorial Institute² for Hastelloy B and Inconel, using a comparable longitudinal-heat-flow apparatus.

Surface Tension

The surface tension of an NaF-BeF₂ (64-36 mole %) mixture has been determined over the temperature range 600-800°C using the maximum-bubble-pressure technique.³ The results are given in Fig. 1.2.5 and compared with earlier measurements⁴ with mixtures LiF-BeF₂-UF₄ (62-37-1 mole %) and LiF-BeF₂-ThF₄-UF₄ (62-36.5-1-0.5 mole %).

Improvements in the experimental procedure and in the instrumentation have resulted in an increase in both the precision and the accuracy of these determinations. The original pressure-sensing and -recording arrangement (a differential-pressure cell and strip-chart recorder) was subject to calibration shifts of the order of $\pm 3\%$. Replacement of these units by a precision manometer resulted in an increase in reproducibility of several orders of magnitude. At the same time, the greater sensitivity of the pressure measurement allowed correction for two effects leading to premature bubble collapse, namely, the rate of bubble formation and fluctuations in the environmental pressure. The total error in this determination is now estimated to be of the order of $\pm 3\%$, as compared with $\pm 8\%$ for the earlier studies.

²H. W. Deem, Battelle Memorial Institute, personal communication.

³W. D. Powers, MSR Quar. Prog. Rep. June 30, 1958, ORNL-2551, p 38.

⁴MSR Quar. Prog. Rep. Apr. 30, 1959, ORNL-2723, p 39.

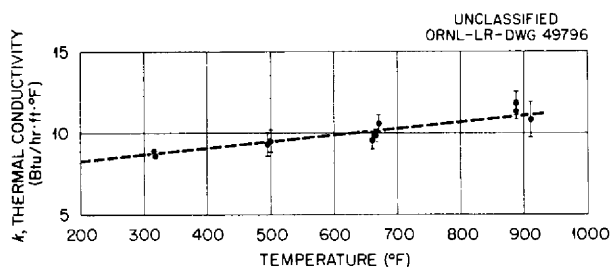


Fig. 1.2.3. Thermal Conductivity of an INOR-8 Specimen.

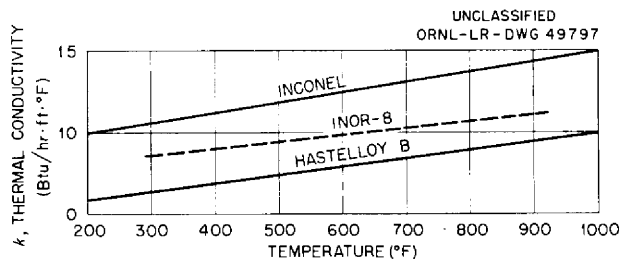


Fig. 1.2.4. Comparison of Thermal Conductivities of INOR-8, Inconel, and Hastelloy B.

To correct for the effect of the depth of immersion of the capillary tube on the bubble pressure, measurements were made at a number of levels (up to 8 mm below the salt surface) for each temperature. From these data, it is possible to make an estimate of the density of the salt. Preliminary results are compared in Fig. 1.2.6 with the density estimated from the correlation by Cohen and Jones;⁵ the agreement is reasonable.

Heat-Transfer Studies

Operation of the system⁶ for determining heat-transfer coefficients with the salt mixture BULT-14 (LiF-BeF₂-UF₄-ThF₄, 67-18.5-0.5-14 mole %) flowing in heated Inconel and INOR-8 tubes was continued. Approximately 4500 hr of primarily isothermal (1150°F) flow have been accumulated. A scheduled shutdown took place after 3750 hr for the purpose of replacing the thermocouples and the oxidized copper power leads on both test sections. On resumption of circulation, the turbine-type flowmeter was found to be inoperable; and for the succeeding 700-hr period, flow rates were determined by using the flow-rpm characteristic⁷ of the pump. The flowmeter signal was spontaneously recovered at 4450 hr. Subsequent comparison of the flow rates as indicated by the turbine meter and the pump characteristic shows a 3% discrepancy, with the flowmeter giving the higher

⁵S. I. Cohen and T. N. Jones, A Summary of Density Measurements on Molten Fluoride Mixtures and a Correlation for Predicting Densities of Fluoride Mixtures, ORNL-1702 (July 1954).

⁶MSR Quar. Prog. Rep. Oct. 31, 1958, ORNL-2626, p 46; MSR Quar. Prog. Rep. July 31, 1959, ORNL-2799, p 39.

⁷MSR Quar. Prog. Rep. Apr. 30, 1959, ORNL-2723, p 41.

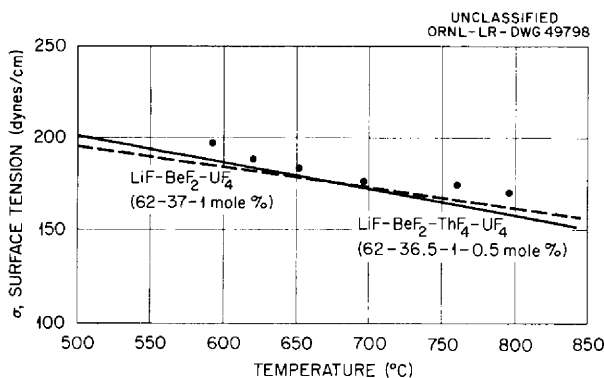


Fig. 1.2.5. Surface Tension of NaF-BeF₂ (64-36 mole %).

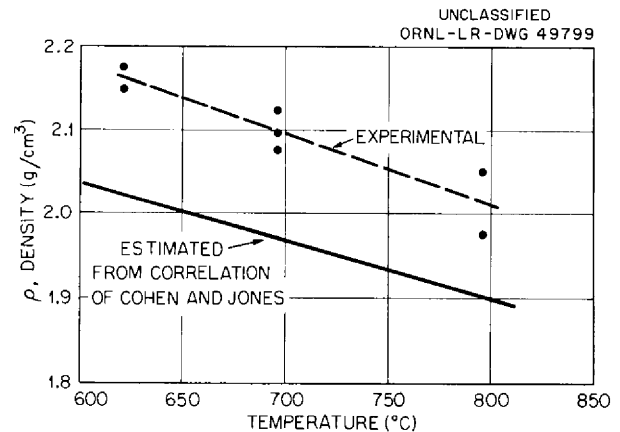


Fig. 1.2.6. Density of NaF-BeF₂ (64-36 mole %).

result. Since the pump curve was obtained initially by calibration with reference to the flowmeter (the performance characteristic for the turbine meter having been established independently), a 3% inconsistency exists in the flow rates for all Δt runs in the MB series. The designations MA and MB have been used to differentiate between the data taken before and after the shutdown, respectively. This flow uncertainty affects directly both the calculated Reynolds modulus and the heat-transfer coefficient.

The experimental results (as the heat-transfer parameter, $N_{Nu}/N_{Pr}^{0.4}$) are shown in Fig. 1.2.7 for the INOR-8 section and in Fig. 1.2.8 for the Inconel section. All the data⁸ have been re-evaluated, using the recently determined values for the heat capacity of the BULT-14 mixture. (See the previous section, "Physical-Property Measurements.") This resulted in an increase in the magnitude of the heat-transfer parameter of about 10%. At the same time, the heat balances (the ratio of the heat gained by the salt in passing through the test section to the electrical energy input) were adversely affected to the extent that all values are now greater than unity (ranging as high as 1.6). A detailed re-examination of the experimental instrumentation and a redetermination of the enthalpy of the salt are planned in an effort to obtain an explanation for this situation.

The data given in Figs. 1.2.7 and 1.2.8 show a general scatter of the order of $\pm 10\%$. However, the variability of the Inconel-tube data within

⁸MSR Quar. Prog. Rep. Oct. 31, 1959, ORNL-2890, p 23.

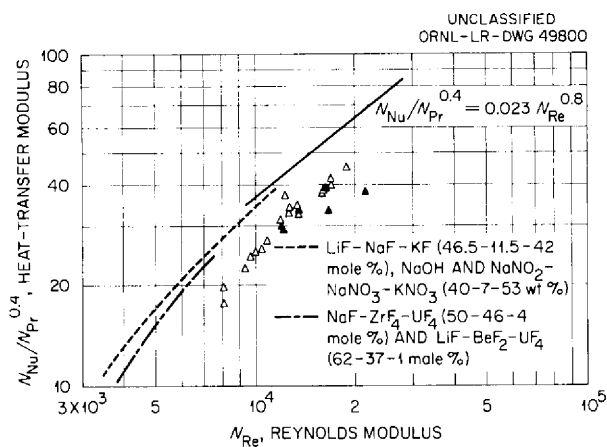


Fig. 1.2.7. Heat Transfer with BULT-14 (LiF-BeF₂-UF₄-ThF₄, 67-18.5-0.5-14 mole %) Flowing in a Heated INOR-8 Tube.

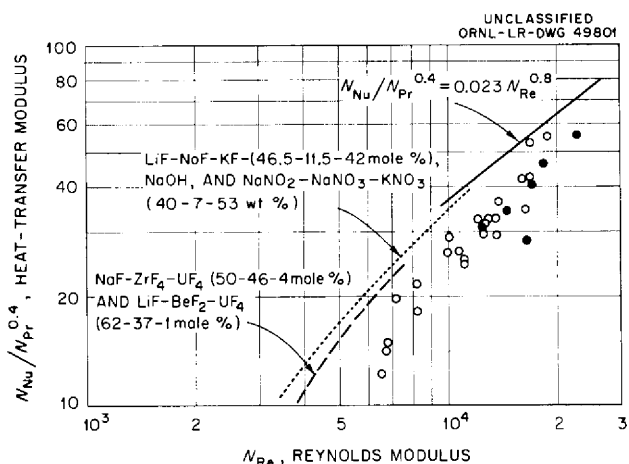


Fig. 1.2.8. Heat Transfer with BULT-14 (LiF-BeF₂-UF₄-ThF₄, 67-18.5-0.5-14 mole %) Flowing in a Heated Inconel Tube.

this scatter band is greater than that observed for the INOR-8 tube. The cause of this increased deviation is not yet understood. Since the salt was drained from the loop during the thermocouple and electrical repair operation, the data have been differentiated as to this aspect (series MA and MB). There does not appear to have been a significant effect, although (for the limited data available) a number of unexpectedly low values of the heat-transfer parameter were calculated. No systematic temporal variation of the heat-transfer coefficient has been observed.

For comparison, the heat-transfer characteristics for a number of previously studied salts⁹⁻¹² are also given in Figs. 1.2.7 and 1.2.8. The data for both the Inconel and INOR-8 tubes are seen to lie about 25% below the general heat-transfer correlation¹³

$$N_{Nu}/N_{Pr}^{0.4} = 0.023 N_{Re}^{0.8}$$

for normal fluids in turbulent flow within circular tubes under moderate Δt conditions, as well as below the experimental results for other molten salts. This discrepancy, if attributed entirely to the lack of experimental data on the thermal conductivity of the BULT-14 salt, would require a decrease in the thermal conductivity by almost a factor of 2 [from the estimated value of $1.3 \text{ Btu}\cdot\text{hr}^{-1}\cdot\text{ft}^{-1}\cdot(^{\circ}\text{F})^{-1}$]. The previously observed⁸ difference between the INOR-8 and Inconel data was found to arise from an error in the value of the tube surface area used in the analysis. After correction, the originally low results for the INOR-8 tube agreed closely with the Inconel-tube data.

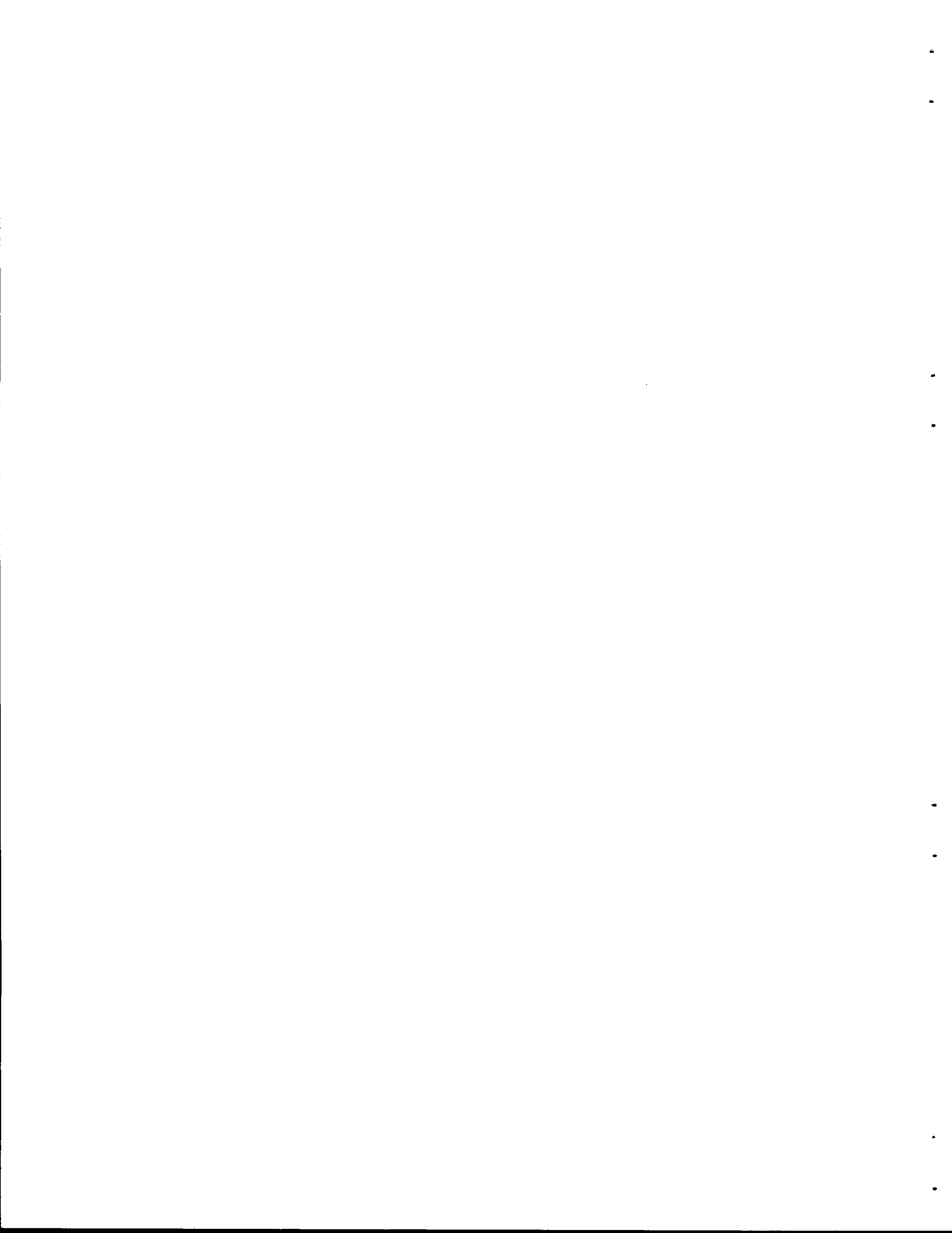
⁹H. W. Hoffman, Turbulent Forced-Convection Heat Transfer in Circular Tubes Containing Molten Sodium Hydroxide, ORNL-1370 (Oct. 3, 1952).

¹⁰H. W. Hoffman, Molten Salt Heat Transfer, ORNL CF-58-2-40 (Feb. 18, 1958).

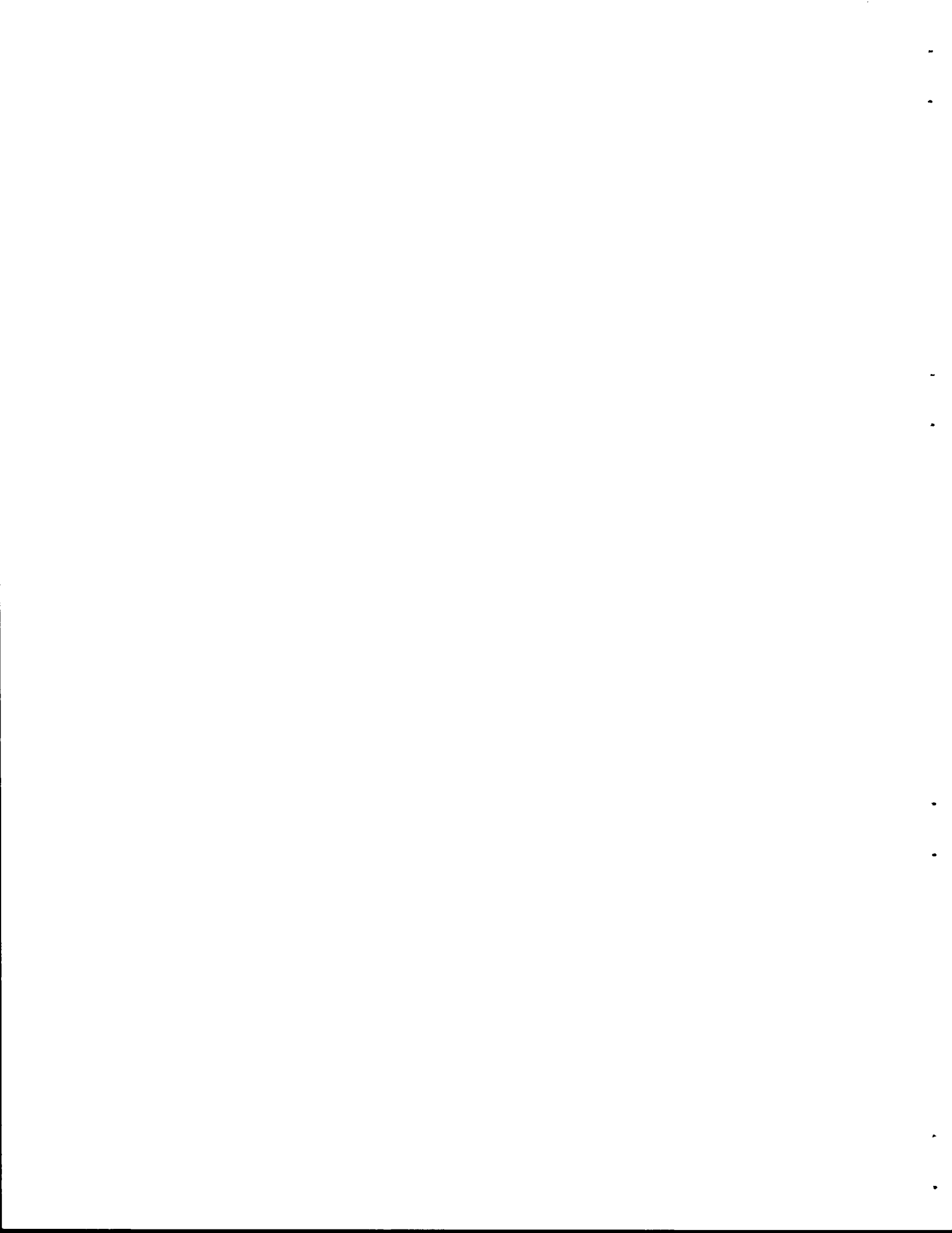
¹¹H. W. Hoffman and S. I. Cohen, Fused Salt Heat Transfer - Part III: Forced-Convection Heat Transfer in Circular Tubes Containing the Salt Mixture $\text{NaNO}_2\text{-NaNO}_3\text{-KNO}_3$, ORNL-2433 (Mar. 1, 1960).

¹²J. C. Amos, R. E. MacPherson, and R. L. Senn, Preliminary Report on Fused Salt Mixture No. 130 Heat Transfer Coefficient Test, ORNL CF-58-4-23 (Apr. 2, 1958).

¹³W. H. McAdams, Heat Transmission, 3d ed., p 219, McGraw-Hill, New York, 1954.



PART 2
MATERIALS STUDIES



2.1 METALLURGY

Dynamic Corrosion Studies

Thermal-Convection Loops

Test results for 16 thermal-convection loops (nine of INOR-8 and seven of Inconel) which were operated with fluoride mixtures are summarized in Tables 2.1.1 and 2.1.2. These tests mark the completion of all phases of the molten-fluoride corrosion program¹ dealing with thermal-convection experiments.

As may be seen in Table 2.1.1, the attack in five of the INOR-8 experiments, all of which operated for one year, was limited to surface roughening and pitting to a maximum depth of 1/2 mil. Figure 2.1.1 is representative of the attack found in these loops. One loop, 1224, which circulated salt 123 (NaF-LiF-BeF₂, 53-46-1 mole %) for 8760 hr at a maximum temperature of 1350°F, showed slightly greater attack, in the form of surface pitting to a maximum depth of 1 mil. Three loops, 1216, 1226, and 1244, exhibited attack in the form of shallow subsurface voids. The maximum depth of attack in loop 1216 was 1-1/2 mils, whereas in 1226 and 1244 the maximum depth of attack was limited to 1/2 mil. No attack, except for light roughening of the surfaces, was found in the cold legs of the loops. Also, examination of the cold regions revealed no deposits or other evidence of mass transfer.

An extremely thin corrosion film was found on the surfaces of several of these loops. As previously discussed,² filming has occurred in a majority of the thermal-convection tests which have operated for more than 3000 hr. Attempts are being made to identify the film, and a discussion of the results obtained is included in the subsequent section, "Analysis of Corrosion Film."

Intergranular and general subsurface voids formed in the hot-leg regions of all seven Inconel loops (Table 2.1.2). The attack ranged from depths of 4 to 7 mils in loops which operated at 1250°F; and from 7-1/2 to

¹J. H. DeVan, J. R. DiStefano, and R. S. Crouse, MSR Quar. Prog. Rep. Oct. 31, 1957, ORNL-2431, p 23.

²MSR Quar. Prog. Rep. July 31, 1959, ORNL-2799, p 50.

Table 2.1.1. Results of Metallographic Examination of INOR-8 Thermal-Convection Loops

Loop No.	Test Period (hr)	Maximum Fluid-Metal Interface Temperature (°F)	Salt No.*	Metallographic Examination	
				Hot-Leg Appearance	Cold-Leg Appearance
1224	8760	1350	123	Moderate surface roughening and pitting to 1 mil	No attack
1226	8760	1250	131	Moderate surface roughening, irregular corrosion film varying from 1/2 mil to 1 mil thick; there are scattered voids within this zone	Light surface roughening, with 1/2-mil corrosion film
1231	8760	1250	134	Light surface roughening and pitting to < 1/2 mil, corrosion film to < 1/2 mil	No attack
1238	8760	1350	134	Light surface roughening	No attack, very shallow corrosion film present
1244	8760	1250	135	Light surface roughening, moderate voids and pits to < 1 mil	No attack
1246	8760	1350	135	Light surface roughening	No attack
1233	8760	1250	133	No attack; very shallow corrosion film present	No attack
1240	8760	1350	133	Light surface roughening	No attack
1216	8760	1350	127	Moderate surface roughening and pitting to < 1/2 mil, light scattered intergranular voids to < 2 mils	No attack

*Compositions:

123	NaF-BeF ₂ -UF ₄ (53-46-1 mole %)	133	LiF-BeF ₂ -ThF ₄ (71-16-13 mole %)
127	LiF-BeF ₂ -ThF ₄ (58-35-7 mole %)	134	LiF-BeF ₂ -ThF ₄ -UF ₄ (62-36.5-1-0.5 mole %)
131	LiF-BeF ₂ -UF ₄ (60-36-4 mole %)	135	NaF-BeF ₂ -ThF ₄ -UF ₄ (53-45.5-1-0.5 mole %)

Table 2.1.2. Results of Metallographic Examination of Inconel Thermal-Convection Loops

Loop No.	Test Period (hr)	Maximum Fluid-Metal Interface Temperature (°F)	Salt No.*	Metallographic Examination	
				Hot-Leg Appearance	Cold-Leg Appearance
1225	8760	1250	123	Moderate surface roughening and pitting to 1 mil; moderate intergranular voids to maximum depth of 7 mils	Light surface roughening
1236	8760	1250	134	Light surface roughening and pitting to 1 mil; moderate intergranular voids to maximum depth of 5 mils	Light surface roughening and pitting to 1 mil
1237	8760	1350	134	Light surface roughening and pitting to 1 mil; heavy intergranular voids to maximum depth of 12 mils	Light surface roughening
1245	8760	1250	135	Moderate surface roughening and pitting to 1 mil; moderate intergranular voids to maximum depth of 6 mils	Light surface pits
1247	8760	1350	135	Moderate surface roughening; heavy general voids to maximum depth of 15 mils	Light surface roughening and pitting to 1/2 mil
1235	7789	1250	133	Light surface roughening and pitting to 1 mil; a few intergranular voids to maximum depth of 4 mils	A few pits to 1 mil
1239	8760	1350	133	Moderate surface roughening; moderate intergranular voids to maximum depth of 7-1/2 mils	Moderate surface roughening and pitting to 1 mil

*Compositions:

123 NaF-BeF₂-UF₄ (53-46-1 mole %)

133 LiF-BeF₂-ThF₄ (71-16-13 mole %)

134 LiF-BeF₂-ThF₄-UF₄ (62-36.5-1-0.5 mole %)

135 NaF-BeF₂-ThF₄-UF₄ (53-45.5-1-0.5 mole %)

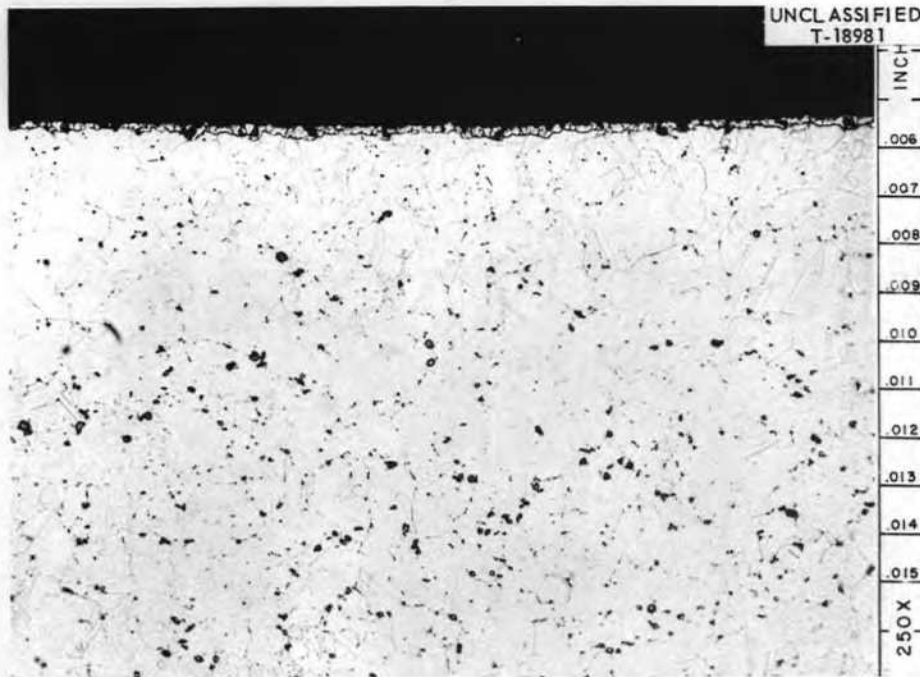


Fig. 2.1.1. Specimen Taken from Hot Leg of INOR-8 Thermal-Convection Loop 1231 at Point of Maximum Loop Temperature (1250°F). Loop was operated for one year with salt mixture $\text{LiF-BeF}_2\text{-ThF}_4\text{-UF}_4$ (62-36.5-1-0.5 mole %). Etchant: 3 parts HCl, 2 parts H_2O , 1 part 10% chromic acid.

15 mils in loops which operated at 1350°F. In the cold-leg regions, surface roughening and pitting occurred to a maximum depth of 1 mil. No evidence of mass-transfer deposits was found in the cold-leg regions.

Inconel Forced-Convection Loops

The status of Inconel forced-convection loops presently in operation is discussed in Sec 1.1 of this report. A report discussing the results for four Inconel loops (9377-1, -2, -3, and -4) was recently issued.³ The results are summarized in Table 2.1.3.

In general, the attack in all four loops followed the characteristic pattern for Inconel loops in contact with fluoride mixtures at higher temperatures; namely, the attack showed a strong dependence on the inside wall

³R. C. Schulze and J. H. DeVan, Examination of Inconel Forced Convection Loops 9377-1, 9377-2, 9377-3 and 9377-4, ORNL CF-60-4-54 (Apr. 6, 1960).

Table 2.1.3. Results of Metallographic Examination of Inconel Forced-Convection Loops

Loop No.	Test Period (hr)	Salt No.*	Maximum Fluid-Metal Interface Temperature (°F)	ΔT (°F)	Reynolds Number	Flow Rate (gpm)	Metallographic Examination
9377-1	3390	126	1300	200	1600	2.0	Intergranular voids to 7 mils
-2	3046	130	1300	200	3000	2	Intergranular voids to 8 mils
-3	8746	131	1300	200	3400	2.0	Intergranular and general sub-surface voids to 14 mils
-4	9574	130	1300	200	2600	1.75	Intergranular and general sub-surface voids to 15 mils

*Compositions:

- 126 LiF-BeF₂-UF₄ (53-46-1 mole %)
- 130 LiF-BeF₂-UF₄ (62-37-1 mole %)
- 131 LiF-BeF₂-UF₄ (60-36-4 mole %)

temperature.⁴ The attack in all the loops was limited to regions where the loop wall temperature exceeded 1200°F, and the depths of attack at these positions were quite consistent when viewed at similar time periods. As can be seen in Table 2.1.3, the rates of attack found at the 3000-hr time interval and the 9000-hr time interval were consistent within 1 mil.

INOR-8 Forced-Convection Loops

As discussed in Sec 1.1, eleven INOR-8 forced-convection loops have completed operation for one year or longer with fused fluoride mixtures. Operation of six of these loops has been terminated, and four of the six loops have been examined (Table 2.1.4). Loop 9354-5, which contained specimens of graphite in the hot-leg section, was discussed previously.⁵ As noted at that time, examination of this loop revealed no manifestations of corrosive attack beyond the start of a thin surface film.

Similar results (Table 2.1.4) were obtained from the recent examinations of loops MSRP-8 and -9, which circulated fluoride mixtures for 9633 and 9687 hr, respectively. Both loops appeared unattacked, except for the development of the thin surface layer. The extent of this layer can be seen in Figs. 2.1.2 and 2.1.3, which show the metallographic appearance of the hot-leg sections from the latter loops. (Results of chemical analyses of some of these layers are discussed in the next section.)

Considerably greater attack was noted, however, in loop 9354-1, which was terminated after 14,563 hr because of a leak which developed in the second heater leg. This loop encountered operational difficulties at two earlier periods, each of which necessitated suspension of operation and the replacement of loop components.⁶ As noted in Table 2.1.4, metallographic examinations of specimens removed from the hot-leg regions revealed general surface roughening and pitting to a maximum depth of 1-1/2 mils (Fig. 2.1.4). Attack elsewhere in the loop appeared negligible. In contrast, two specimens removed from the hot legs after 3000 hr (at the time of the first of the component failures) revealed no attack.

⁴W. D. Manly et al., "Metallurgical Problems in Molten Fluoride Systems," Second U.N. Intern. Conf. Peaceful Uses Atomic Energy, Geneva, 1958, paper A/Conf 15/P/1990, p 12 (June 1958).

⁵MSR Quar. Prog. Rep. July 31, 1959, ORNL-2799, p 55.

⁶MSR Quar. Prog. Rep. Oct. 31, 1958, ORNL-2626, p 56.

Table 2.1.4. Results of Metallographic Examination of INOR-8 Forced-Convection Loops

Loop No.	Test Period (hr)	Salt No.*	Maximum Fluid-Metal Interface Temperature (°F)	ΔT (°F)	Reynolds Number	Flow Rate (gpm)	Metallographic Examination (Maximum Attack)
9354-5	8,950	130	1300	200	3000	2.5	No attack**
MSRP-8	9,633	124	1300	200	4000	2	No attack**
MSRP-9	9,687	134	1300	200	2300	1.8	No attack**
9354-1	14,563	126	1300	200	2000	2.5	Heavy surface roughening and pitting to 1-1/2 mils (nickel deposits were found in the cooler coil)

*Compositions:

- 124 NaF-BeF₂-ThF₄ (58-35-7 mole %)
- 126 LiF-BeF₂-UF₄ (53-46-1 mole %)
- 130 LiF-BeF₂-UF₄ (62-37-1 mole %)
- 134 LiF-BeF₂-ThF₄-UF₄ (62-36.5-1-0.5 mole %)

**Corrosion film found on interior surfaces of the tubing.

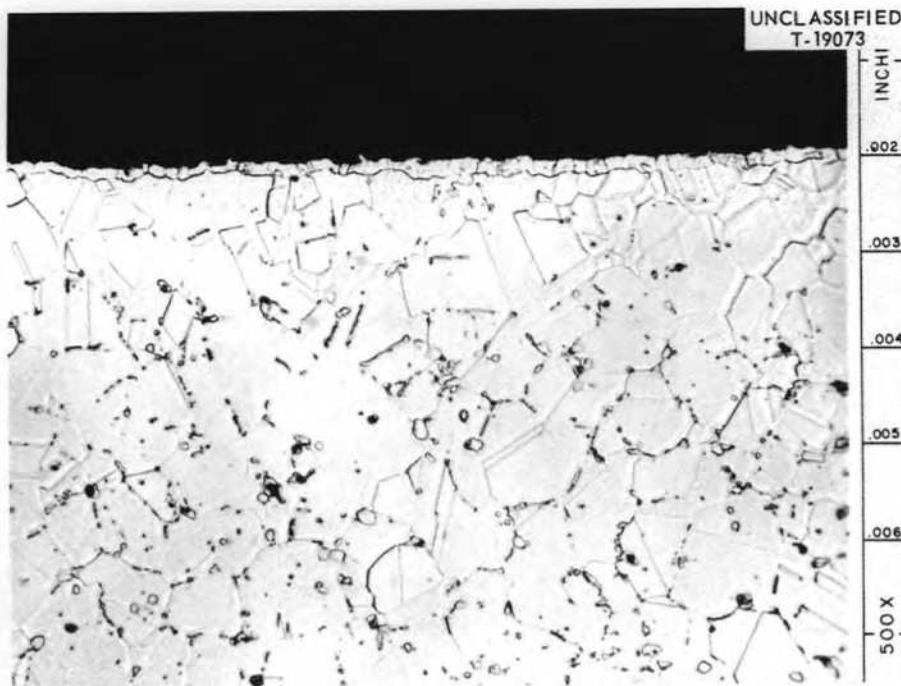


Fig. 2.1.2. Appearance of Specimen Removed from Point of Maximum Salt-Metal Interface Temperature (1300°F) of INOR-8 Forced-Convection Loop MSRP-8. Loop was operated for 9633 hr with salt mixture NaF-BeF₂-ThF₄ (58-35-7 mole %). Etchant: 3 parts HCl, 2 parts H₂O, 1 part 10% chromic acid.

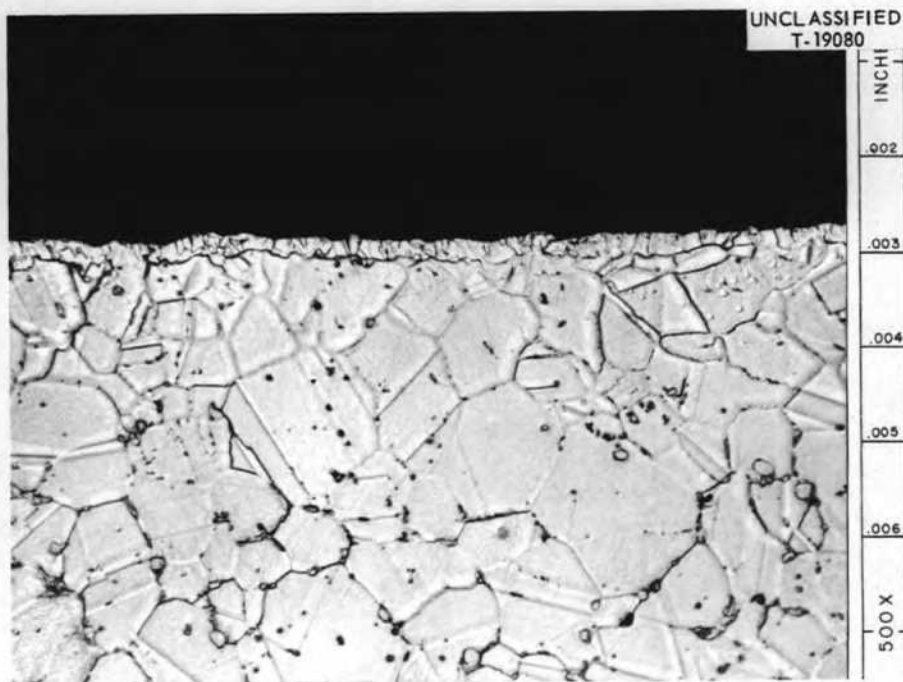


Fig. 2.1.3. Specimen Removed from Point of Maximum Salt-Metal Interface Temperature (1300°F) from INOR-8 Forced-Convection Loop MSRP-9. Loop was operated for 9687 hr with salt mixture LiF-BeF₂-ThF₄-UF₄ (62-36.5-1-0.5 mole %). Etchant: 3 parts HCl, 2 parts H₂O, 1 part 10% chromic acid.

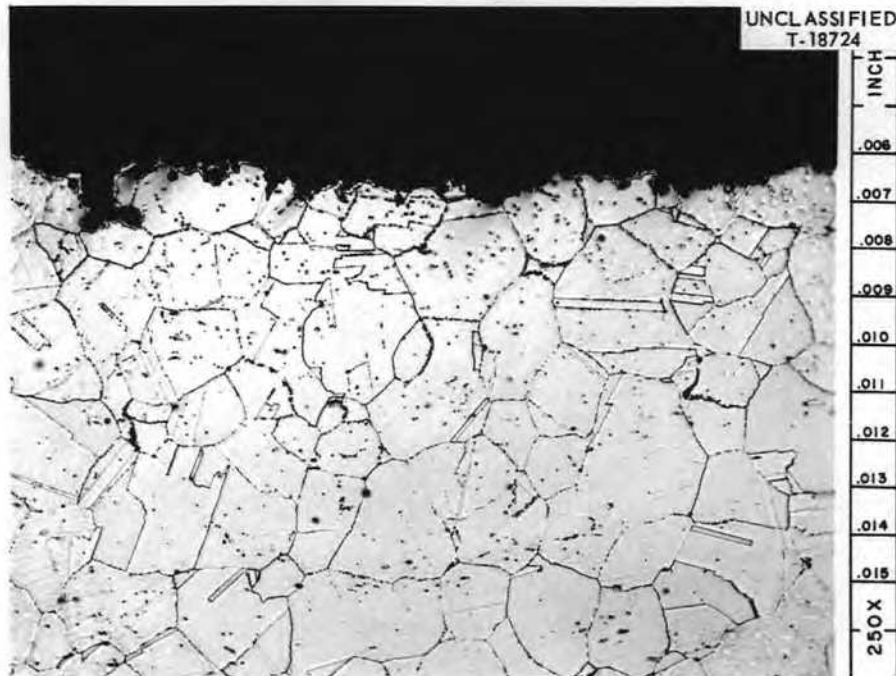


Fig. 2.1.4. Specimen Removed from INOR-8 Forced-Convection Loop 9354-1 at Point of Maximum Salt-Metal Interface Temperature (1300°F) Showing Maximum Attack Found. Loop operated for 14,563 hr with salt mixture LiF-BeF₂-UF₄ (53-46-1 mole %). Etchant: 3 parts HCl, 2 parts H₂O, 1 part 10% chromic acid.

Examinations of the cold-leg regions at the end of this test revealed magnetic metal crystals loosely adherent to the cold-leg wall. This deposit was obtained for chemical analyses by sectioning the length of tubing over which it appeared into approximately 6-in. segments and then scraping out the deposited material. The lengths of tubing and the quantities and compositions of material removed are listed in Table 2.1.5. The deposit was composed predominantly of nickel and contained only minor amounts of iron and chromium, with the greatest concentration of chromium being found where the material was first precipitated from the salt. Molybdenum, which comprised 17 wt % of the base metal, was present in only insignificant concentrations. Altogether the weight of the deposit totaled 22 g.

The abnormally high rate of attack and mass transport of nickel in this loop necessarily implies that an extremely effective oxidant was made available to the salt circulating in the loop. An indication of the nature of this oxidant was afforded by after-test salt analyses, which indicated

Table 2.1.5. Chemical Analysis of Deposit*

Specimen	Length of Tubing (in.)	Weight of Deposit (g)	Weight %			Mo (ppm)
			Ni	Cr	Fe	
1	11-1/8	1.9000	88.2	7.33	0.23	7035
2	42-1/8	4.4994	94.3	1.22	1.34	6380
3	18	4.4134	92.5	1.26	1.37	6215
4	32-7/8	4.0994	92.5	1.95	1.39	7850
5	24-5/8	7.1898	94.3	0.68	0.81	5690

*Deposit contained small amounts of salt residue.

that a relatively large percentage of UF_4 had been converted to UO_2 during the test. The production of UO_2 most probably was affected by H_2O contamination which entered the loop during one or more of the tubing failures. Reaction of this contaminant with UF_4 would also produce HF , which is potentially capable of oxidizing nickel as well as other constituents of INOR-8.

Analysis of Corrosion Film. - Chemical and metallurgical studies were undertaken to investigate the nature and causes of the thin corrosion films observed in long-term INOR-8 corrosion loops, as discussed above. The film appears as a continuous second phase which extends below the exposed surfaces to a thickness of 1/2 mil or less. No transition or diffusion zone has been evident between the film and the base metal (Figs. 2.1.1, 2.1.2, and 2.1.3). In thermal-convection loops the film has been observed both in hot- and cold-leg specimens; in forced-convection loops it has been found only along the tubing between the pump exit and the end of the second heater leg.

Comparative hardnesses of the film and parent metal of one of the specimens were recently determined by using a Bergman microhardness tester with a 1-g load. The portion of the film examined was approximately 1/3 mil thick and was removed from the point of maximum salt-metal interface temperature of INOR-8 forced-convection loop 9354-5.⁷ On the basis of the

⁷MSR Quar. Prog. Rep. July 31, 1959, ORNL-2799, p 55.

1-g load, the film was found to have a DPH (diamond pyramid hardness) of 518, and the DPH for the parent metal was 269. A check of the base metal using the Tukon hardness tester with a 200-g load indicated a DPH of 218. Although the numbers based on the Bergman tester appear to be slightly high, the values obtained demonstrate that the film is approximately twice as hard as the parent metal, as shown in Fig. 2.1.5.

Since none of the films have been more than 1/2 mil thick, it has been extremely difficult to determine their chemical composition. However, qualitative analyses of these films were recently carried out with the aid of C. E. Zachary of the Metallographic Group. These analyses were made on material "scrubbed" from the inside surfaces of the tubes with a corundum slurry, the specimens being weighed before and after to determine the amount of material removed. The resulting mixture of slurry and metal, along with an unused sample of the slurry as a blank, was then submitted for spectrographic analysis.

Analyses obtained for several different specimens of this surface film are listed in Table 2.1.6. The films were composed primarily of nickel and

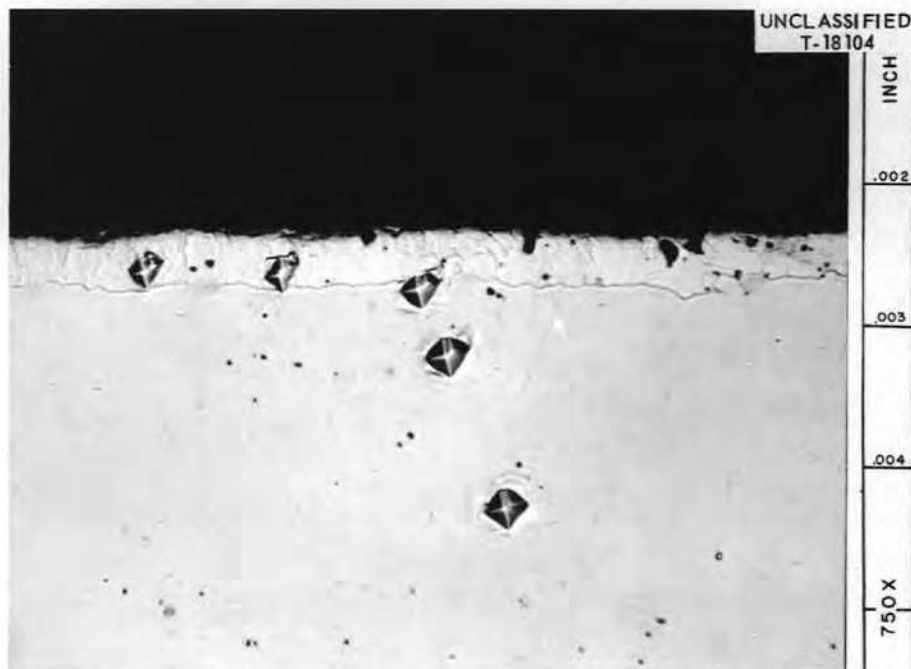


Fig. 2.1.5. Hardness Measurements Made on Specimen Removed from Point of Maximum Salt-Metal Interface Temperature (1300°F) of INOR-8 Forced-Convection Loop 9354-5.

Table 2.1.6. Spectrographic Analyses of Surface Films

Loop from Which Specimen Was Removed	Location	Approximate Temperature of Specimen (°F)	Salt Circulated	Spectrographic Analysis (wt %)			
				Ni	Cr	Fe	Mo
1226	Cold leg	1078	131	62	4.3	29	4.7
9354-5	End of first heater leg	1269	130	80	1.5	14.5	4
9354-5	End of second heater leg	1296	130	70.6*			29.4*
MSRP-7	End of second heater leg	1300	133	67.9*			32.1*

*These analyses assume Ni + Mo = 100%.

contained smaller amounts of chromium, iron, and molybdenum. At present, there is no apparent correlation of the film composition with any of the test loop variables (temperature, time, salt, etc.). Interestingly, however, analyses of the specimen removed from the end of the second heater leg of forced-convection loop 9354-5 showed it to have a composition approximately the same as the β -phase (Ni_4Mo) of the Ni-Mo system.

Graphite Brazing Studies

The development of techniques for brazing graphite to itself and to metals is of continuing interest for molten-salt power reactor systems with a high-breeding-ratio potential. A study of these procedures has been under way during the past year, and the progress has been reported in the last few progress reports.^{8,9} Recent findings are summarized in this report.

The promising brazing characteristics of the 48% Ti-48% Zr-4% Be brazing alloy were discussed in the last report.⁹ In order to demonstrate the general feasibility of brazing assemblies of graphite tubes to metal headers, a demonstration assembly was fabricated with this alloy. An exploded view of the assembly is shown in Fig. 2.1.6.

The first step was to braze the CT-158 fine-grained extruded graphite tubing to a molybdenum ring using the Ti-Zr-Be alloy. The molybdenum ring was used as a transition layer between the graphite and the INOR-8 base plate. Because of its low coefficient of thermal expansion and its ability to absorb shearing stresses, the molybdenum acts as a buffer and tends to minimize the possibility of shearing in the graphite by stresses which result from the large difference in thermal expansion between graphite and INOR-8.

The final assembly was made by brazing the molybdenum in the graphite-molybdenum subassemblies to the INOR-8 plate with a commercially available alloy, Coast Metals No. 53 (Ni-Cr-B-Si-Fe). The completed assembly is shown in Fig. 2.1.7.

⁸MSR Quar. Prog. Rep. July 31, 1959, ORNL-2799, p 71-72.

⁹MSR Quar. Prog. Rep. Oct. 31, 1959, ORNL-2890, p 33-35.

UNCLASSIFIED
Y-32366

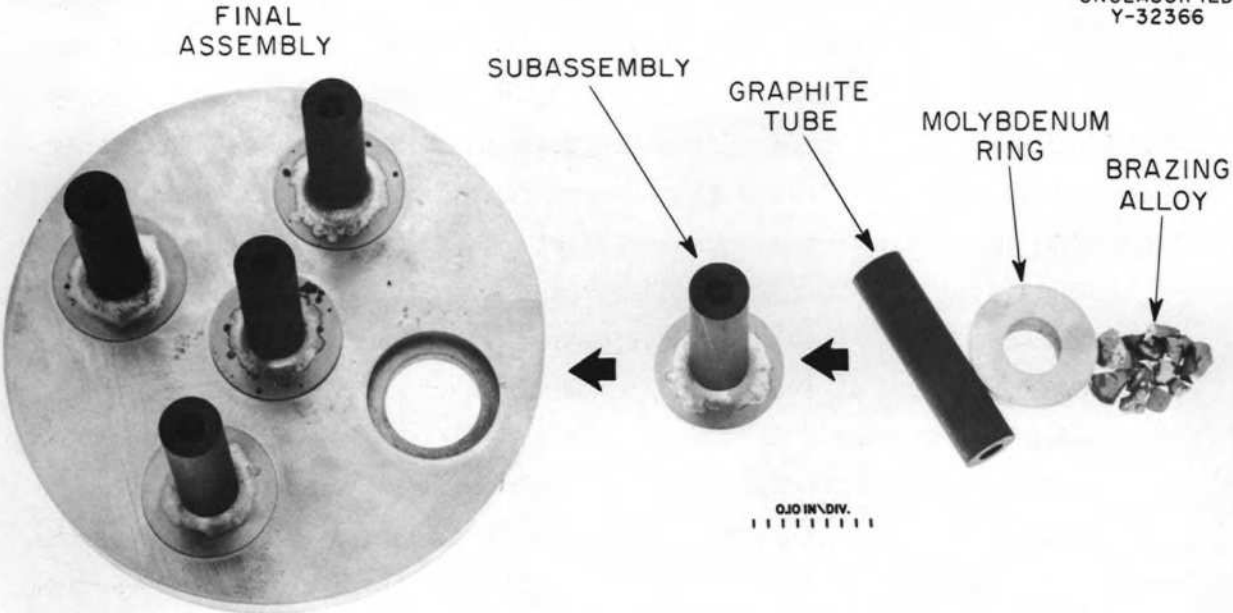


Fig. 2.1.6. Sequence for Assembly of Graphite Tube to INOR-8 Plate.

UNCLASSIFIED
Y-33370

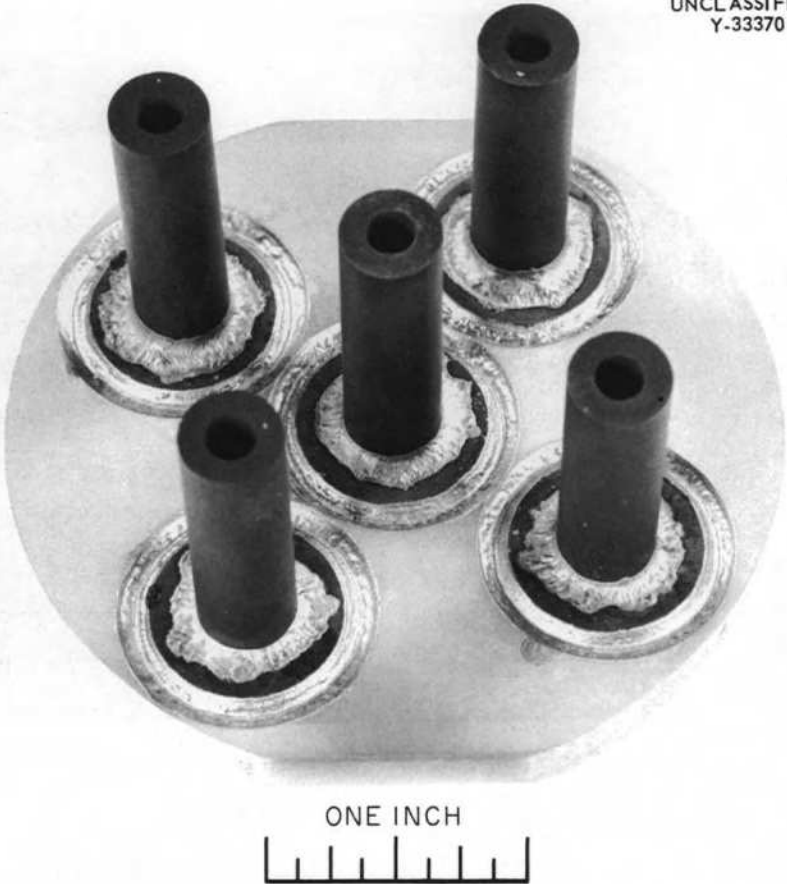


Fig. 2.1.7. Completed Assembly of Graphite Tube to INOR-8 Plate.

The utilization of the Ti-Zr-Be alloy for molten-salt reactor applications has been shown to be severely limited by virtue of its poor corrosion resistance to fluoride salts.⁹ A brazing-alloy development program was subsequently initiated for the express purpose of obtaining brazing alloys which wet and flow on graphite at reasonable brazing temperatures (< 1300°C) and which are corrosion resistant to the fused salts. The corrosion-resistant 82% Au-18% Ni alloy¹⁰ was selected as a potential starting material, and it may find use in certain selected applications. Corrosion-resistant carbide-forming elements such as tantalum or molybdenum were added to promote wetting.

Promising ternary compositions were selected through an analysis of the available binary phase diagrams of the Au-Ni-Ta and Au-Ni-Mo systems. To date, 10-g buttons of approximately forty Au-Ni-Ta and thirty Au-Ni-Mo alloys have been arc-cast and evaluated. Figures 2.1.8 and 2.1.9, respectively, indicate the compositions of these alloys. The flow behavior, in vacuum, of small fragments of alloys in the Au-Ni-Mo system on graphite at 1300°C is shown in Fig. 2.1.10.

Flowability studies have been conducted with these alloys on both graphite-to-graphite joints and graphite-to-molybdenum joints. The alloy compositions in the two systems which flow well on graphite-to-graphite joints are enclosed by dashed lines in Figs. 2.1.8 and 2.1.9. However, alloys containing lower percentages of carbide-forming elements flow adequately on graphite-to-molybdenum joints and are more ductile than those required for graphite-to-graphite joints.

The 35% Au-35% Ni-30% Mo alloy has been investigated in view of its application for joints of both types. Figure 2.1.11 shows joints containing low-permeability graphite tubes butt-brazed to a 1/4-in.-thick molybdenum plate and to an AGOT graphite plate. The alloy was preplaced around the outside diameter of the graphite tubes before induction brazing. Full penetration of the braze through the joints and subsequent filleting on the inside diameters can be seen. A photomicrograph of a graphite-to-molybdenum joint brazed with this alloy is shown in Fig. 2.1.12.

¹⁰E. E. Hoffman *et al.*, An Evaluation of the Corrosion and Oxidation Resistance of High-Temperature Brazing Alloys, ORNL-1934 (October 1956).

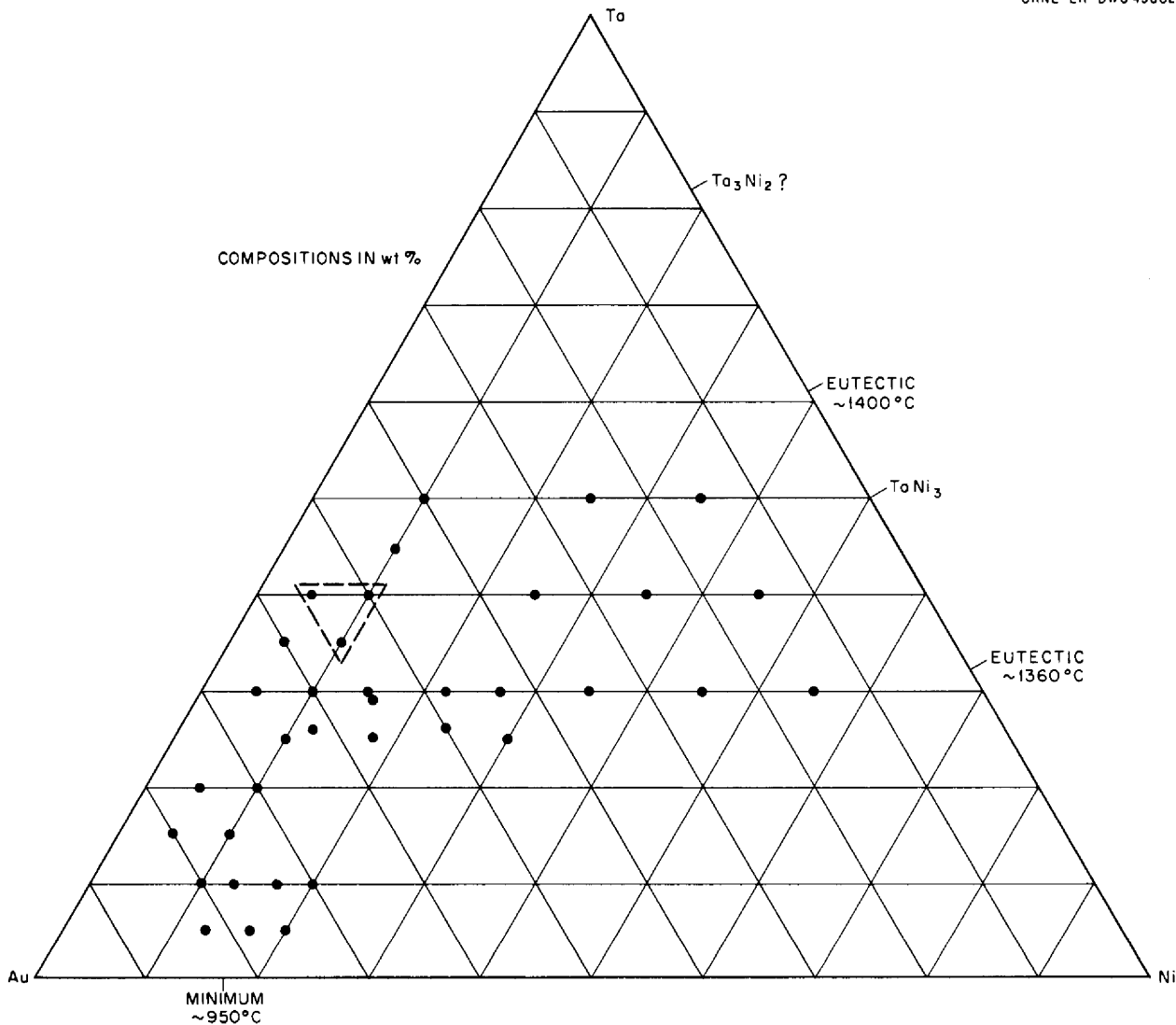


Fig. 2.1.8. Compositions of Experimental Au-Ni-Ta Alloys Prepared for Graphite Brazing Studies.

Preliminary thermal-cycling and leak-test studies, coupled with metallographic examinations, indicate that those alloys which flow best on graphite are brittle and tend to crack, as shown in Fig. 2.1.13. The brittleness of these alloys is also evidenced by their relative ease of crushing as arc-melted buttons. It should be possible, however, to obtain adequate flow on graphite-to-molybdenum joints with alloys of improved ductility by reducing the molybdenum or tantalum contents. This possibility is being investigated.

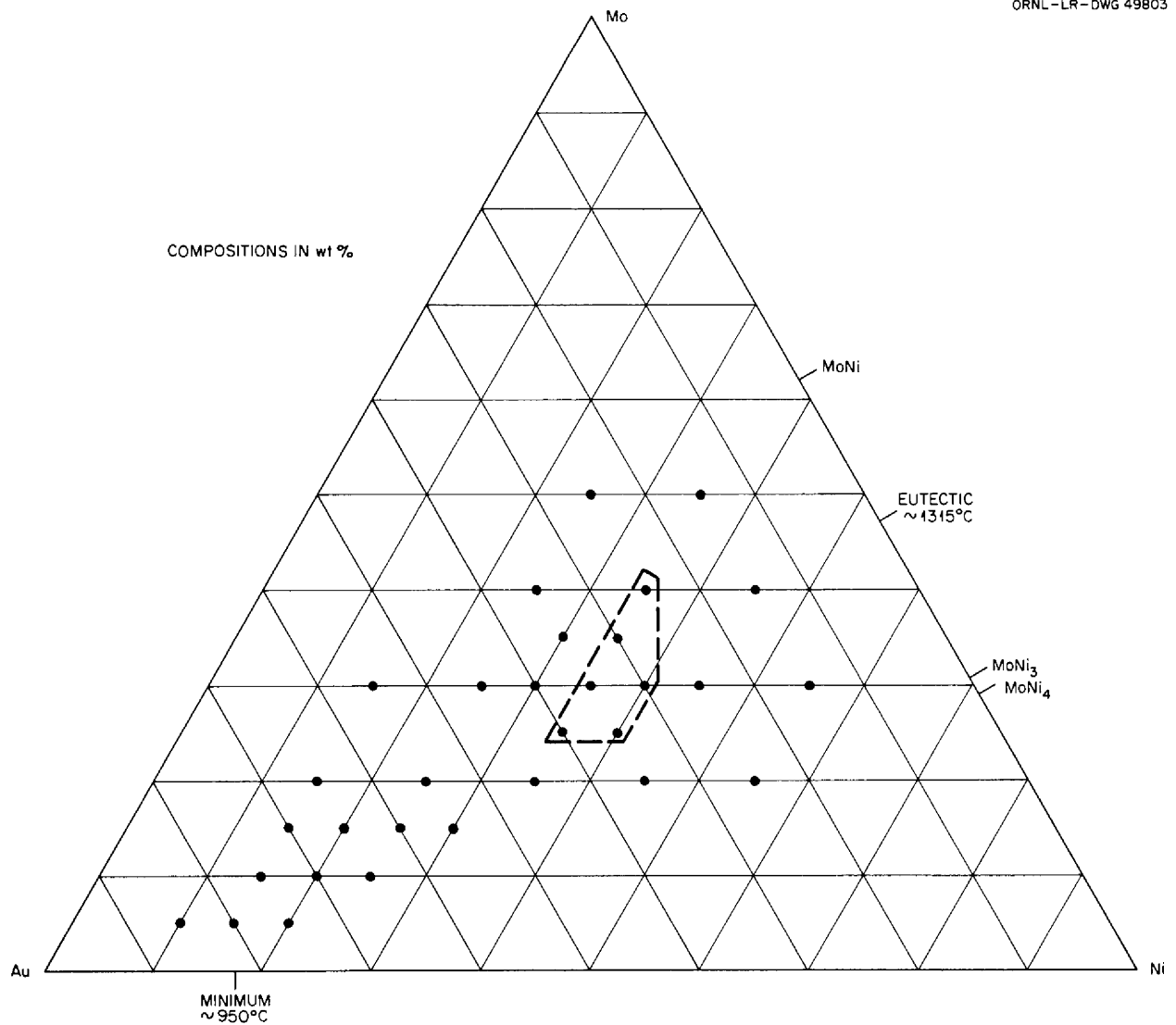


Fig. 2.1.9. Compositions of Experimental Au-Ni-Mo Alloys Prepared for Graphite Brazing Studies.

The porous graphites, such as type AGOT, have greater joint strengths, as evidenced by the mechanical testing of T-joint specimens. Specimens of AGOT graphite fail deep in the parent material, while low-permeability graphite specimens fail at the graphite-braze-metal interface. The deep penetration of brazing alloy into the pores of the AGOT graphite is shown in Fig. 2.1.14; no evidence of this condition has been observed in the low-permeability material. The small-sized pores in this type of graphite reduce the possibility of a mechanical "keying" action and reduce the braze-graphite contact area.

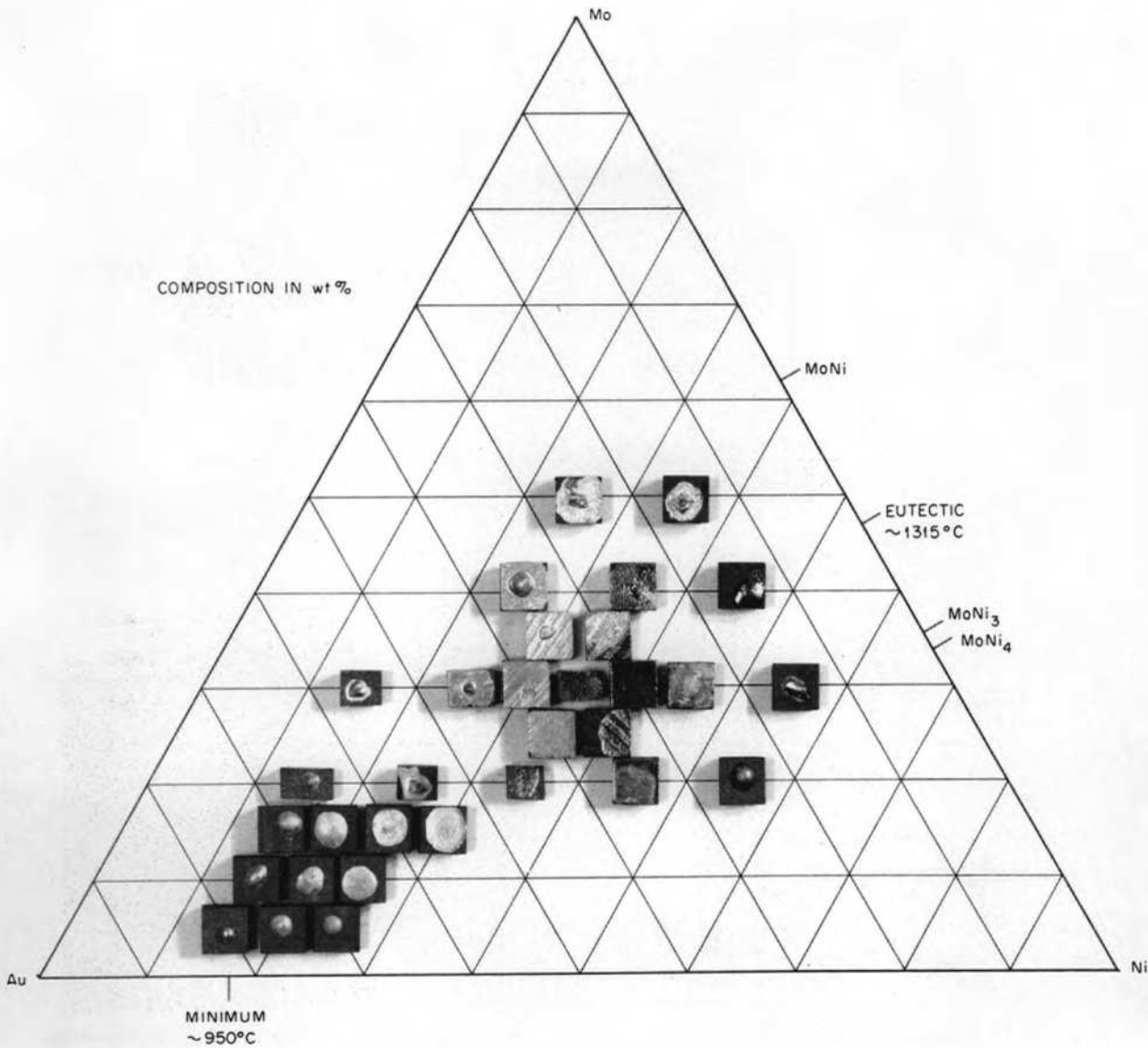


Fig. 2.1.10. Flow Behavior of Au-Ni-Mo Alloys on Graphite at 1300°C.

Remedies for this problem seem to lie in improved joint designs and/or the development of new brazing alloys with stronger bonding characteristics and lower coefficients of thermal expansion. Studies along these lines are being made.

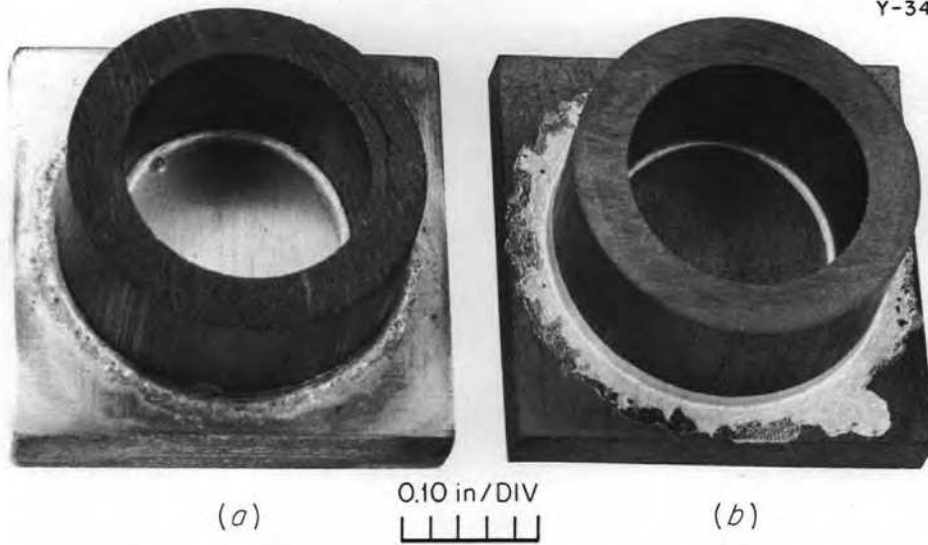


Fig. 2.1.11. (a) Type RLM-24 Graphite Tubing Induction-Brazed to Molybdenum with 35% Au-35% Ni-30% Mo. (b) Type RLM-24 Graphite Tubing Induction-Brazed to Type AGOT Graphite with 35% Au-35% Ni-30% Mo.

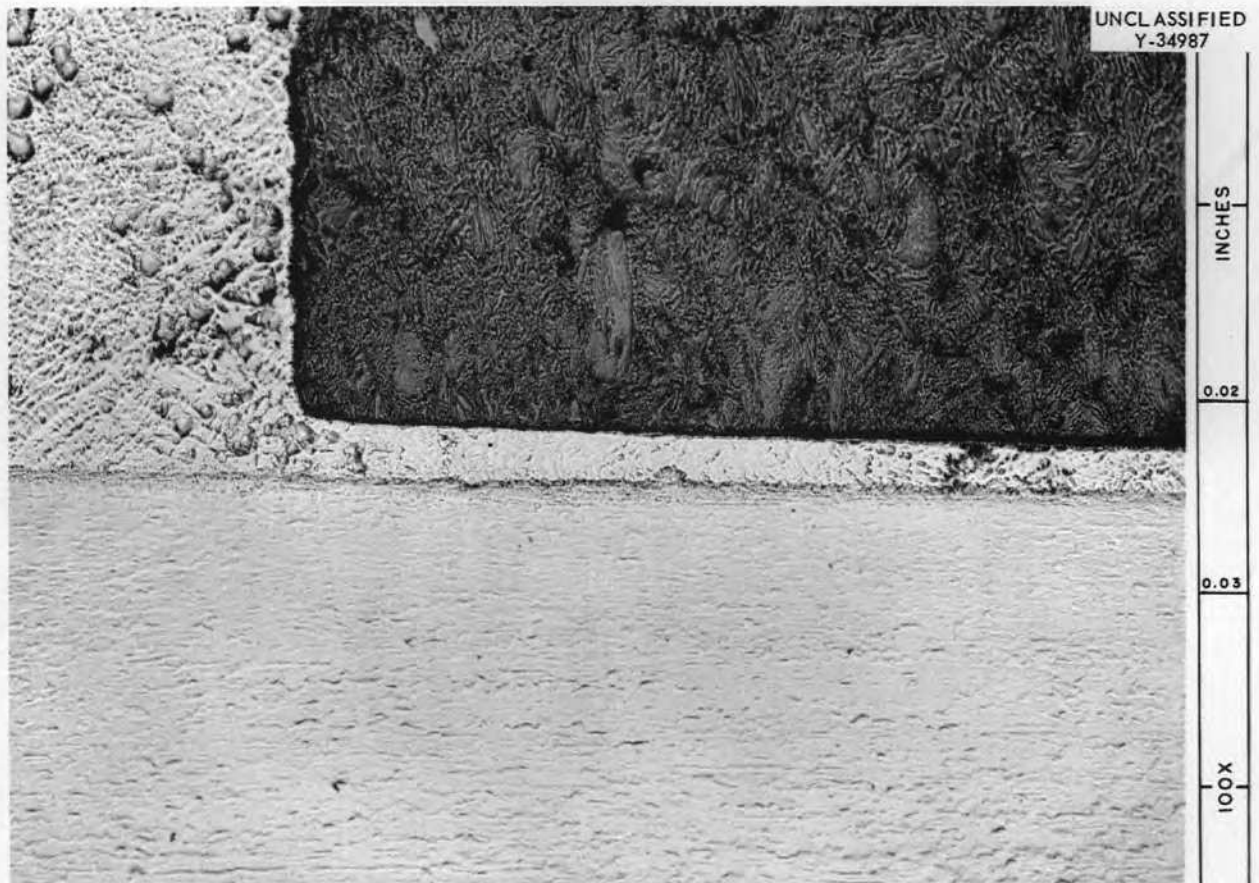


Fig. 2.1.12. Photomicrograph of Type RLM-24 Graphite Tubing Induction-Brazed to Molybdenum with 35% Au-35% Ni-30% Mo.

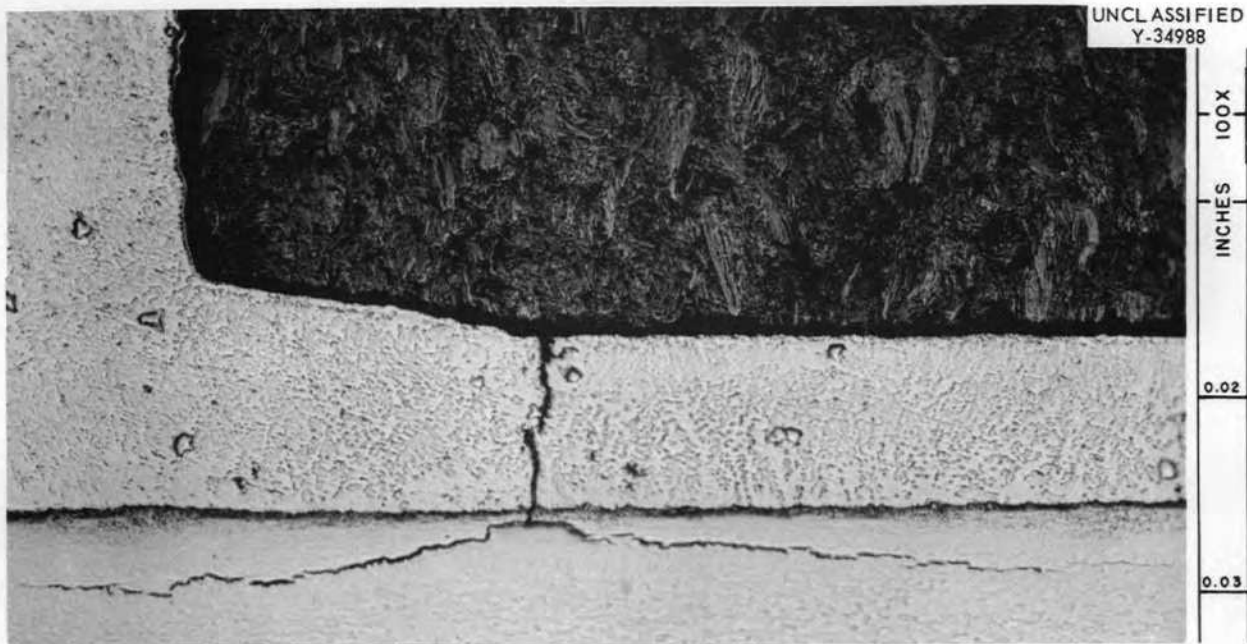


Fig. 2.1.13. Photomicrograph of Type RLM-24 Graphite Tubing Induction-Brazed to Molybdenum with 35% Au-35% Ni-30% Mo and Thermally Cycled 16 Times from 700°C to Room Temperature.

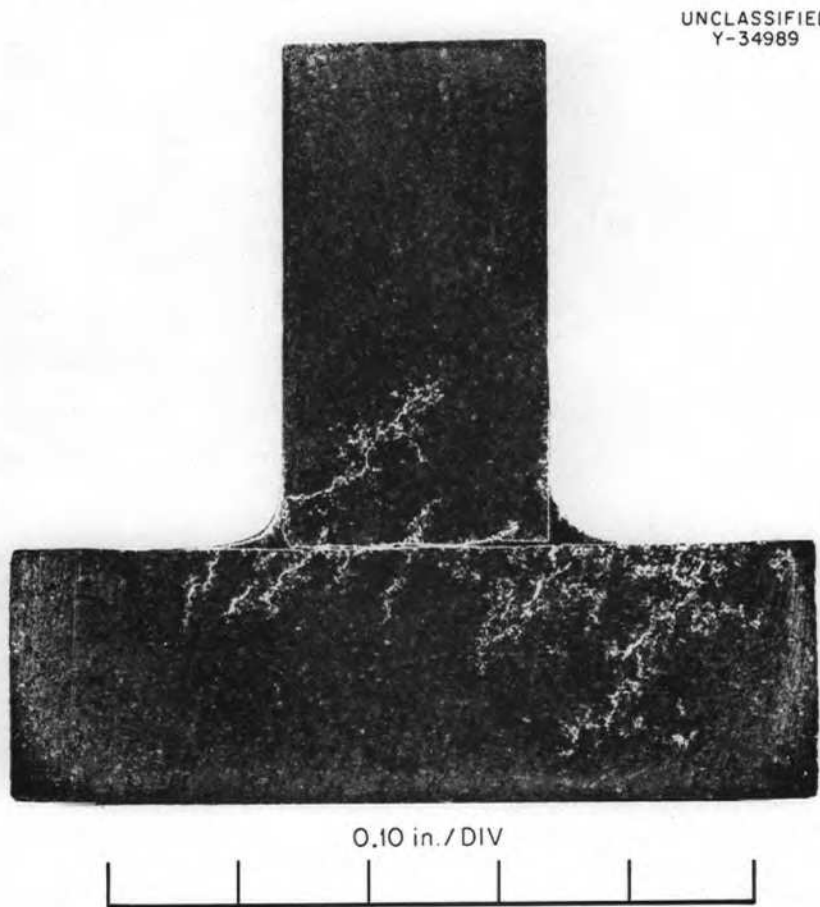


Fig. 2.1.14. Photomacrograph of Type AGOT Graphite-to-Graphite T-Joint.

General Corrosion Studies

Permeation of Graphite by Molten Salts

The use of unclad graphite as a moderator in a molten-salt reactor requires that not more than a small percentage of the graphite pore space be filled with salt. To ensure this condition, a test program¹¹ has been in progress to study the permeation of various potential grades of graphite by molten salt (BULT 14-.5U) at 1300°F and for various times and pressures.

Thirty-one grades of graphite have been tested under the conditions described above. All grades were manufactured as low-permeability grades except seven: CCN, CEY-B, R-0013, GT-123, SM-1, TSF, and AGOT. Results of the screening tests are summarized in Table 2.1.7. There are now four grades, B-1, S-4-LB, GT-123-82, and CS-112-S, that meet the permeation specification, under the screening-test conditions, that less than 0.5% of the bulk volume of graphite be filled with salts. These results are from specimens taken from single pieces of graphite that were relatively small.

In an attempt to determine the effect of pressure on permeation, 20 grades of graphite that were available at the time this test was assembled were screened at a lower pressure. Three or more specimens of each of the 20 grades were exposed simultaneously for 100 hr to LiF-BeF₂-ThF₄-UF₄ (67-18.5-14-0.5 mole %, BULT 14-.5U) at 1300°F (704°C) and 95 psig, a potential reactor fluoride-salt pressure. The results of this test are compared in Table 2.1.8 with those obtained from previous tests in which the pressure was 150 psig. This test suggests that if the reactor pressure were 95 psig, four additional grades, CT-150, CEY-1350, CT-158, and CEY-G, might be brought within the MSRP specification.

The grades of graphite that showed the greatest reductions in quantity of salt permeation as a result of the lower pressure have the highest percentage of small pores comprising their total accessible voids. These graphites also are those that were fabricated as relatively small shapes.

Under the assumption that other reactor conditions will not significantly modify permeation, it appears that for some grades of graphite,

¹¹W. H. Cook and D. H. Jansen, A Preliminary Summary of Studies of INOR-8, Inconel, Graphite and Fluoride Systems for the MSRP for the Period May 1, 1958 to Dec. 31, 1958, ORNL CF-59-1-4, p 1-20.

Table 2.1.7. Permeation of Various Grades of Graphite by LiF-BeF₂-ThF₄-UF₄ (67-18.5-14-0.5 mole %, BULT 14-5U) at 150 psig

Test conditions:
 Temperature: 1300°F (704°C)
 Exposure period: 100 hr

All densities and percentages are averages of three with the exception of those with numerical superscripts, which denote the number of values averaged

Graphite Grade	Graphite Apparent Density (g/cc)	Bulk Volume of Graphite Permeated (%)	Shape	Specimen Dimensions, Nominal (in.)		
				Diameter or OD	ID	Length(s)
B-1	1.91	0.0 ₂	Rod	0.90 ^a		0.50
S-4-LB	1.90 ⁽⁴⁾	0.2 ⁽⁴⁾	Block	0.50		0.75
GT-123-82 ^b	1.91 ⁽⁶⁾	0.3 ⁽⁶⁾	Rod	0.50 ^a		1.50
CS-112-S	1.89 ⁽⁴⁾	0.5 ⁽⁴⁾	Rod	0.90 ^a		0.50
RH-1	1.89 ⁽⁶⁾	0.6	Rod	0.90 ^a		0.50
CEY-1350	1.90	0.7	Pipe	1.24 ^a	0.86 ^a	0.25
CEY-G	1.88	0.9	Pipe	1.25 ^a	0.86 ^a	0.50
S-4-LA	1.89 ⁽⁴⁾	1.0 ⁽⁴⁾	Block	0.50		0.75
CEY	1.91 ⁽⁶⁾	1.0 ⁽⁶⁾	Pipe	1.24 ^a	0.85 ^a	0.50, 0.25
CT-150	1.80	1.8	Pipe	0.53 ^a	0.26 ^a	1.50
R-0009 ^b	1.92 ⁽⁶⁾	1.9 ⁽⁶⁾	Block	0.50		1.50
CEY-82 ^b	1.87	1.9	Pipe	1.25 ^a	0.86 ^a	0.50
R-4 ^b	1.92 ⁽¹³⁾	2.0 ⁽¹³⁾	Block	0.50		1.50
R-0009 RG ^b	1.90 ⁽⁶⁾	2.6 ⁽⁶⁾	Block	0.50		1.50
CT-158 ^b	1.76 ⁽⁴⁾	3.6 ⁽⁴⁾	Pipe	0.40 ^a	0.19 ^a	1.50
186 ^b	1.86 ⁽⁶⁾	3.8 ⁽⁶⁾	Bar	0.50		1.50
CCN ^b	1.92	4.2	Block	0.50		1.50
CEY-B ^b	1.79	4.3	Pipe	1.25 ^a	0.86 ^a	0.50

Table 2.1.7 (continued)

Graphite Grade	Graphite Apparent Density (g/cc)	Bulk Volume of Graphite Permeated (%)	Shape	Specimen Dimensions, Nominal (in.)		
				Diameter or OD	ID	Length(s)
S-4 ^b	1.85	4.8	Block	0.50		1.50
R-0025 ^c	1.87 ⁽²⁴⁾	5.7 ⁽²⁴⁾	Block	0.50		1.50, 0.50
RLM-24 ^d	1.83 ⁽⁶⁾	5.7 ⁽¹³⁾	Pipe	0.50		1.50, 0.50
ATJ-82 RG ^b	1.83	6.4	Block	0.50		1.50
R-0013 ^b	1.87 ⁽⁶⁾	6.6 ⁽⁶⁾	Block	0.50		1.50
MH4LM-82	1.81 ⁽²⁴⁾	8.2 ⁽²⁴⁾	Block	0.50		1.50, 0.50
CS-82 RG ^b	1.80	8.1	Block	0.50		1.50
GT-123	1.79	8.9	Rod	0.50		1.50
ATL-82	1.80	10.8	Block	0.50		1.50
MH4LM	1.76	11.4	Block	0.50		1.50
SM-1	1.72	13.9	Block	0.50		1.50
AGOT ^b	1.68 ⁽¹⁷⁾	13.9 ⁽¹⁷⁾	Bar	0.50		1.50, 0.50
TSF ^b	1.67	14.4	Bar	0.50		1.50

^aThese are the original dimensions of the graphite as manufactured.

^bThese were previously reported in MSR Quar. Prog. Oct. 31, 1959, ORNL-2890, p 44.

^cSpecimens for R-0025 were taken from a piece 39 in. in diameter and 11 in. long.

^dSpecimens for RLM-24 were taken from the walls of a 5-in.-OD, 3-5/8-in.-ID, 26-in.- long pipe.

Table 2.1.8. Permeation of Various Grades of Graphite by LiF-BeF₂-ThF₄-UF₄ (67-18.5-14-0.5 mole %, BULT 14-.5U) at 95 and 150 psig

Test conditions:

Temperature: 1300°F (704°C)

Exposure period: 100 hr

Graphite Grade	Bulk Volume of Graphite Permeated (%) ^a		P95:P150 ^c
	At 95 psig	At 150 psig ^b	
CT-158	0.04	3.6	0.0 ₁
CT-150	0.3	1.8	0.2
CEY-1350	0.2	0.7	0.3
CEY-G	0.3	0.9	0.3
CEY-82	1.0	1.9	0.5
CS-82 RG	5.3	8.1	0.6
CEY-B	3.0	4.3	0.7
GT-123	6.6	8.9	0.7
GT-123-82	0.2 ₅	0.3	0.8
MH4LM	8.9	11.4	0.8
R-0013	5.4	6.6	0.8
SM-1	12.2	13.9	0.9
S-4	4.4	4.8	0.9
ATL-82	10.6	10.8	1.0
ATJ-82 RG	6.3	6.4	1.0
R-0009 RG	2.6	2.5	1.0
R-4	2.3	2.2	1.0
186	4.1	3.8	1.1
AGOT	16.1	14.6	1.1
R-0009	2.2	1.8	1.2

^aEach value is an average of three or more values.

^bThese data have been reported previously; they are included here for comparison purposes.

^cThe ratio of the per cent of the bulk volume of the graphite permeated by BULT 14-.5U at 95 psig to that at 150 psig.

salt permeation can be decreased appreciably by proper pressure reductions. However, a specific grade or grades of graphite chosen for a reactor should be thoroughly investigated, since the low-permeability grades are still relatively new.

Studies of fluoride permeation of graphite as a function of time have been initiated with AGOT, S-4, and R-4 grades, which were chosen because they are in plentiful supply. A partially completed series of tests indicates that a 1-hr exposure of these grades to BULT 14-.5U at 1300°F (704°C) under a pressure of 150 psig produced the same degree of permeation as did 100-hr exposures under like conditions.

Grade R-4 graphite is one in which relatively large, accessible voids were partially filled with carbon to decrease its permeability. The graphite was impregnated with pitch, and the pitch was thermally converted to amorphous carbon. Metallographic examinations indicated that the original voids were approximately two-thirds filled with carbon. An exploratory test was made to determine the relationship of permeability vs location in this grade of graphite.

A standard permeation screening test as described above was made on four specimens from the original surface of the graphite and three specimens approximately 1/2 to 1 in. away from this surface. The specimens were nominally 1/2 in. in diameter and 1-1/2 in. long. The bulk volume of the graphite permeated by BULT 14-.5U averaged 1.4% (0.7 to 2.7%) for specimens that were located at the surface and 3.0% (2.3 to 4.2%) for those not at the surface. More tests would be necessary to fully evaluate the variations in the fluoride-salt permeability of grade R-4. However, these data indicate that for the impregnation technique used the lowest permeability values extend over short distances, 1/2 to 1 in. The average percentage for all seven specimens was 2.1, which compares well with a 1.9 average value in previous tests for six similar specimens from random positions.

Grade AGOT graphite was permeated with molten bismuth as a pretreatment to a standard fuel permeation test.¹² The purpose of the bismuth permeation was twofold: (1) to determine if the bismuth would occupy the pore spaces in the graphite and exclude fuel from these pores and (2) to

¹²MSR Quar. Prog. Rep. Oct. 31, 1959, ORNL-2890, p 43.

determine if the bismuth which had permeated the graphite pores would be retained within them during reactor temperature and pressure cycles. The latter was important not only in maintaining resistance to salt permeation but also in preventing contact of the bismuth with the nickel-base alloy container, since nickel-base alloys have limited corrosion resistance to bismuth at temperatures as low as 520°F (270°C).¹³

Results of the standard fuel-permeation test with the bismuth-impregnated graphite showed that the bismuth suppressed the permeation by fuel but did not eliminate it. Chemical analyses of six successive 1/16-in.-thick layers machined from the graphite specimen showed a decreasing uranium content as shown in Table 2.1.9.

Bismuth was not completely retained in the graphite pores during the fuel-permeation test, and this resulted in some attack of the Inconel container by the bismuth.

Bismuth impregnation will be tested to determine its effectiveness in inhibiting fuel permeation of low-permeability small-pore-diameter graphite, as the graphite becomes available.

¹³Liquid Metals Handbook, p 176, June 1952.

Table 2.1.9. Effect of Impregnation with Bismuth in Inhibiting Fuel Permeation of AGOT Graphite

Pretreatment conditions: molten bismuth at 1022°F (550°C),
200 hr, 125 psig
Fuel-permeation conditions: fuel 130 at 1300°F (704°C), 100
hr, 150 psig

Depth of Cut (in.)	Uranium Analyses (mg of U per g of graphite)	
	Untreated Graphite	Pretreated Graphite
0*-1/16	6.6	2.6
1/16-1/8	7.5	2.6
1/8-3/16	7.2	2.4
3/16-1/4	7.6	1.7
1/4-5/16	7.4	1.3
5/16-3/8	7.3	0.9

*Surface of specimen.

✓ Removal of Oxygen Contamination from Graphite

Work has continued on methods for removing oxygen contamination from graphite as a means of eliminating precipitation of UO_2 from $\text{LiF}\text{-BeF}_2\text{-UF}_4$ salt systems. As previously reported,¹⁴ an expensive method of purging graphite of oxygen contaminants has been found. Other methods investigated include the use of preheated hydrogen and the thermal decomposition of ammonium bifluoride, $\text{NH}_4\text{F}\cdot\text{HF}$.

In a single test, flushing an AGOT-grade graphite crucible with preheated hydrogen for 50 hr at 1300°F (704°C) prior to charging it with fuel 130 ($\text{LiF}\text{-BeF}_2\text{-UF}_4$, 62-37-1 mole %) did not detectably alter the quantity of uranium that is normally precipitated from fuel 130 by contaminants of this graphite.

The test system was evacuated for 15 hr at less than $2\ \mu$ Hg pressure at 1300°F (704°C) prior to the hydrogen flushing operation. The hydrogen ($\sim 99.5\%$ H_2) was passed through a commercial deoxygenation unit and a moisture trap, was heated to 1300°F (704°C), and was then passed through the test system, which was also at 1300°F (704°C). The calculated flow rate of the hydrogen was $2.8\ \text{ft}^3/\text{hr}$. The charge of fuel 130 for the test was stored in a chamber integral with the test unit. Therefore the system was not opened to the atmosphere during the transfer of frozen fuel to the graphite crucible at 1300°F (704°C). Following the fuel transfer, the test unit was evacuated ($< 2\ \mu$ Hg pressure) and sealed and was then held at temperature for 100 hr. Radiographic examinations were used to detect the quantity of uranium that precipitated.

The value of hydrogen as a gettering agent for the contaminants of graphite will be further investigated as a function of temperature and/or time. It is also planned to determine whether a catalyst will make the hydrogen an effective gettering agent.

A test has been completed in which oxygen contaminants were partially or completely removed from a crucible of AGOT-grade graphite with a nominal bulk volume of 190 cc by the thermal decomposition of 1 g of $\text{NH}_4\text{F}\cdot\text{HF}$. The graphite crucible containing crystals of $\text{NH}_4\text{F}\cdot\text{HF}$ was sealed in a vacuum of 5 in. Hg in an Inconel container. The residual gas in the container

¹⁴MSR Quar. Prog. Rep. Oct. 31, 1959, ORNL-2890, p 44.

was pure argon. The test unit was heated from room temperature to 1300°F (704°C). The heatup of the argon plus the thermal decomposition of the $\text{NH}_4\text{F}\cdot\text{HF}$ to form NH_3 and HF raised the pressure of the system to 35 psig. After 22 hr, the system was evacuated to less than 1 μ , and a solid charge of fuel 130 was placed in the graphite crucible. The unit had been designed so that this could be accomplished with the crucible at 1300°F (704°C) and without opening the system to the atmosphere. The ratio of the bulk volume of graphite to the volume of fuel 130 at 1300°F (704°C) was 27:1.

Uranium precipitation was not detected by radiographic examinations after 90- and 1000-hr exposures. Normally, in an untreated graphite-fuel 130 system, the precipitation of uranium occurs in 5 hr or less. The absence of the precipitate in the test suggests that the pretreatment with the $\text{NH}_4\text{F}\cdot\text{HF}$ was effective in removing the oxide contaminants. The test is being continued to determine whether tenaciously held oxide contaminants might eventually cause precipitation. Past data concerning uranium precipitation in graphite-fuel 130 systems indicate that this should not happen.

Compatibility of INOR-8 and Graphite

The tendency for INOR-8 to carburize when under pressure and in direct contact with graphite was investigated. A modified stress-rupture apparatus was used to hold grade TSF graphite in contact with INOR-8 (heat 1665) at 1000 psi in fuel 30 ($\text{NaF-ZrF}_4\text{-UF}_4$, 50-46-4 mole %). The test system was maintained at 1300°F (704°C) for 3400 hr. Metallographic examination (Fig. 2.1.15) indicated that carburization had occurred to a depth of about 14 mils. Two successive sets of millings, each 7 mils thick, taken from the INOR-8 platen at the metal-graphite contact surface analyzed 0.38 and 0.12 wt % carbon, respectively. Nominal carbon content of the INOR-8 is 0.067 wt %. The other side of the platen not in contact with the graphite and the surfaces of the female threads in the platen were examined metallographically; no carburization was detected on them.

A test is currently in progress to determine whether the rate of carburization of INOR-8 is dependent upon the stress on the material. An INOR-8 specimen is being tested in a strongly carburizing medium while being subjected to various stress concentrations.

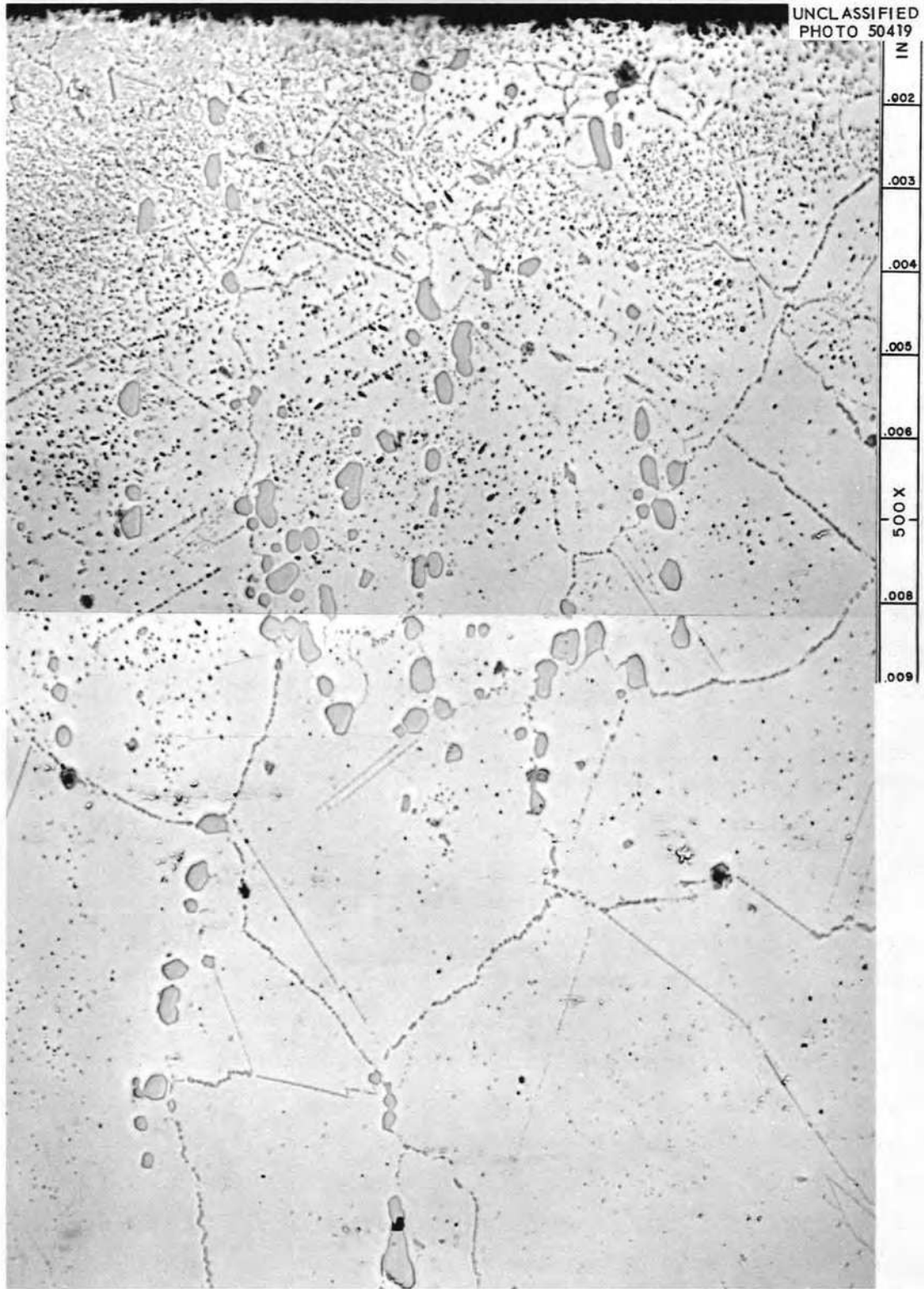


Fig. 2.1.15. Surface of INOR-8 (Heat No. 1665) Platen Which Was Held in Contact with Grade TSF Graphite for 3400 hr at 1000 psi in Fuel 30.

Corrosion Resistance of Brazing Alloys to Fluoride Fuel

Since a barren-salt-to-fuel-salt heat exchanger may be used in the Molten-Salt Reactor, brazing alloys which could be used in fabricating such equipment have been examined for corrosion resistance to fuel 130 (LiF-BeF₂-UF₄, 62-37-1 mole %), a potential reactor fuel.

Five different brazing materials, three nickel-base alloys, one gold-base alloy, and pure copper, were chosen which had exhibited good resistance to fuels 30 and 44 (the NaF-ZrF₄-base fuels). The tests were conducted by brazing small coupons together to form lap joints of Inconel to Inconel and of INOR-8 to INOR-8. Ten of these joints were suspended in an enlarged section in the hot leg of each of three thermal-convection loops. The loops were operated for 1000, 5000, and 10,000 hr at hot-leg temperatures of 1300°F (704°C). The results from the 1000- and 5000-hr tests have been reported previously.¹⁵

The 10,000-hr test has been terminated and examined, and the results are listed in Table 2.1.10. All the brazed joints showed good corrosion resistance when used to join INOR-8. However, Inconel joints brazed with Coast Metals No. 52 and 53 and General Electric No. 81 were attacked.

The results from the 1000-, 5000-, and 10,000-hr corrosion tests indicate that several brazing materials suitable for joining INOR-8 or Inconel have adequate corrosion resistance to the type of fluoride salt represented by fuel 130.

An alloy development program is being conducted by the Welding and Brazing Group in an effort to develop brazing alloys which would be useful in joining graphite to graphite and graphite to metal. As these alloys are developed, they are corrosion-tested to determine their potential use for Molten-Salt Reactor applications. Recent work has been done primarily on gold-base alloys containing various amounts of tantalum, nickel, and other minor constituents to provide proper flowability and melting point. The results of corrosion tests on these alloys in different fuel salts are listed in Table 2.1.11. A moderate concentration of tantalum was detected spectrographically on the inside walls of the nickel container from the 60% Au-30% Ta-10% Ni test. This dissimilar-metal mass transfer was not

¹⁵MSR Quar. Prog. Rep. Oct. 31, 1959, ORNL-2890, p 46.

Table 2.1.10. Results of Corrosion Tests on Brazing Alloys
in LiF-BeF₂-UF₄ (62-37-1 mole %, Fuel 130)
in a Thermal-Convection Loop

Test conditions:
Time: 10,000 hr
Temperature: 1300°F (704°C)

Nominal Composition of Brazing Material (wt %)	Metallographic Results	
	Base Material	
	INOR-8	Inconel
Coast Metals No. 52 (89 Ni-4 B-5 Si-2 Fe)	No attack observed; no porosity	Diffusion voids to 3 mils in depth below surface
Coast Metals No. 53 (81 Ni-8 Cr-4 B-4 Si-3 Fe)	No attack or poros- ity	Severe porosity 15 mils deep
General Electric No. 81 (70 Ni-20 Cr-10 Si)	No attack observed	Complete attack; severe porosity through fillet
82 Au-18 Ni	No attack	No attack
Pure copper	No attack or dif- fusion voids	No attack; small diffusion voids are present in fillet

intense enough to be detected on the nickel capsule by metallographic examination.

The relatively large weight gain on the graphite-to-molybdenum T-joint was due to pickup of fuel by the graphite. The two alloys listed last in the table showed good resistance to fuel 30, which was used in this test to simulate the components of a proposed pump-loop test being planned.

Table 2.1.11. Results of Fuel Corrosion Tests on Newly Developed Brazing Alloys

Test conditions:

Time: 100 hr

Temperature: 1300°F (704°C)

Alloy Composition (wt %)	Test Container	Type of Test Specimen	Fuel Used as Bath*	Weight Change (mg)	Metallographic Results.
60 Au-30 Ta-10 Ni	Nickel capsule	Alloy button	130	-3	Slight, scattered sub- surface voids to 1 mil in depth
62 Au-26 Ta-12 Ni	Nickel capsule	Graphite-Mo T-joint	130	+36	Slight, scattered sub- surface voids to 2 mils in depth
58 Au-27 Ni-8 Ta- 3 Mo-2 Cr-2 Fe	Inconel capsule	Alloy button	30	-0.9	No attack observed
63 Au-29 Ni-3.5 Mo- 2.5 Cr-2 Fe	Inconel capsule	Alloy button	30	N.A.**	No attack observed

*130: LiF-BeF₂-UF₄ (62-37-1 mole %)30: NaF-ZrF₄-UF₄ (50-46-4 mole %)

**Not available.

2.2 CHEMISTRY AND RADIATION EFFECTS

Phase Equilibrium Studies

The System LiF-BeF₂-ZrF₄

For a minimum temperature of 500°C the LiF-BeF₂ binary system can serve as a fuel solvent for a combined total of about 15 mole % UF₄ and ThF₄, together or singly, and there are indications that both the oxide tolerance and the corrosivity of fuels are improved by the presence of a relatively high proportion of the quadrivalent cations. Thus, to minimize uranium inventories and yet retain the advantages of a more "acidic" fuel, the addition of ZrF₄ is an attractive possibility; optimized fuels in the future may well be chosen from the quinary system LiF-BeF₂-ZrF₄-ThF₄-UF₄.

In order to estimate whether such quinary mixtures - suitable as reactor fuels and containing 60 to 75 mole % LiF - are molten at 500°C, preliminary studies of the phase relationships in the system LiF-BeF₂-ZrF₄ were made. The equilibrium phases present in quenched samples of seven LiF-BeF₂-ZrF₄ mixtures show that at 60 to 75 mole % LiF, at least 15 mole % ZrF₄ can be contained in liquid solutions of LiF-BeF₂ at 500°C. The composition sections 3LiF·ZrF₄-2LiF·BeF₂ are not quasi-binary at any temperature interval, because of the occurrences of the primary-phase field of an unidentified phase on these composition sections. This phase is probably a ternary compound of LiF-BeF₂-ZrF₄ containing at least 75 mole % LiF. The compound is uniaxial negative and has such low birefringence that only the average refractive index, 1.418, could be measured. At each of the four compositions where it was observed, the optical properties of the ternary compound were identical, from which fact one may infer that the compound forms little or no solid solution in the ternary system. An x-ray diffraction standard pattern for the compound has been derived.

The System NaF-ZrF₄-ThF₄

Renewed attention has been directed to the phase studies in the system NaF-ZrF₄-ThF₄, because the system NaF-ZrF₄-ThF₄-UF₄ could provide alternative converter-breeder reactor fuels and because of possible advantages for fuel reprocessing cycles. Current efforts are concerned with

the determination of phase relationships in the composition area least studied previously,¹ that of compositions containing less than 50 mole % NaF. The determination of the refractive indices of the ZrF₄-ThF₄ solid-solution compositions furnishes a definitive method of establishing tie lines in the ZrF₄-ThF₄ solid-solution primary-phase area of the system NaF-ZrF₄-ThF₄. This information, once obtained, will be used to construct fractionation paths in this primary-phase area. The combination of fractionation paths and liquidus isotherms on the diagram will indicate the composition of the liquid and the solid phase in equilibrium for each composition in the primary-phase area. The experimental determinations of the refractive indices of the ZrF₄-ThF₄ solid-solution series and of the fractionation paths for the ZrF₄-ThF₄ solid-solution primary-phase area are in progress.

The System NaF-ThF₄-UF₄

The similarity of crystal properties of ThF₄ and UF₄ is conducive to similarities in the compounds formed by these substances with other metal fluorides. This is reflected by several similarities in the phase diagrams for the systems NaF-ThF₄ and NaF-UF₄, but not all the compounds in the two systems occur with identical NaF/XF₄ molecular ratios. Each of the equilibrium phases in the system NaF-ThF₄ takes significant amounts of UF₄ into solid solution, and also the solid phases in the system NaF-UF₄ form solid solutions by including ThF₄.

Continuing studies of the phase equilibria in the system NaF-ThF₄-UF₄ provide additional evidence that the two isostructural crystal forms of the compounds 4NaF·ThF₄ and 3NaF·UF₄ form a continuous solid solution in spite of the difference in stoichiometry of the end members. Phase data from some 15 thermal-gradient quenching experiments indicate that the composition of the solid solution is confined to the line β-4NaF·ThF₄-β-3NaF·UF₄. On the other hand, at higher temperatures, where the alpha modifications are stable, partial solubility of UF₄ occurs in α-4NaF·ThF₄, and of the ThF₄ in α-3NaF·UF₄, so that the alpha-modification solid solutions contain constant proportions of NaF, either 80 or 75 mole %. The

¹R. E. Thoma (ed.), Phase Diagrams of Nuclear Reactor Materials, ORNL-2548, p 82.

solubility of UF_4 in $\alpha\text{-4NaF}\cdot\text{ThF}_4$ is limited to approximately 13 mole %, and the solubility of ThF_4 in $\alpha\text{-3NaF}\cdot\text{UF}_4$ is limited to approximately 4 mole %. In Fig. 2.2.1 are shown the results obtained from thermal-gradient quenching experiments on the composition line $4\text{NaF}\cdot\text{ThF}_4\text{-}3\text{NaF}\cdot\text{UF}_4$. It is unusual for isostructural crystal modifications to occur for a pair of $\text{MF}\cdot\text{XF}_4$ compounds whose molecular ratios, MF/XF_4 , are not identical. Considerable evidence exists which indicates that within the system $\text{NaF}\text{-ThF}_4\text{-UF}_4$, there is a similar continuous solid solution between the isostructural cubic pairs $3\text{NaF}\cdot 2\text{ThF}_4$ and $5\text{NaF}\cdot 3\text{UF}_4$, and limited solubility

UNCLASSIFIED
ORNL-LR-DWG 48668A

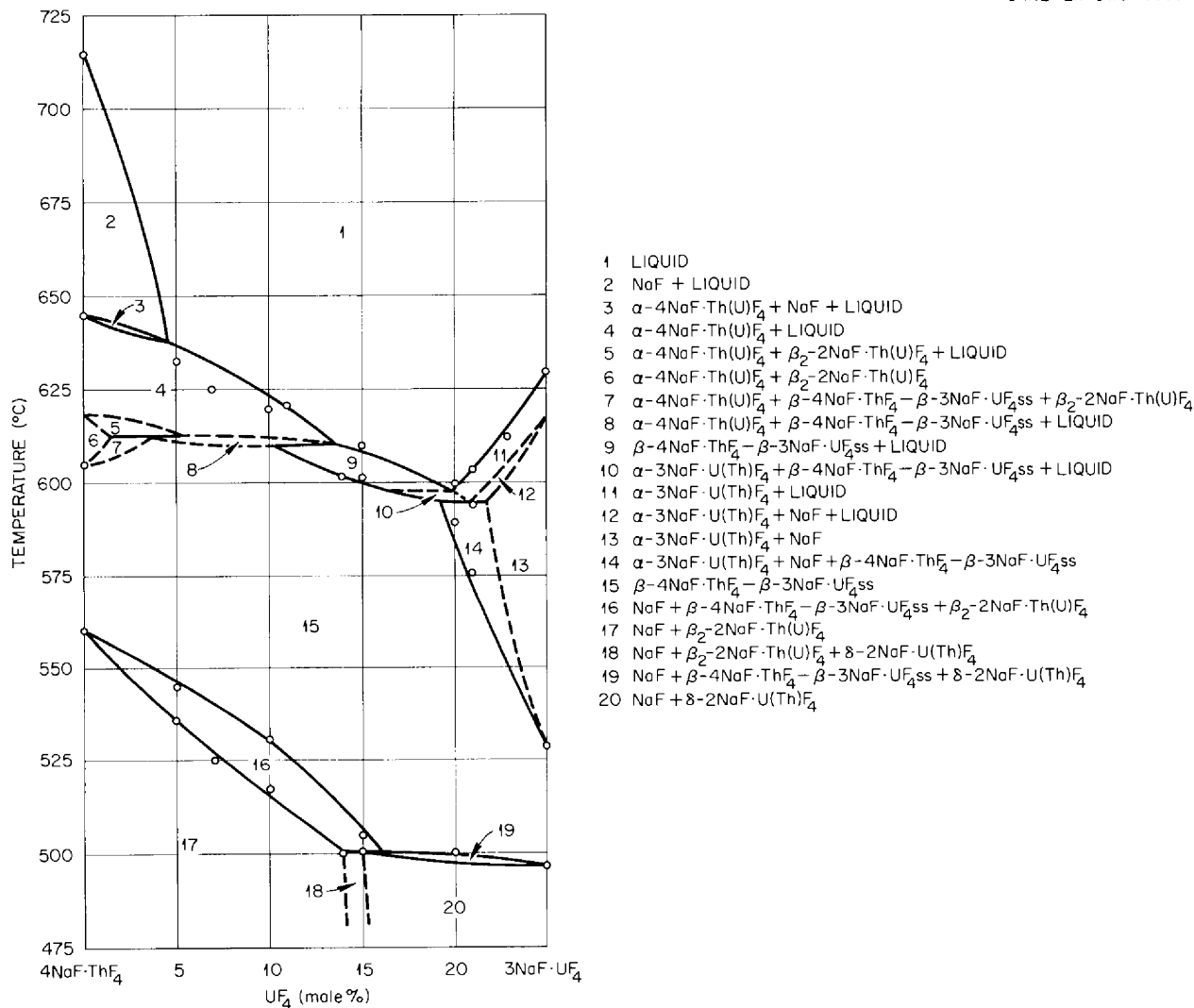


Fig. 2.2.1. System $\text{NaF}\text{-ThF}_4\text{-UF}_4$; The Section $4\text{NaF}\cdot\text{ThF}_4\text{-}3\text{NaF}\cdot\text{UF}_4$.

between the nonisostructural pairs $2\text{NaF}\cdot\text{ThF}_4$ - $2\text{NaF}\cdot\text{UF}_4$ and $\text{NaF}\cdot 2\text{ThF}_4$ - $\text{NaF}\cdot 2\text{UF}_4$.

Phase Diagrams for Fluoride Systems

Detailed descriptions of the phase equilibria in systems of alkali fluorides with zirconium, thorium, and uranium fluorides have recently appeared in an annual report,² and a comprehensive compilation of diagrams of such systems, along with others of significance to fluid-fuel reactor development, all of which were investigated at ORNL, has also been issued.¹

Fission-Product Behavior and Reprocessing Chemistry

Extraction of Uranium and Protactinium from $\text{LiF}\text{-BeF}_2\text{-ThF}_4$ Mixtures

The advantages of a molten-salt nuclear reactor as a thermal breeder could be greatly enhanced by improved processes for recovering U^{233} and protactinium from a blanket salt. A recent review of various oxide precipitation reactions³ provides examples of the potential usefulness of oxide precipitants in molten-salt mixtures containing uranium, thorium, rare earths (represented as cerium), and beryllium to selectively remove these elements from solution as oxides. The development of a suitable chemical reprocessing scheme based on these reactions has been pursued with favorable results.

In the proposed blanket material, $\text{LiF}\text{-BeF}_2\text{-ThF}_4$ (67-18-15 mole %), the problem is to remove trace quantities of U^{233} , produced by the breeding process, in the presence of rather large thorium concentrations. The difference in the behavior of uranium and thorium in reacting with calcium oxide, as illustrated in Fig. 2.2.2, provides the basis for oxide separation schemes, although calcium oxide is not the preferred additive.

The production of U^{233} by thermal breeding is achieved by the decay of Pa^{233} . However, Pa^{233} will also absorb neutrons by a similar reaction to produce U^{234} . Hence, isolation of Pa^{233} from the neutron flux field removes an important source of nuclear poisoning. An oxide precipitation

²Reactor Chem. Ann. Prog. Rep. Jan. 31, 1960, ORNL-2931, p 3-27.

³Reactor Chem. Ann. Prog. Rep. Jan. 31, 1960, ORNL-2931, p 84.

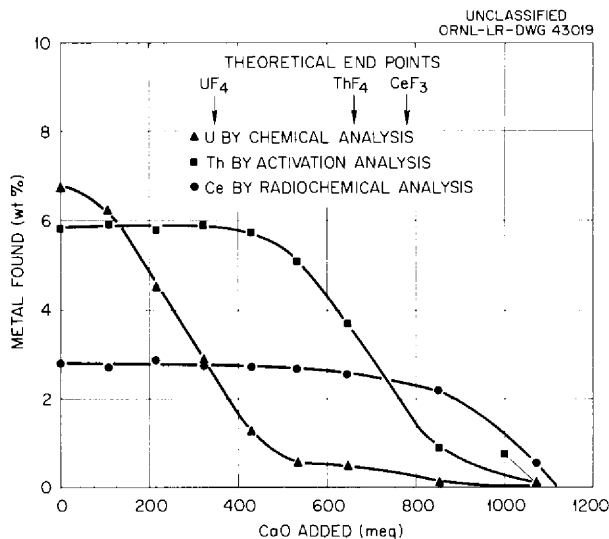


Fig. 2.2.2. Reaction of CaO with UF₄, ThF₄, and CeF₃ in LiF-NaF (60-40 mole %) at 750°C.

scheme for protactinium removal appears to be useful for accomplishing this objective.

Since the treatment to recover uranium and protactinium should not cause serious alterations in the composition of the blanket material, the choice of precipitants is probably limited to BeO, ThO₂, UO₂, or possibly water vapor. The reaction of BeO with trace quantities of UF₄ dissolved in LiF-BeF₂-ThF₄ (67-18-15 mole %) is illustrated in Fig. 2.2.3. In three separate experiments, the addition of approximately 30 g of BeO per kg of melt effectively removed approximately 2000 ppm of dissolved uranium. Roughly comparable results were obtained on using either ThO₂ or BeO to precipitate uranium from the proposed blanket mixture in the experiments summarized by Fig. 2.2.4.

The precipitation of protactinium from solution in LiF-BeF₂-ThF₄ (67-18-15 mole %) was examined in a separate series of experiments. Initially, the removal of Pa²³³ activity, obtained by the irradiation of thorium, was followed as BeO and CaO were added, giving results typified by Fig. 2.2.5. Following each precipitation experiment, the protactinium was successfully redissolved by hydrofluorination *in situ*. The removal of an estimated 50 ppm of Pa²³¹, labeled with Pa²³³, by reaction with BeO is illustrated in Fig. 2.2.6. Similar results, shown in Fig. 2.2.7, were

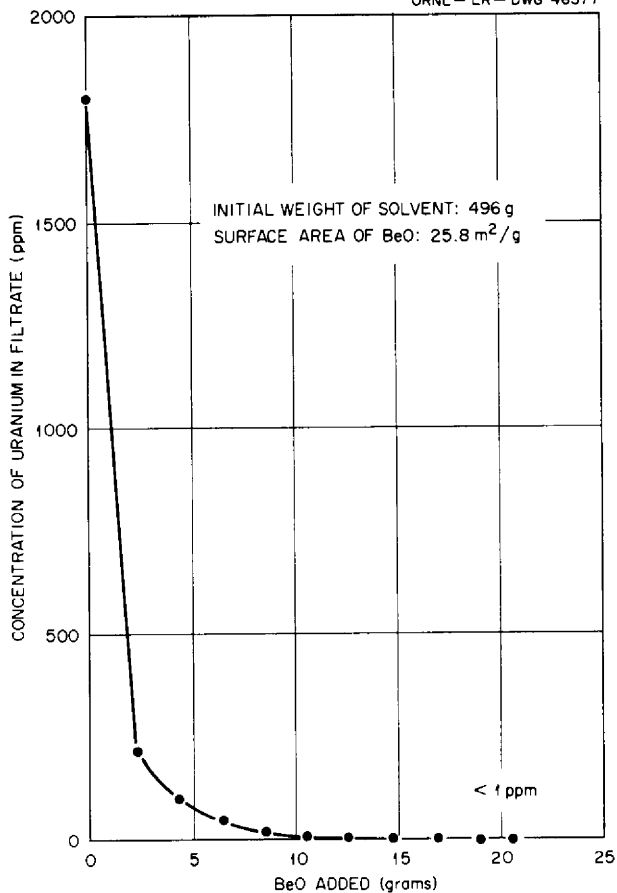


Fig. 2.2.3. Extraction of Uranium from LiF-BeF₂-ThF₄ (67-18-15 mole %) at 650°C.

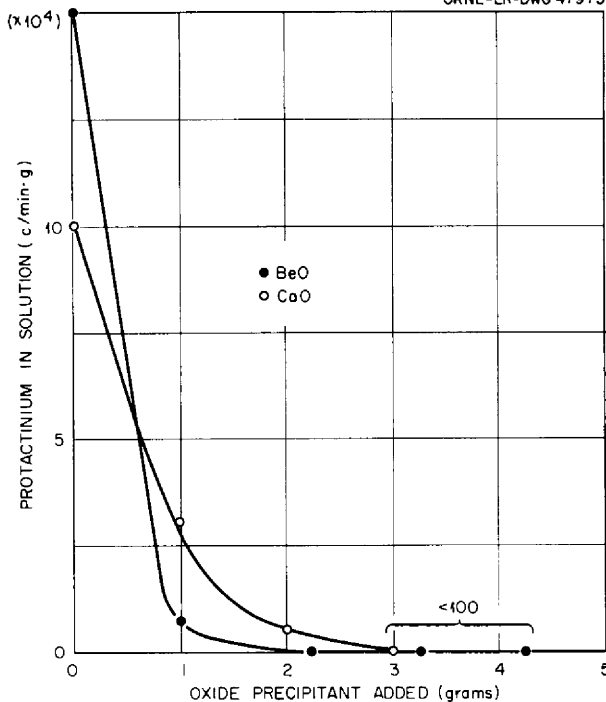


Fig. 2.2.5. Removal of Protactinium (Pa²³³) from Solution in LiF-BeF₂-ThF₄ (67-18-15 mole %) by Reaction with BeO and CaO at 650°C.

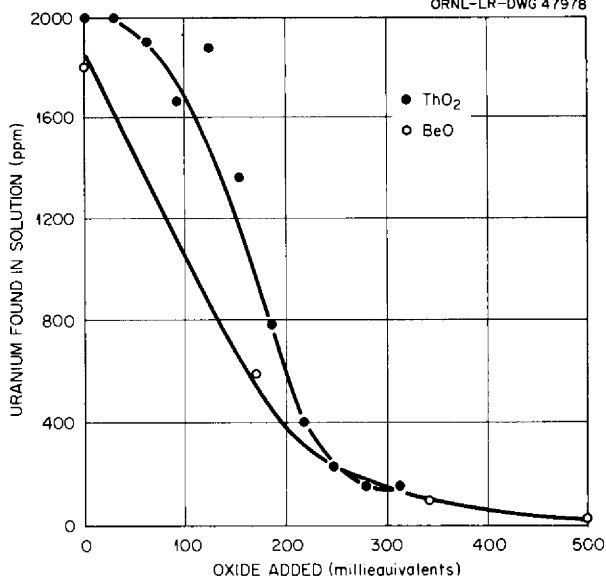


Fig. 2.2.4. Reactions of ThO₂ and BeO with UF₄ in LiF-BeF₂-ThF₄ (67-18-15 mole %) at 650°C.

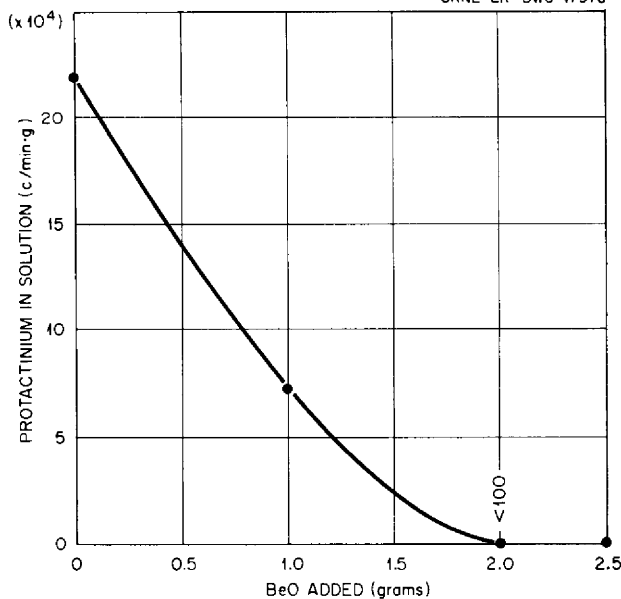


Fig. 2.2.6. Removal of Protactinium (Pa²³¹ Labeled with Pa²³³) from Solution in LiF-BeF₂-ThF₄ (67-18-15 mole %) by Reaction with BeO at 650°C.

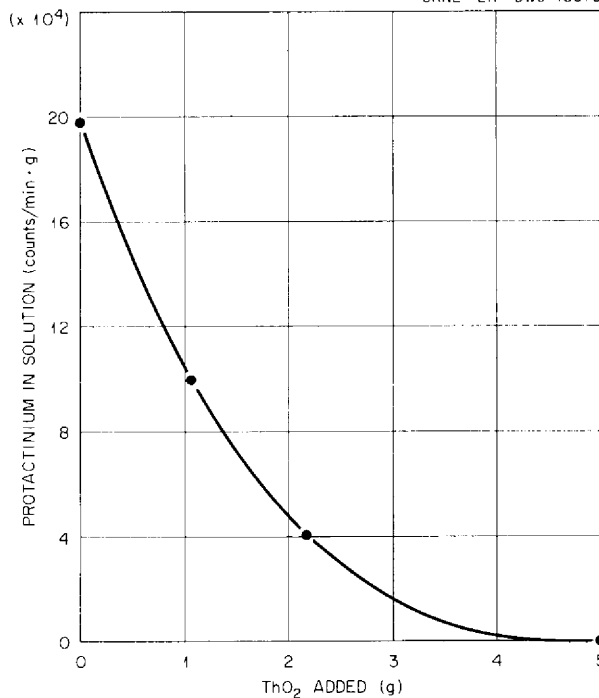


Fig. 2.2.7. Removal of Protactinium (Pa^{231} Labeled with Pa^{233}) from Solution in $\text{LiF}\text{-BeF}_2\text{-ThF}_4$ (67-18-15 mole %) by Reaction with ThO_2 at 650°C .

obtained with ThO_2 as the precipitant. Such examples demonstrate that realistic quantities of both uranium and protactinium can be precipitated from solution in the proposed blanket melt for a molten-salt breeder reactor by using oxide reactions.

Current studies are directed toward the effect of added oxide on the composition of the blanket material and toward solid-liquid separations following precipitation reactions. Since BeO and ThO_2 are ceramic materials, they can be processed into shapes having variable densities and surface areas, and if adherent precipitates of uranium and protactinium form on BeO or ThO_2 ceramic bodies, the separation from the liquid would be facilitated. Preliminary results on the relative reaction rates with BeO , extruded into 1/16-in.-dia \times 1/4-in.-long cylinders having average surface areas of $8.5 \text{ m}^2/\text{g}$, are shown in Fig. 2.2.8. In another experiment, an apparent adherence of UO_2 to extruded ceramic bodies of BeO was demonstrated (Fig. 2.2.9) by the disappearance of uranium from molten

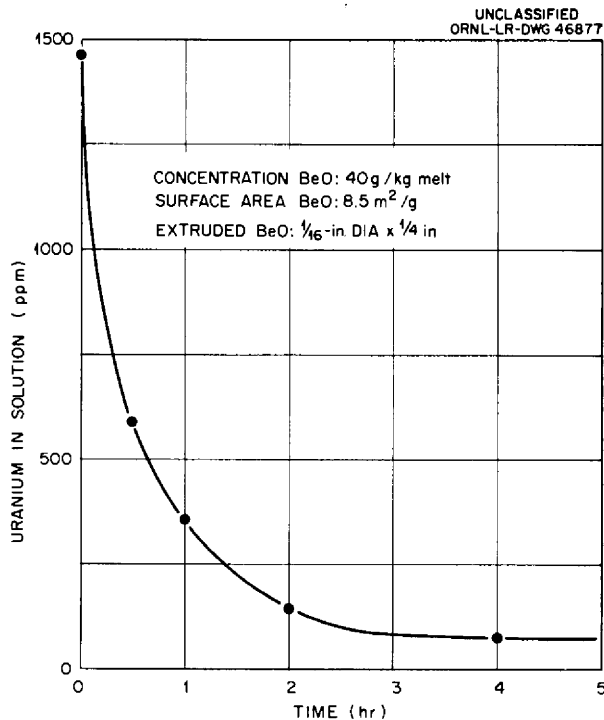


Fig. 2.2.8. Reaction of BeO with UF₄ in LiF-BeF₂-ThF₄ (67-18-15 mole %) at 650°C.

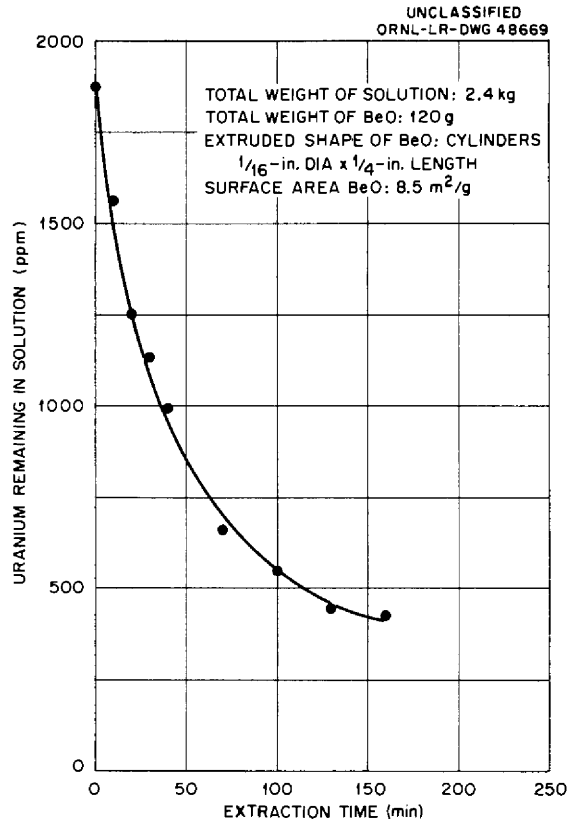
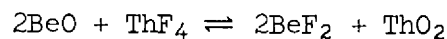


Fig. 2.2.9. Extraction of UF₄ in LiF-BeF₂-ThF₄ (67-18-15 mole %) by Reaction with Extruded BeO at 650°C.

LiF-BeF₂-ThF₄ (67-18-15 mole %) collected from a solid bed by forcing the liquid phase through a nickel screen, having approximately 900- μ openings, into a separate container. The analyses shown in Fig. 2.2.9 were obtained after hydrofluorination of the separated liquid.

The effect of an added oxide precipitant is determined by the equilibrium for the reaction of the oxide with the fluoride components. For example, the equilibrium reaction



influences the conditions which must be maintained to avoid precipitation of thorium during the extraction of protactinium and uranium. The relative stability of BeO and ThO₂ in LiF-NaF (60-40 mole %), as evidenced by the reaction of calcium oxide with dissolved BeF₂ and ThF₄, is shown in Fig. 2.2.10. If BeO is added to ThF₄ dissolved (8 wt % Th) in this same solvent, an equilibrium which apparently involves both solid

oxides is encountered (Fig. 2.2.11). With more BeF_2 present, as in the case of the solvent $\text{LiF}-\text{BeF}_2$ (63-37 mole %), shown in Fig. 2.2.12, no precipitation of ThO_2 occurs when BeO is added to a solution again containing 8 wt % thorium. Further study of this reaction is in progress.

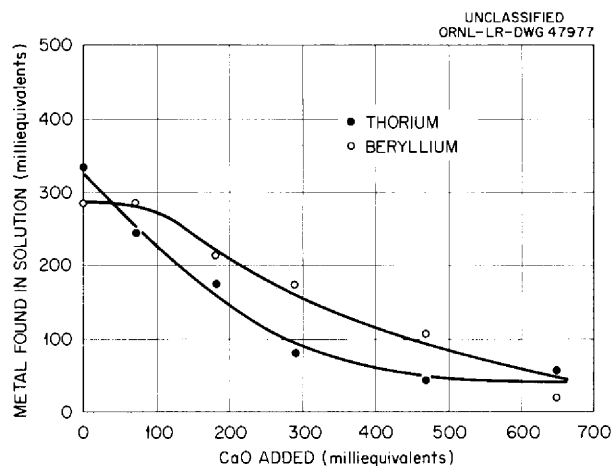


Fig. 2.2.10. Reaction of CaO with ThF_4 and BeF_2 in $\text{LiF}-\text{NaF}$ (60-40 mole %) at 750°C .

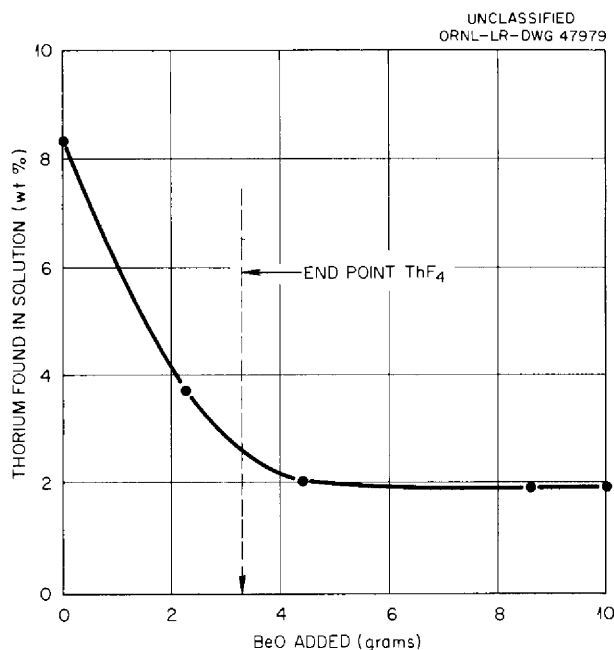


Fig. 2.2.11. Reaction of BeO with ThF_4 in $\text{LiF}-\text{NaF}$ (60-40 mole %) at 750°C .

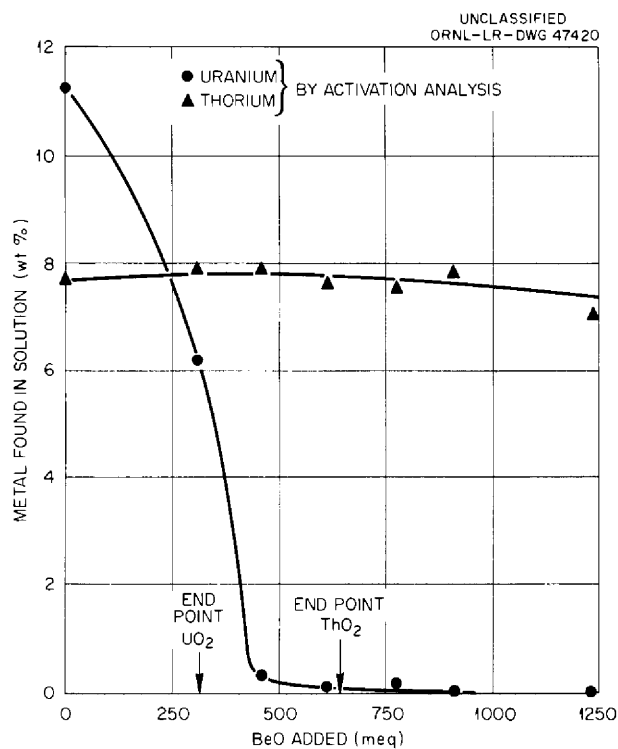


Fig. 2.2.12. Reaction of BeO with UF_4 and ThF_4 in $\text{LiF}-\text{BeF}_2$ (63-37 mole %) at 600°C .

The insolubility of uranium oxide in comparison with thorium oxide was not anticipated from the relative stability of the crystals and hence must depend on as-yet-unelucidated solution behavior, but the feasibility of extracting uranium and protactinium from solution in LiF-BeF₂-ThF₄ (67-18-15 mole %) seems well established for the concentrations of uranium and protactinium to be expected in the proposed blanket of a two-region molten-salt breeder reactor. Of further interest in this connection is the experimental observation that protactinium was precipitated from solution in the presence of approximately 1000 to 2000 ppm uranium. This suggests that the precipitated oxide of protactinium is more stable than UO₂. A study of the possible application of this reaction to a one-region molten-salt breeder reactor is now in progress, as are studies to provide further experimental information for exploiting the reactions of BeO and ThO₂ with uranium and protactinium in a chemical reprocessing scheme.

Chemistry of Corrosion Processes

Effect of Oxide on LiF-BeF₂-ThF₄ and LiF-BeF₂-ThF₄-UF₄ Mixtures

The applicability of thermal-gradient quenching techniques for obtaining information on the effect of oxide in LiF-BeF₂-ThF₄ and LiF-BeF₂-ThF₄-UF₄ melts at high temperatures has been explored. Oxide was included in the equilibrated samples by substituting beryllium oxide for a fraction of the BeF₂ contained in the mixtures LiF-BeF₂-ThF₄ (67-18-15 mole %) and LiF-BeF₂-ThF₄-UF₄ (67-18-14.5-0.5 mole %). Samples with increments of BeO between 0.006 and 2.9 wt % were annealed in the temperature ranges between 450 and 550°C for one week before quenching. Deductions concerning the reactions occurring at the high temperatures were made by noting the phases present in the quenched samples as revealed by petrographic and x-ray diffraction examinations.

In LiF-BeF₂-ThF₄ the occurrence of ThO₂ was found only in samples containing 0.3 wt % or more BeO. However, the samples containing 0.06, 0.03, and 0.006 wt % BeO gave rise to an unidentified, highly birefringent phase (refractive index: high $N \cong 1.70$, low $N \cong 1.55$), which might well be a thorium oxyfluoride. In none of these samples were traces of unreacted BeO observed.

In the quaternary mixtures, BeO was added in increments upward from 0.3 wt %. At 0.3 wt % BeO, the only oxide phase encountered was UO₂. At 0.8 wt % and upward, both UO₂ and ThO₂ were observed, mixed but uncombined between 450 and 500°C and as a UO₂-ThO₂ solid solution at temperatures above 500°C. The results of these experiments appear to corroborate the sequential precipitation of ThO₂ and UO₂ previously noted by Watson and Shaffer^{3,4} when BeO is used as a precipitant in LiF-BeF₂ melts, and also indicate that UO₂-ThO₂ solid solutions are readily formed at much lower temperatures in fused-salt media than by solid-state reaction.

No quantitative conclusions regarding the solubility of BeO can be made from these quenching experiments, partly because of the possibility that small amounts of BeO remain dissolved in the glassy portion of the quenched samples without noticeably altering the refractive index of the glass. However, the detection of a distinguishable oxygen-containing phase at concentrations as low as 0.003 wt % BeO in samples that would have otherwise corresponded to complete liquefaction can be regarded as evidence that the oxide tolerance of the sample was less than 30 ppm.

Radiotracer Studies of the Role of Cr⁰ Diffusion as a Controlling Factor in Corrosion by Molten Fluorides

A thorough understanding of the solid-state diffusion of chromium in MSRE alloys is an important aspect of corrosion studies. The present state of knowledge in this field has been summarized recently⁴ and will appear in topical reports.⁵

A large number of the chromium diffusion coefficients available in the literature⁶ were applicable only at temperatures above 900°C. However, extrapolation of this information to temperatures of reactor interest (600 to 900°C) could be misleading if the diffusion mechanism

⁴W. R. Grimes, G. M. Watson, et al., Radiotracer Techniques in the Study of Corrosion by Molten Fluorides, for presentation at Copenhagen Conference on the Uses of Radioisotopes, September 1960.

⁵R. B. Evans et al., Self-Diffusion of Chromium in Nickel-Based Alloys, ORNL report (in press).

⁶P. L. Gruzin and G. B. Federov, Doklady Akad. Nauk S.S.S.R. 105, 264-67 (1955).

were to change within the extrapolated region. Accordingly, self-diffusion coefficients of chromium in nickel-base alloys in the temperature range 600 to 900°C were determined both by monitoring the depletion of tracer from melts containing Cr^{51}F_2 and by successively electropolishing the metal to obtain the concentration profile of the tracer in the alloy.

As reported previously,^{7,8} the diffusion coefficients change from 10^{-16} cm^2/sec at 600°C to about 10^{-13} at 800°C but can vary from 10^{-16} to 10^{-15} cm^2/sec at 600°C depending on the annealing history of the Inconel. Low diffusion coefficients are found in samples exhibiting large grain growth. At temperatures above 800°C the diffusion coefficients in Inconel as measured by the different techniques were the same, but at lower temperatures there were discrepancies in such a direction as to suggest the emergence of a grain-boundary-path mechanism. With INOR-8 no such differences were found. Also, the self-diffusion coefficients of chromium in INOR-8 and Inconel appear to be about the same if the higher values found for Inconel at low temperatures are adopted as the basis of comparison.

In order to obtain corrosion data directly amenable to analysis, two anisothermal convection loops of INOR-8 were placed in operation under identical conditions with tracer CrF_2 , but no corrodant, in the melt. The first loop, No. 1248, was operated for 500 hr and then drained and examined to obtain the values for the self-diffusion coefficients of chromium in INOR-8 shown in Fig. 2.2.13. A small difference was noticeable between the values obtained by the various methods used; the coefficients obtained on total specimen counts tended to be low at high temperatures and vice versa. The reason for this trend is not immediately apparent and is presently ascribed to small systematic errors which lie within the over-all experimental precision of ± 0.4 of a logarithmic cycle as normally encountered in such studies.

In order to determine the validity of the self-diffusion coefficients determined in loop 1248 for the prediction of chromium diffusion rates under corrosive conditions, the second loop, No. 1249, was operated under

⁷MSR Quar. Prog. Rep. June 30, 1958, ORNL-2551, p 95.

⁸MSR Quar. Prog. Rep. Oct. 31, 1959, ORNL-2890, p 55.

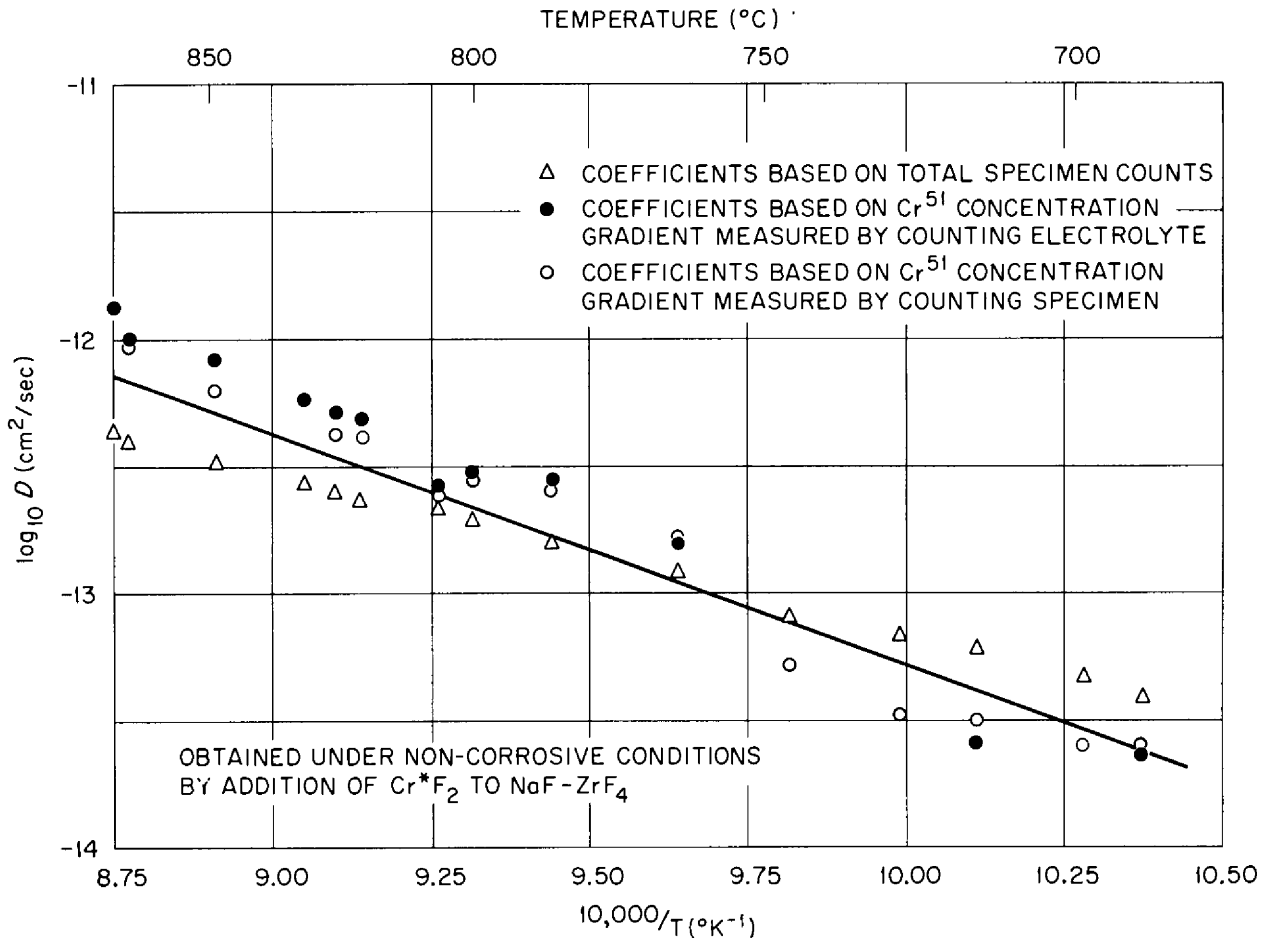
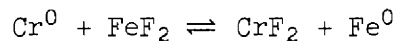


Fig. 2.2.13. Self-Diffusion Coefficients for Cr⁵¹ in INOR-8; Loop 1248.

noncorrosive conditions for 792 hr and then a corrosive agent (FeF₂) was added without otherwise disturbing the operation. After 264 hr of operation under corrosive conditions, the loop was drained and examined. As expected, the presence of FeF₂ in the solution caused the chromium concentration at the surface of the metal to be reduced to essentially zero. The reaction⁹



has an equilibrium quotient of 1.5×10^4 at 600°C and greater at higher

⁹C. M. Blood et al., Activity Coefficients of Ferrous Fluoride and of Nickel Fluoride in Molten Sodium-Fluoride-Zirconium-Fluoride Solutions, Paper No. 75, Division of Physical and Inorganic Chemistry, 132nd Meeting of the American Chemical Society, New York (Sept. 8-13, 1957).

temperatures, so that FeF_2 is a drastic oxidant for Cr^0 but has little effect on the Ni-Mo matrix of the alloy. In Fig. 2.2.14, the results obtained with a specimen from loop 1249 are compared with the results obtained with the corresponding specimen from loop 1248, showing that the experimental points agree well with the calculated curves.

Figure 2.2.15 shows the concentration profiles in the specimens as calculated from the diffusion coefficients shown in Fig. 2.2.13. Curve 1 gives the expected concentration of tracer for 1056 hr of operation under noncorrosive conditions. Curve 2 represents the expected tracer-concentration profile in the specimen from loop 1249, altered from curve 1 by adding FeF_2 after 792 hr of operation. Curve 3 shows the actual tracer-concentration profile in the same specimen as calculated from the ratio

UNCLASSIFIED
ORNL-LR-DWG 46402

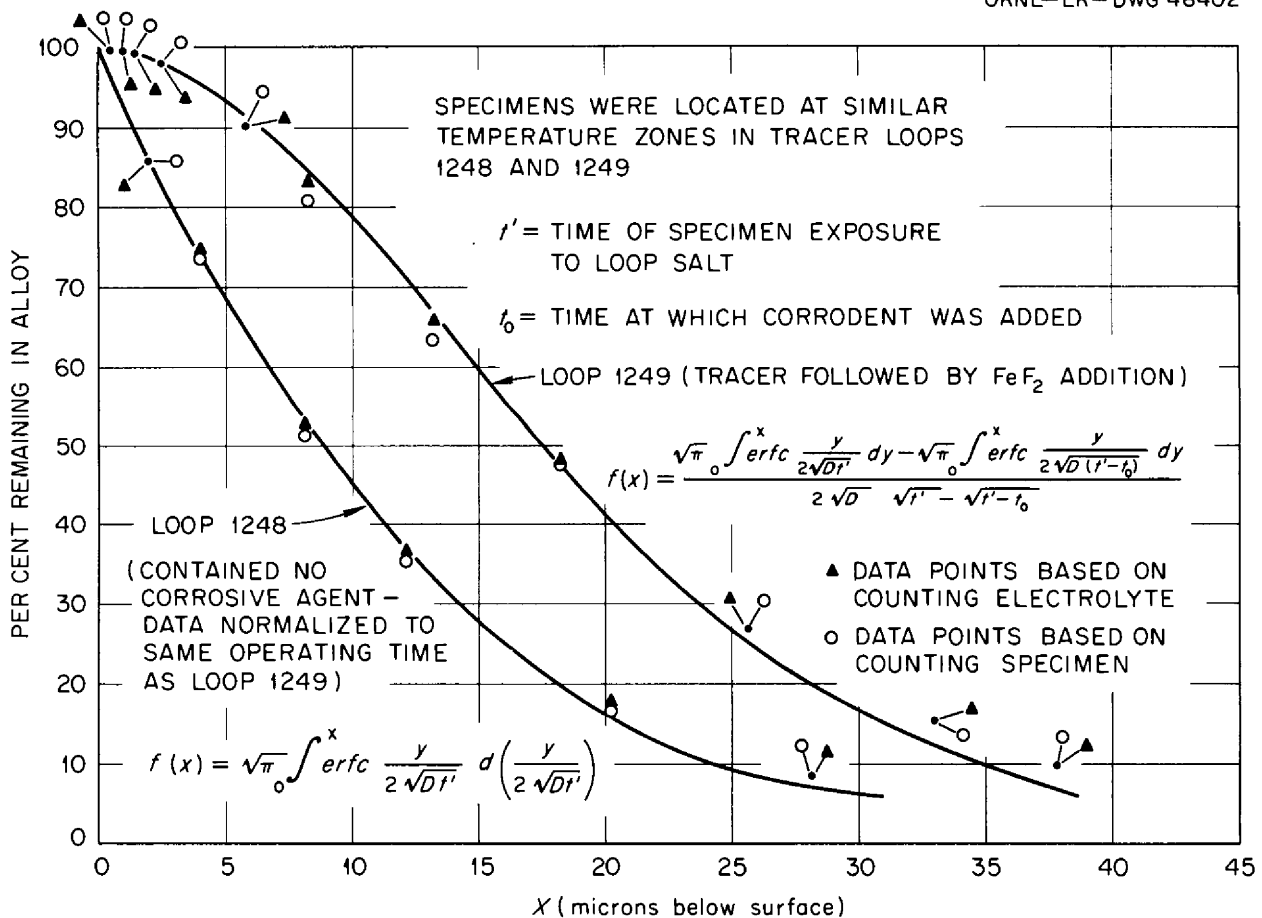


Fig. 2.2.14. Per Cent of Tracer Remaining in Alloy as a Function of Depth Removed from Specimen Surface by Electropolishing.

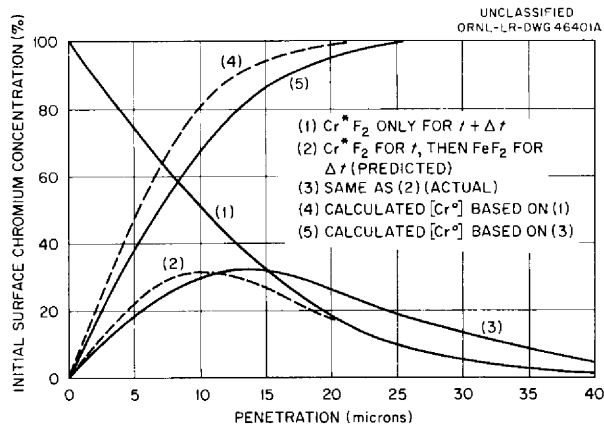
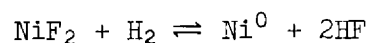


Fig. 2.2.15. Various Chromium-Concentration Profiles at 813°C in INOR-8 Loop Specimens.

of the activity of the corroded specimen to that of the salt. Disagreements at a depth of about 25 μ or greater may arise from a lack of precision resulting from the fact that, at these penetrations, only about 25% of the tracer remains. However, in many other specimens the experimentally determined tracer concentrations at the greater penetrations were found to be greater than calculated. The deviations are within the experimental uncertainty, but the trend is always in the same direction, which suggests that the effect is real. In any case, a relatively minor contribution to the over-all diffusion rates is involved. Curves 4 and 5 of Fig. 2.2.15 represent the total chromium-concentration profile in INOR-8 after 264 hr of selectively leaching the chromium, showing that considerable reliance can be placed on both the diffusion coefficients and the mathematical analyses employed for treating metal diffusion in corrosion tests with thermal-convection loops.

The Free Energy of Formation of NiF_2

Determinations of the free energy of formation of NiF_2 , based on measurements of the equilibrium constant for the reaction



in molten LiF-BeF_2 as a solvent, and including experiments on saturated solutions in equilibrium with solid NiF_2 , have given less negative values

than those found in the literature. This resolves much of a long-standing discrepancy previously noted in connection with the empirical corrosion results in nickel alloys, and also with a marked difference in the solution behavior in fluoride melts of Ni^{++} as compared with Fe^{++} and Cr^{++} ions. The details, as discussed in a recent report,¹⁰ lead to free energies of formation of -123 and -126 kcal/mole, compared with a literature estimate¹¹ of -128 and -131, at 600 and 500°C, and further suggest that the entropy of fusion of NiF_2 is nearer to 10 e.u. than to 5 e.u.

Analysis of Corrosion Test Loops

Periodic sampling of the melts in the forced-circulation corrosion test loops has continued.¹² There are now four loops in operation, and two have been terminated recently.

The oldest loop, MSRP-12, an INOR-8 loop containing $\text{LiF-BeF}_2\text{-ThF}_4\text{-UF}_4$ (62-36.5-1.0-0.5 mole %), continues to operate without sampling in order to conserve the supply of salt in the loop.¹³ It has now operated for more than 13,500 hr.

Loop 9377-5, an Inconel loop charged with the same salt as MSRP-12, has shown a continuing increase in chromium concentration for almost 12,000 hr and now contains 0.6 wt % Cr^{++} , which is far in excess of the amount attributable to equilibrium with normal fuel. A further indication of extraneous oxidation is found in the decrease in uranium concentration, as though UO_2 were being precipitated.

Loop MSRP-13, an INOR-8 loop charged with $\text{LiF-BeF}_2\text{-UF}_4$ (70-10-20 mole %), operated for 8200 hr before failing because of an inadvertent freezing. As shown in Fig. 2.2.16, the chromium concentration climbed at an increasing rate; although this type of curvature is atypical, the terminal Cr^{++} ion concentration is not exceptionally high for a fuel containing 20 mole % UF_4 .

¹⁰C. M. Blood et al., Reactor Chem. Ann. Prog. Rep. Jan. 31, 1960, ORNL-2931, p 39.

¹¹L. Brewer et al., The Chemistry and Metallurgy of Miscellaneous Materials: Thermodynamics (ed. by L. L. Quill), pp 65, 110 McGraw-Hill, New York, 1950.

¹²MSR Quar. Prog. Rep. Oct. 31, 1959, ORNL-2890, p 59.

¹³MSR Quar. Prog. Rep. Oct. 31, 1959, ORNL-2890, p 61.

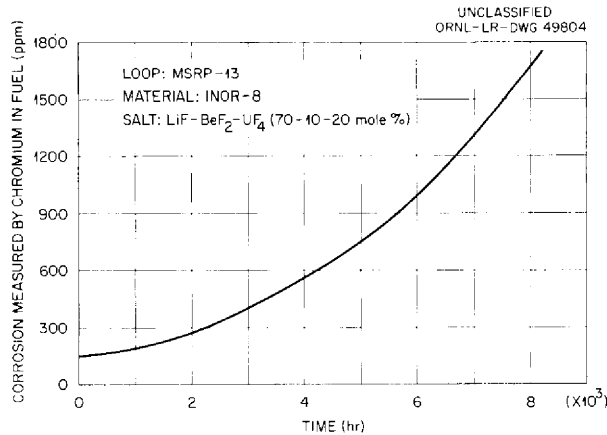


Fig. 2.2.16. Corrosion of INOR-8 by a Fuel Containing 20 mole % UF₄.

Loop MSRP-14, constructed of INOR-8 and charged with LiF-BeF₂-ThF₄-UF₄ (67-18.5-14-0.5 mole %), has operated for 2300 hr. So far, the Cr⁺⁺ ion concentration has not exceeded 300 ppm and has returned to near this value after a dilution resulting from the addition of fresh melt to restore the liquid level; a steady-state concentration of Cr⁺⁺ at several hundred ppm is characteristic of normal behavior.

Loop MSRP-15, a duplicate of MSRP-14, has operated for 4000 hr without any difficulties and currently exhibits a Cr⁺⁺ concentration of 500 ppm; the approach to the presumed steady-state level was made in less than 500 hr, which is also a characteristic of normal behavior.

Loop MSRP-16, another duplicate of MSRP-14, exhibited low Cr⁺⁺ ion concentrations for 2750 hr before pump failure.

Corrosion Equilibria with Unalloyed Cr⁰

In order to better understand the corrosion behavior of Cr⁰, LiF-BeF₂-ThF₄ (67-18-15 mole %) salt has been circulated over 1800 g of pure chromium metal in an isothermal assembly constructed of Inconel. The plan of the experiment was to determine the concentration of chromium in the fluoride melt without UF₄ as a function of temperature, and then to add UF₄ as an oxidizing agent. Two separate attempts, each involving analyses of samples drawn over a period of months, gave unsatisfactory results; the Cr⁺⁺ concentration did not follow a consistent pattern. The first assembly was behaving so erratically after 2230 hr of operation

that it was drained for examination. A deposition of chromium metal had taken place at the liquid level in the pump bowl, which was a cold spot in spite of precautions to maintain isothermal conditions. The second experiment is still under surveillance.

Melting Points of Chromous Fluoride and Chromic Fluoride

Melting points were determined for both CrF_2 and CrF_3 . Solutions of these compounds result from the corrosion of chromium-containing alloys by fluoride fuels. Both compounds were previously reported to melt near 1000°C .¹⁴

Conventional thermal analysis procedures showed pure CrF_2 to have a melting point of $900 \pm 10^\circ\text{C}$.

Chromic fluoride required special precautions because it disproportionates into CrF_2 and volatile CrF_5 at high temperatures.¹⁵ To prevent disproportionation, the samples were sealed in platinum capsules containing a helium atmosphere. Capsules were heated to various temperatures, and the cooled product was checked visually for evidence of melting. Melting was deemed to have occurred in a capsule heated to 1419°C , but not in one heated to 1388°C ; therefore the melting point is $1404 \pm 25^\circ\text{C}$. Possibly the previously reported low value was depressed due to admixture with CrF_2 resulting from disproportionation.

Graphite Compatibility

Intercalation of Graphite

Studies were continued relative to the conditions under which intercalation of graphite does or does not occur. Although certain molten salts can damage graphite by the formation of intercalation compounds, no evidence of such an effect has been found with breeder fuels.^{16,17} Also,

¹⁴L. Brewer, "The Fusion and Vaporization Data of the Halides," p 201 in The Chemistry and Metallurgy of Miscellaneous Materials: Thermodynamics (ed. by L. L. Quill), McGraw-Hill, New York, 1950.

¹⁵Reactor Chem. Ann. Prog. Rep. Jan. 31, 1960, ORNL-2931, p 186.

¹⁶MSR Quar. Prog. Rep. Oct. 31, 1956, ORNL-2890, p 66-67.

¹⁷Reactor Chem. Ann. Prog. Rep. Jan. 31, 1960, ORNL-2931, p 70.

most of the fission products have been either melted as fluorides in graphite crucibles or included as major constituents of fluoride melts in graphite; again no evidence of intercalation has been noticed. It appears likely that reactor fuels melt at too high a temperature to favor the formation of intercalation compounds. For example, it was found that although pure FeCl_3 at 300°C crumbles graphite tubes in about 2 hr to form an intercalated powder, NaCl-FeCl_3 (70-30 mole %) shows no effect at 750°C . Dilution is also important, since intercalation was not found with NaCl-FeCl_3 (46-54 mole %) at 200°C for 7-1/2 hr; the maximum concentration of cations known to have intercalating proclivities in the MSRE is expected to be much less than 0.01 at. %.

Permeation of Graphites by Molten Fluoride Fuels

Continued tests on the permeation of graphite by $\text{LiF-BeF}_2\text{-ThF}_4\text{-UF}_4$ (67-18.5-14-0.5 mole %) and $\text{LiF-BeF}_2\text{-ThF}_4$ (67-18-15 mole %) are summarized in Table 2.2.1. Most of the permeating salt in the CEY samples was found, by chemical analyses, to be near the exposed ends, and there was a selective depletion in the uranium concentration relative to other fuel constituents with increasing distance from the ends.

Table 2.2.1. Permeation of Graphites Expressed as Weight Gains

Temperature: 1300°F
 Pressure: 60-75 psig

Graphite	Weight Gains (%)	
	$\text{LiF-BeF}_2\text{-ThF}_4$	$\text{LiF-BeF}_2\text{-ThF}_4\text{-UF}_4$
AGOT		20-23
S-4		3.4-6.0
GT-123	0.2	0.2
MH4LM-85	10.5	10.4
CEY* (RLM-24)	1.0	0.1-0.2
CEY**	1.0	1.0

*This graphite is in the form of extruded tubing, 1-1/4-in. OD x 7/8-in. ID.

**This graphite is in the form of 1/2-in.-OD extruded tubing.

Radiation Effects

Behavior of a Rare-Earth Fission Product in a Graphite-Molten-Salt System

In a graphite-moderated fused-salt reactor, retention of fission products in the graphite could appreciably reduce the breeding efficiency. The effect of xenon has been evaluated in other reports.¹⁸ Rare earths also comprise an important part of the high-cross-section fission products. Europium has been selected as a typical rare earth, with useful tracer properties and a high cross section, for study in a molten-salt-graphite system. To provide a background for future work with irradiated specimens, AGOT graphite was treated with LiF-BeF₂-UF₄-ThF₄ (67-18.5-0.5-14 mole %), containing a tracer quantity of Eu^{152,154} as described below.

A group of three AGOT graphite specimens in the form of rods, 0.75-in. diameter and 3-in. length, were exposed to the tagged fuel for 1 hr at 700°C under a helium pressure of 30 psia and under conditions which should have given penetration of at least 15 wt %. Examination of these rods revealed that the degree of impregnation, as evidenced by weight gains, was only about 1%. Although the impregnation was not satisfactory, and there was considerable difference between rods, contact radioautographs were made of the ends of 0.5-in. lengths sectioned from the three rods. Figure 2.2.17 illustrates the variation found along a rod. Visual observation of a sectioned face by stereomicroscope revealed salt deposits in large random pores or interconnecting faults extending inward from the outer surface of the graphite rod.

Other AGOT graphite specimens have been treated with fuel salt containing europium by a different method. A hole 0.3 in. in diameter was drilled 2.5 in. along the axis of a graphite rod 0.9 in. in diameter and 3 in. long, and this hole was filled with fuel containing Eu^{152,154}. The rod was then lowered into a molten-salt bath to a depth of approximately 2.75 in. This operation was carried out in a controlled-atmosphere vacuum-tight furnace. A thick Lucite window in the top of the furnace container permitted observation during treatment of the graphite.

One AGOT rod was maintained in the molten-salt bath for 24 hr at a temperature of 700°C under a helium pressure of 7.4 psia. Upon recovery

¹⁸Reactor Chem. Ann. Prog. Rep. Jan. 31, 1960, ORNL-2931, p 37.

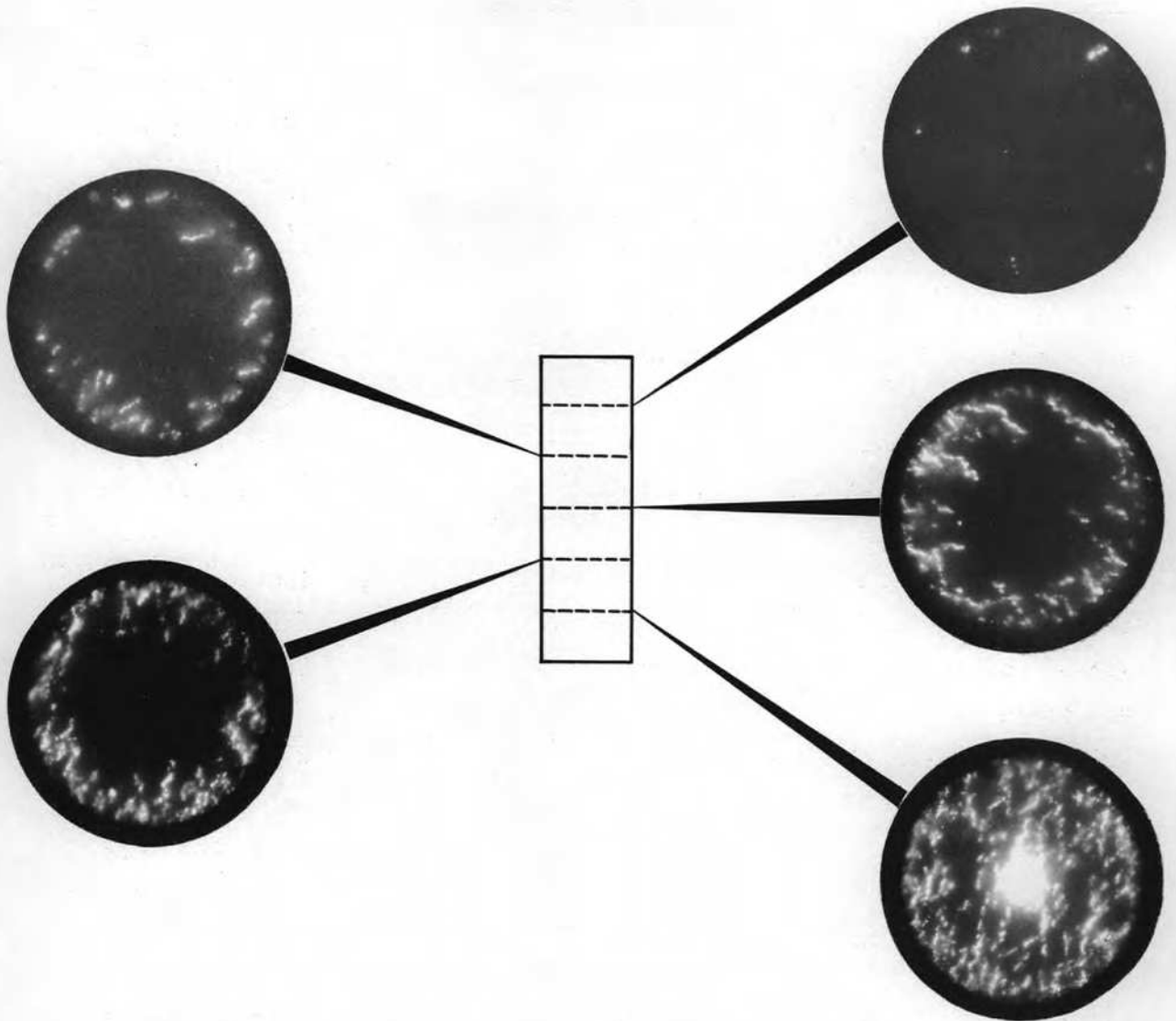


Fig. 2.2.17. Radioautographs Showing Variation of Penetration of BULT-14 Salt Containing $\text{Eu}^{152,154}$ into AGOT Graphite Rod.

of the specimen and removal of the inner plug of salt, no penetration of the graphite by the salt was noted, as might have been anticipated from the fact that the rod was incompletely immersed, and hence no pressure difference was available for pushing the salt into the graphite. The rod was then cut into 0.5-in. sections and a 24-hr contact radioautograph made using Kodak type M x-ray film. No blackening of the film was observed.

A second graphite rod was treated for 24 hr, as described above, except that the helium pressure was cycled twice between 7.4 and 35 psia during the last 2 hr in an attempt to develop a pressure difference. The attempt was again unsuccessful, and no blackening of the film was produced by a 24-hr contact period.

The sections of both rods were then placed in contact with film for six days, and a very slight darkening of the film occurred in the position of the axial hole in each section. Gamma-ray analysis of the very small amount of radioactivity in the graphite sections indicated that the film darkening was due to the uranium and thorium content of the salt rather than $\text{Eu}^{152,154}$ activity. These limited data indicate that europium remains in the salt as expected and does not deposit on graphite surfaces.

A third AGOT specimen is being treated under a vacuum of 100 to 200 μ at 550°C and then under a helium pressure of 41 psia at 700°C to induce penetration of the graphite walls by tracer-bearing salt. Once permeation of europium activity by this treatment has been accomplished, the arrangement will be reversed so that the graphite specimen containing europium will be exposed to clean salt, permitting the leaching or interchange of the europium activity between the tagged and nontagged salt to be followed.

Preparation of Purified Materials

Purification, Handling, and Service Operations

The use of purified fuels has been somewhat greater than had been anticipated, so that a stockpile of fuels of current interest no longer exists, although four batches of beryllium-based fuels were processed recently. Several capsules for in-pile testing were filled with a purified fuel containing U^{235} and Li^7 .

The large-scale production facility has recently been operated almost continuously to treat 950 kg of fluoride melts for use in recovery processes under development by the Chemical Technology Division.

2.3 FUEL REPROCESSING

NO₂-HF Solutions

Further investigation of the dissolution of LiF-BeF₂-ThF₄-UF₄ (62-36.5-1.0-0.5 mole %) in anhydrous hydrogen fluoride containing nitrogen dioxide showed that under proper conditions the UF₄ is dissolved along with the LiF and BeF₂. Salt of this composition was contacted several times successively with liquid HF containing 5 mole % NO₂, each pass with 7 ml of solvent per gram of original salt. Essentially all the LiF and BeF₂ and 73% of the UF₄ dissolved in the first two treatments, and the rest of the uranium dissolved in the third. Thorium fluoride was not soluble, and rare earths were sufficiently insoluble that the dissolved salt was decontaminated by a factor greater than 50.

A large power reactor would probably use a fuel salt containing less UF₄ than in this experiment, probably around 0.3 mole %, and perhaps no ThF₄. Such a salt could be dissolved with HF-NO₂ solutions in two contacts. Since UF₄ is dissolved along with the LiF and BeF₂, the section of the fluoride volatility plant used for recovering uranium from the fuel salt could be eliminated. The LiF and BeF₂ solubilities may be such that the total fuel-salt solubility is lower than for aqueous HF solutions, thus requiring a somewhat larger plant for the same processing capacity.

Aqueous NH₄F

In tests with blanket salt, LiF-BeF₂-ThF₄-UF₄ (67-18.5-14-0.5 mole %), some component, probably LiF, interfered with ThF₄ solubility. A sample of salt was added to 50% NH₄F solution at 100°C. After 1 hr all the BeF₂ and UF₄ dissolved, the respective concentrations being 13 and 2.15 mg/ml; but only 12 to 15% of the LiF and ThF₄ dissolved, their respective solubilities being 2.2 and 9.3 mg/ml. After one day, during which time the pH decreased considerably due to loss of NH₃ from the ammonium fluoride solution, all the solubilities were lower except that of BeF₂. Neutralization with NH₄OH did not restore the original solubilities. In every case all the BeF₂ present was in solution, in agreement with its very high solubility in water. The solid phases containing ThF₄ obtained upon

freezing this salt were $3\text{LiF}\cdot\text{ThF}_4$ solid solution and a little $\text{LiF}\cdot 2\text{ThF}_4$; such compounds generally do not have properties similar to those of the components, LiF and ThF_4 . In this case the solubility of ThF_4 in equilibrium with the compounds is much lower than that in equilibrium with pure ThF_4 .

No satisfactory process has been found for decontaminating salts containing large amounts of ThF_4 . The fluoride volatility process is entirely satisfactory for processing these salts if they are used in the blanket of a two-region breeder reactor, since decontamination is not required for many years, if ever. However, decontamination would be required if these salts are used for fuel, as they might be in a one-region converter reactor.

Protactinium Removal

A method for economically removing protactinium from the blanket of a molten-salt breeder reactor at a rate competitive with its decay would be advantageous. A single experiment was made to investigate the possibility that a volatile fluoride might be formed. Natural protactinium (Pa^{231}) was added to $\text{LiF}\text{-BeF}_2\text{-ThF}_4\text{-UF}_4$ (67-18.5-14-0.5 mole %) to a concentration of 0.012 wt %, and the salt was fluorinated for 2 hr at 650°C . No measurable amount of protactinium was removed from the salt, but the uranium was removed.

INTERNAL DISTRIBUTION

- | | |
|---------------------------|-------------------------|
| 1. R. G. Affel | 48. M. T. Kelley |
| 2. L. G. Alexander | 49. F. Kertesz |
| 3. E. S. Bettis | 50. B. W. Kinyon |
| 4. D. S. Billington | 51. M. E. Lackey |
| 5. F. F. Blankenship | 52. J. A. Lane |
| 6. E. P. Blizard | 53. D. A. Lee |
| 7. A. L. Boch | 54. R. S. Livingston |
| 8. C. J. Borkowski | 55. H. G. MacPherson |
| 9. W. F. Boudreau | 56. W. D. Manly |
| 10. G. E. Boyd | 57. E. R. Mann |
| 11. M. A. Bredig | 58. L. A. Mann |
| 12. E. J. Breeding | 59. W. B. McDonald |
| 13. R. B. Briggs | 60. H. F. McDuffie |
| 14. W. E. Browning | 61. J. R. McNally |
| 15. D. O. Campbell | 62. H. J. Metz |
| 16. W. H. Carr | 63. R. P. Milford |
| 17. G. I. Cathers | 64. E. C. Miller |
| 18. C. E. Center (K-25) | 65. J. W. Miller |
| 19. R. A. Charpie | 66. K. Z. Morgan |
| 20. R. S. Cockreham | 67. J. P. Murray (Y-12) |
| 21. J. H. Coobs | 68. M. L. Nelson |
| 22. F. L. Culler | 69. G. J. Nessle |
| 23. J. H. DeVan | 70. W. R. Osborn |
| 24. D. A. Douglas | 71. L. F. Parsly |
| 25. L. B. Emlet (K-25) | 72. P. Patriarca |
| 26. W. K. Ergen | 73. A. M. Perry |
| 27. J. Y. Estabrook | 74. D. Phillips |
| 28. D. E. Ferguson | 75. W. D. Reel |
| 29. A. P. Fraas | 76. P. M. Reyling |
| 30. E. A. Franco-Ferreira | 77. J. T. Roberts |
| 31. J. H. Frye, Jr. | 78. M. T. Robinson |
| 32. W. R. Gall | 79. H. W. Savage |
| 33. A. T. Gresky | 80. J. L. Scott |
| 34. J. L. Gregg | 81. H. E. Seagren |
| 35-37. W. R. Grimes | 82. E. D. Shipley |
| 38. E. Guth | 83. M. J. Skinner |
| 39. C. S. Harrill | 84. G. M. Slaughter |
| 40. M. R. Hill | 85. A. H. Snell |
| 41. E. E. Hoffman | 86. E. Storto |
| 42. H. W. Hoffman | 87. C. D. Susano |
| 43. A. Hollaender | 88. J. A. Swartout |
| 44. A. S. Householder | 89. A. Taboada |
| 45. W. H. Jordan | 90. E. H. Taylor |
| 46. G. W. Keilholtz | 91. R. E. Thoma |
| 47. C. P. Keim | 92. D. B. Trauger |

- | | |
|----------------------|-----------------------------------------------------------------------|
| 93. F. C. VonderLage | 100. C. E. Winters |
| 94. G. M. Watson | 101. J. Zasler |
| 95. A. M. Weinberg | 102-105. ORNL - Y-12 Technical Library,
Document Reference Section |
| 96. M. E. Whatley | 106-145. Laboratory Records Department |
| 97. J. C. White | 146. Laboratory Records, ORNL R.C. |
| 98. G. D. Whitman | 147-148. Central Research Library |
| 99. G. C. Williams | |

EXTERNAL DISTRIBUTION

- 149. D. H. Groelsema, AEC, Washington
- 150. Division of Research and Development, AEC, ORO
- 151-727. Given distribution as shown in TID-4500 (15th ed.) under Reactors-Power category (75 copies - OTS)